DEVELOPMENT OF TARGETED DELIVERY SYSTEMS FOR EARLY DETECTION AND GENETICALLY THERAPEUTIC INTERVENTION OF CARDIOVASCULAR DISEASE

ZHILI KANG

Development of targeted delivery systems for early detection and genetically therapeutic intervention of cardiovascular disease

By

Zhili Kang

A thesis submitted to the School of Graduate Studies

in partial fulfillment of the requirements

for the degree of Master of Science

School of Pharmacy

Memorial University of Newfoundland

August, 2003

St. John's Newfoundland Canada

Your file Votre référence
ISBN: 0-612-99083-4
Our file Notre référence
ISBN: 0-612-99083-4

Abstract

Atherosclerosis is a primary cause of heart disease and stroke. It is known that early detection of atherosclerotic lesions would significantly reduce the risk. One of the objectives in this thesis is to evaluate a noninvasive radioimaging method for detecting early atherosclerotic plaques. A novel polyiodinated cholesterol analog, cholesteryl 1,3-diiopanoate glyceryl ether (C2I), radiolabeled with ^{125}I, was incorporated into acetylated low density lipoprotein (AcLDL) which is considered as an atherosclerotic plaque seeking carrier. ^{125}I-C2I was also prepared as a chylomicron-like emulsion. ^{125}I-C2I/AcLDL or ^{125}I-C2I emulsion was intravenously injected into apoE/LDL receptor (LDLR) double knockout mice that serve as an atherosclerosis animal model. The *ex vivo* images of radioactivity accumulated in the aortas 24 hours postinjection were compared to the atherosclerotic lesions revealed by histological studies. It was found that both ^{125}I-C2I/AcLDL and ^{125}I-C2I emulsion resulted in accumulation of radioactivity at the site of early atherosclerotic lesions, and therefore may be useful for early detection of atherosclerosis.

Treatments for atherosclerosis include general lipid-lowering strategies and approaches toward etiology. Among the multiple risk factors associated with atherosclerosis, familial hypercholesterolemia (FH) is the first genetic disorder recognized to cause severe premature atherosclerosis. Ultimate treatment for FH depends on gene therapy which can correct its LDLR deficiency. The second part of this thesis focused on the development of a liver-targeting liposome vector for systemic gene therapy, with the objective of delivering mouse LDLR gene to the liver of the LDLR-

knockout mouse, an animal model closely resembling human FH conditions. A peptide from the circumsporozoite protein (CS) of malaria parasites was chosen as the liver-targeting ligand. Cationic liposome/protamine/DNA (LPD) complex conjugated with the malaria peptide was prepared by different protocols and primarily investigated *in vitro* to transfect cultured cells with a reporter gene, either the chloramphenicol acetyltransferase (CAT) gene or the enhanced green fluorescent protein (EGFP) gene. Peptide-LPD complex showed higher CAT/EGFP expression in HepG2 cells (human hepatoma cell line) than LPD itself, whereas no significant difference was observed in Hela cells (human cervical cancer cell line, control). However, these results were still preliminary and somewhat inconsistent. Further studies are needed.

Finally, chapter 4 summarized other work using LDL as a potential targeting carrier for lipophilic antitumor drugs. A prodrug, dipalmitoyl-5-fluorodeoxyuridine (dpFUdR), was synthesized and incorporated into LDL. The antiproliferative effect of the resultant LDL-dpFUdR was investigated in human cervical cancer cells.

Key words: atherosclerosis • apoE/LDLR knockout mice • AcLDL • emulsion • cholesteryl 1,3-diiopanoate glyceryl ether (C2I) • early detection • familial hypercholesterolemia (FH) • gene therapy • cationic liposome • LPD • malaria peptide • transfection • liver targeting • dipalmitoyl-5-fluorodeoxyuridine (dpFUdR) • LDL • antiproliferation

Acknowledgments

I wish to sincerely appreciate my supervisor, Dr. Hu Liu, who has provided me the opportunity to enter into the field of science and guided the development of my research abilities. His devotion to research has inspired me to make learning a life-long experience.

I am also grateful to the members of my supervisory committee, Dr. Thomas Scott for his knowledgeable advisement and experienced research skills, and Dr. Lili Wang for her valuable suggestions and great assistance in my writing. They have given me the continuing encouragement that I will never forget.

Thanks should be extended to Ms. Judy Foote (Histology Unit), Mr. Howard Gladney and Ms. Kathryn Williams (EM Unit) for their technical assistance, to Ms. Margaret Connors (School of Pharmacy) for her help, and to everyone in Dr. Liu's laboratory, including Krista, Anas, and Wei, for the friendly working environment.

I dedicate this thesis to all the people who have positively influenced me, particularly my husband, Jinguo Wang, and my newborn daughter, Amy. I could not have completed my projects without Jinguo's unconditional support and helpful discussions. Other people standing out in my mind are my parents (Jishan Kang and Xiugai Yang) and my parents-in-law (Xuebin Wang and Xianxu Lü), who encouraged my education and supported my family.

Projects in this thesis were funded by operating grants from the Canadian Institutes of Health Research (CIHR) and the Research Infrastructure Fund from Memorial University of Newfoundland. The author was a recipient of a graduate research

scholarship in pharmacy from the Health Research Foundation, Canada's Research-Based Pharmaceutical Companies (Rx&D) and the CIHR.

Table of contents

List of tables

Page

List of figures

Page

List of abbreviations

AcLDL	Acetylated low density lipoprotein
apo	apolipoprotein
bp	base pairs
Bq	Becquerel
BSA	Bovine serum albumin
BVs	Blood vessels
C2I	Cholesteryl 1,3-diiopanoate glyceryl ether
CAT	Chloramphenicol acetyltransferase
CDTA	trans-1,2-Diaminocyclohexane-tetraacetic acid hydrate
CE	Cholesteryl ester
CI	Cholesteryl iopanoate
cpm	Counts per minute
CS	Circumsporozoite (protein)
CT	Computed tomography
CVD	Cardiovascular disease
d	Density
D5W	5% dextrose water
DCC	Dicyclohexylcarbodiimide
DMAP	Dimethylaminopyridine
DMEM	Dulbecco's Modified Eagle's Medium
DMF	N,N-dimethylformamide

DMSO	Dimethylsulfoxide
DOTAP	1,2-Diolelyl-3-trimethylammonium-propane
dpFUdR	3',5'-Dipalmitoyl-5-fluoro-2'-deoxyuridine
DPPE	DL-α-phosphatidylethanolamine dipalmitoyl
ECL	Enhanced chemiluminescence
EDTA	Ethylenediaminetetraacetic acid
EGFP	Enhanced green fluorescent protein
ELISA	Enzyme linked immunosorbent assay
EM	Electron microscopy
EtBr	Ethidium bromide
FBS	Fetal bovine serum
FdUMP	5-Fluoro-2'-deoxyuridine-5'-monophosphate
FH	Familial hypercholesterolemia
FITC	Fluorescein isothiocyanate
FU	5-Fluorouracil
FUdR	5-Fluoro-2'-deoxyuridine
HDL	High density lipoprotein
hLDLR	Human low density lipoprotein receptor
HPLC	High performance liquid chromatography
HRP	Horseradish peroxidase
i.v.	intravenous
IC_{50}	50% growth-inhibitory concentration

IVUS	Intravascular ultrasound
kb	kilobases
kDa	kilo-Dalton
LDL	Low density lipoprotein
LDLR	Low density lipoprotein receptor
LPD	Cationic liposomes/protamine/DNA
MeOH	Methanol
mLDLR	Mouse low density lipoprotein receptor
MOPS	4-Morpholinepropanesulfonic acid, sodium salt
MR	Magnetic resonance
MTT	3-[4,5-Dimethylthiazol-2-yl]-2,5-diphenyltetrazolium bromide
OCT	Optical coherence tomography
OxLDL	Oxidized low density lipoprotein
PBS	Phosphate buffered saline
PC	L-α-phosphatidylcholine
PE	R-phycoerythrin
PMSF	Phenylmethylsulfonyl fluoride
Rf	Retention factor
RT-PCR	Reverse transcription polymerase chain reaction
SD	Standard derivation
SDS-PAGE	Sodium dodecyl sulfate polyacrylamide gel electrophoresis
SE	Standard error

SEM	Standard error of the mean
SMC	Smooth muscle cell
TBE	Tris-boric acid-EDTA
TBST	Tris-buffered saline-Tween
TE	Tris-EDTA
TLC	Thin layer chromatography
TS	Thymidylate synthase
US	Ultrasound
UV	Ultraviolet
VLDL	Very low density lipoprotein

Chapter 1. Introduction and overview

1.1 Atherosclerosis and the development of atherosclerotic lesions

Atherosclerosis is a slowly developing, chronic degenerative disease of blood vessels (BVs), which is characterized by the accumulation of lipids and fibrous elements in the wall of large and medium arteries. It is the primary cause of cardiovascular disease (CVD) including coronary heart disease and stroke. In economically privileged populations such as those of western societies, atherosclerosis is responsible for about 50% of all deaths [Lusis, 2000].

It is now clear that atherogenesis is a long-term process developed in an inflammatory and hyperlipidemic environment. The atherosclerotic lesions are focal areas of intimal thickening formed through a very complex interaction between the vessel wall and blood components [Lusis, 2000; Glass and Witztum, 2001]. A primary initiating event is the deposit of lipid particles, low density lipoprotein (LDL), within the subendothelial matrix of the intima. When circulating LDL level is raised, both the transport of LDL into BVs and retention of LDL by BVs are increased. LDL particles diffuse passively through endothelial cell junctions and aggregate in the matrix of BVs, where they undergo certain modifications such as oxidation, lipolysis, and proteolysis. The accumulation of modified LDL stimulates the overlying endothelial cells to produce a

number of pro-inflammatory factors that can attract blood mononuclear cells and platelets. The monocytes then enter into the intima and subsequently differentiate to macrophages. The modified LDL can be rapidly taken up by macrophages via scavenger receptors, resulting in the formation of foam cells. The death of foam cells leaves behind a growing mass of extracellular lipids and other cell debris. In parallel, smooth muscle cells (SMCs) abnormally proliferate and transmigrate from the media to intima. The intimal SMCs secrete extracellular matrix and give rise to a fibrous cap on the luminal aspect of the lipid core. The continuation of these processes leads to the formation of fibrolipid atherosclerotic plaques which may be rich in both connective tissue and lipid [Woolf, 2001].

Typically, an atherosclerotic lesion, or plaque, consists of: (1) matrix-rich connective tissue including collagen, proteoglycans, and fibronectin elastic fibers; (2) crystalline cholesterol, cholesteryl esters, and phospholipids, which are derived largely from the plasma LDL; and (3) cells such as monocyte-derived macrophages, T-lymphocytes, and SMCs [Libby, 1995]. Proportions of these components vary in different plaques, and have important impact on the natural history of the lesion. The local increase in volume of the plaque leads to narrowing of the arterial lumen (stenosis), and if this is sufficiently severe as to reduce the cross-sectional area of the lumen by 75% or more, or the diameter by 50% or more, the blood flow will be compromised and the patient is

likely to develop stable angina [Stary et al., 1995]. However, a plaque with a thin cap and a massive lipid/necrotic core is more likely to develop intimal injury, resulting in the rupture of the plaque. When it is disrupted, the underlying tissues are exposed to the blood, activating platelets and the clotting cascade. Large numbers of platelets then attach to the plaque surface and crosslink with fibrin to form a thrombus or blood clot. Although usually mildly stenotic, these so-called rupture-prone or vulnerable plaques are found to be more closely associated with life-threatening clinical situations than the severely stenotic lesions, such as unstable angina, acute myocardial infarction, stroke and sudden death due to the development of serious ventricular arrhythmias [Falk et al., 1995; Fayad and Fuster, 2001; Corti et al., 2002].

1.2 Lesion types and progressing phases of atherosclerosis

In morphological terms, atherosclerosis can be defined as a systemic disorder involving the intima of large elastic and muscular arteries such as the aorta, the epicardial coronary, femoral and carotid arteries [Corti et al., 2002]. In humans, early atherosclerotic lesions can usually be found in the aorta in the first decade of life, the coronary arteries in the second decade, and the cerebral arteries in the third or fourth decades. Because of differences in blood flow dynamics, there are preferred sites of

lesion formation within the arteries such as regions of arterial branching or curvature where flow is turbulent [Gimbrone, 1999].

According to the criteria of the American Heart Association Committee on Vascular Lesions, atherosclerotic lesion can be categorized to six types (Table 1.1) [Stary et al., 1994; Stary et al., 1995].

Table 1.1. Pathological classification of human atherosclerotic lesions

Lesion types	Main histology	Earliest onset	Clinical correlation
Type I lesion (initial)	Isolated macrophage foam cells	From first decade	Clinically silent (early lesions)
Type II lesion (fatty steak)	Mainly intracellular lipid accumulation		
Type III lesion (intermediate)	Type II changes & small extracellular lipids	From third decade	Clinically silent or overt (advanced lesions or raised lesions)
Type IV lesion (atheroma)	Fibrolipid plaques with confluent extracellular lipid pools		
Type V lesion (fibroatheroma)	Lipid core & fibrotic layer, or multiple lipid cores & fibrotic layers (Va), or mainly calcific (Vb), or mainly fibrotic (Vc)	From forth decade	
Type VI lesion (complicated)	Surface defect, hematoma-hemorrhage, thrombus		

Based on gross pathological and clinical findings, the progression of coronary atherosclerotic disease can also be classified into five phases [Fuster et al., 1992; Fuster, 1994].

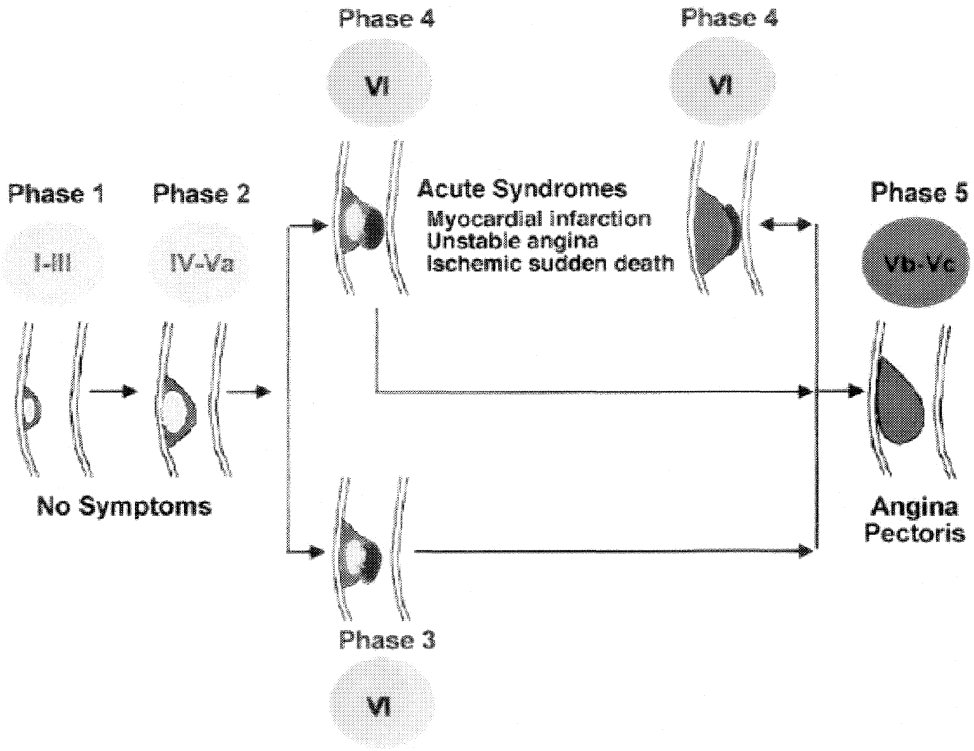

Figure 1.1. Phases and lesion morphology of the progression of coronary atherosclerosis (Copied from Fayad and Fuster, 2001 with permission)

As shown schematically in Figure 1.1, phase 1 is represented by a small plaque that is categorized as type I to III lesions. It is present in most people under the age of 30 years and usually progresses very slowly. Phase 2 is characterized by the presence of plaques that, although not necessarily very stenotic, have a high lipid content that is very prone to rupture (types IV and Va lesions). Disruption of phase 2 plaques may lead to the formation of either mural or occlusive thrombus, representing acute phase 3 or phase 4, respectively. Phase 3, consisting of type VI lesions, could possibly progress into stenosis, resulting in angina. Phase 4 may be associated with acute coronary syndromes and type VI lesions of phase 4 can also evolve into a fibrotic phase (phase 5) characterized by more stenotic plaques that may proceed to occlusive lesions (types Vb and Vc lesions). This process of occlusion from late stenotic plaques tends to be silent because the preceding severe stenosis and ischemia enhance protective collateral circulation [Fuster et al., 1992; Fayad and Fuster, 2001].

1.3 Etiology of atherosclerosis and familial hypercholesterolemia (FH)

Epidemiological studies over the past 50 years have revealed numerous risk factors for atherosclerosis. These can be grouped into factors with a significant genetic component, and those that are largely environmental [Lusis, 2000; Glass and Witztum, 2001]. As listed in Table 1.2, the common forms of CVD result from the combination of

an unhealthy environment, genetic susceptibility and our increased lifespan. Among the many risk factors, there is a complex interaction between some factors; for example, the effects of hypertension on CVD are considerably amplified if cholesterol levels are high. Moreover, the relatively elevated atherogenic lipoproteins appear to be of primary importance, as raised level of plasma cholesterol is a prerequisite for most forms of the disease. Even in the absence of other known risk factors, an elevated cholesterol level is probably sufficient to drive the development of atherosclerosis in humans and experimental animals [Glass and Witztum, 2001].

Plasma cholesterol is carried by several lipoprotein particles that perform the complex physiologic tasks of transporting dietary and endogenously produced lipids [Packard and Shepherd, 2001]. Chylomicrons provide the primary means of transporting dietary lipids, while very low density lipoprotein (VLDL), LDL, and high density lipoprotein (HDL) function to transport endogenous lipids. In humans, LDL is the main vehicle for the delivery of cholesterol to peripheral tissues, and it is taken up by cells via LDL receptors (LDLRs) that recognize the apolipoprotein (apo) B-100 on its surface. The circulating level of LDL is determined in large part by the rate of liver uptake through the hepatic LDLR pathway, as evidenced by the fact that lack of functional LDLR is responsible for the massive accumulation of LDL-bound cholesterol in patients with homozygous familial hypercholesterolemia (FH) [Brown and Goldstein, 1986].

Table 1.2. Risk factors for the development of atherosclerosis

Factors with a strong genetic component	Environmental factors
Elevated levels of LDL and VLDL	High fat diet
Low levels of HDL	Smoking
Elevated levels of lipoprotein(a)	Lack of exercise
Hypertension	Infectious agents
Diabetes mellitus	Low antioxidant levels
Obesity	
Gender (male)	
Family history	
Elevated levels of homocysteine	
Elevated levels of hemostatic factors, e.g. fibrogen	
Metabolic syndrome, such as insulin resistance	
Systemic inflammation	
Depression and other behavioural traits	

FH is the first genetic disorder recognized to cause myocardial infarction, a fatal clinical consequence of atherosclerosis [Goldstein et al., 2001]. To this day, it remains the most typical example used to illustrate relations between high plasma cholesterol levels and coronary atherosclerosis [Stehbens, 2001].

FH results from a mutation in the gene specifying LDLR, one of the most extensively studied receptors in genetics. Five classes of gene mutations at the LDLR locus have been identified and each class can be subdivided into multiple alleles through

molecular characterization. More than 420 different mutant alleles have been found in different FH patients. Many of these mutations disrupt receptor function in meaningful ways [Goldstein et al., 2001]. The clinical characterizations of FH include a lifelong elevation of LDL concentration, deposition of LDL-derived cholesterol in tendons and skin (xanthomas), as well as in arteries, and premature atherosclerosis. Inherited as an autosomal dominant trait, FH homozygotes (two mutant alleles at the LDLR locus, either identical or different) are more severely affected than are heterozygotes (one normal allele and one mutant allele). Heterozygotes occur in the population at a frequency of about 1 in 500, placing FH among the most common monogenic diseases in humans. Cholesterol levels in heterozygotes elevate twofold from birth (350 to 550 mg/dl) and coronary atherosclerosis generally develops after age 30. Homozygotes, on the other hand, number 1 in 1 million persons and have severe hypercholesterolemia (650 to 1000 mg/dl). Coronary heart disease begins in childhood and frequently causes death from myocardial infarction before age 20.

In addition to the finding of a raised level of LDL cholesterol from childhood, diagnosis of FH also requires either the demonstration of a decrease in LDLR activity, the documentation of mutation in the LDLR gene, or the presence of other clinical features such as tendon xanthomas, premature atherosclerosis, and autosomal dominant transmission [Goldstein et al., 2001].

1.4 Imaging modalities for the detection of atherosclerotic lesions

It is known that early identification of patients at high risk for development of CVD and subsequent intervention with lifestyle changes and, where necessary, drug therapy would have substantial benefit for reducing cardiovascular morbidity and mortality [Corti et al., 2002]. Besides evaluation of clinical risk factors, which are not adequate and sometimes not timely, directly imaging atherosclerosis at its early stage is a promising approach for identifying patients who are at increased risk for cardiovascular events. It may also provide a tool for better understanding the plaque biology, monitering a patient's response to therapy, and testing new therapeutic approaches. Currently, a number of invasive and noninvasive methods are used to study atherosclerosis, and most of them identify luminal diameter or stenosis, wall thickness, and plaque volume.

Angiography, a traditional imaging technique, remains the "gold standard" for evaluating luminal narrowing or stenosis resulting from the formation of atherosclerotic plaque. It may also reveal advanced lesions, plaque disruption, luminal thrombosis, and calcification [Fayad and Fuster, 2001]. However, angiography can only provide limited information about histopathological features of individual plaques, which is, as summarized in the section 1.1, more valuable for prediction of lesion progression. As an invasive method, angiography is associated with significant risk.

Angioscopy uses visible light to image the plaque surface. As it can reveal surface features of the plaque, intravascular angioscopy is able to detect thrombus formation and lipid accumulation, although it has not gained significant clinical use. It is also invasive and cannot evaluate deeper plaque components [Thieme et al., 1996].

Catheter-based ultrasound or intravascular US (IVUS) is a new approach to arterial vascular wall imaging with high-resolution [York and Fitzgerald, 1998]. This invasive modality directly provides cross-sectional tomographic images of the vessel and lesion area. Diagnostic applications of IVUS include detection of angiographically unrecognized disease, detection of intermediate lesions (40-75% stenosis) and calcification, and certain risk estimation for intervention of atherosclerosis. The limitation of IVUS is its low sensitivity in detection of thrombus and lipid-rich lesions.

Some other new invasive techniques, namely, optical coherence tomography (OCT), Raman spectroscopy and near-infrared spectroscopy, are undergone exploration and have shown promise in characterizing lesion compositions with high resolution [Pasterkamp. et al., 2000]. Noninvasive methods, such as B-mode ultrasound (US), computed tomography (CT), magnetic resonance (MR) imaging and nuclear scintigraphy, are obviously safer and easier for practice than the above invasive techniques.

Ultrasound and Doppler flow studies have been used extensively to measure severity of stenosis in peripheral arteries. It is also the dominant clinical method for

evaluation of carotid artery disease including carotic atherosclerosis. Measurements of carotid and aortic wall thickness as well as qualitative and quantitative analysis of plaque such as calcification, lipid accumulation, and thrombus can also be determined by surface and transesophageal US, and each of these features is correlated with the evaluated risk of CVD [Gronholdt, 1999; Fazio et al., 1993]. However, this usage has not yet been standardized and integrated into clinical practice, and requires further study.

CT is a kind of X-ray-based technique, which demonstrates high sensitivity to calcification. It is therefore capable of noninvasively detecting human coronary artery calcification in the clinic, which in general represents the burden degree of atherosclerotic plaque. However, CT has limited capability to characterize soft tissue such as lipids, a feature associated with plaque vulnerability. With the development of multidetector scanners, CT technology continues to improve and significant potential still exists for the early identification of patients at increased risk [Callister et al., 1999].

High-resolution MR imaging is the leading imaging modality for characterization of atherosclerotic lesions on the basis of biophysical and biochemical information. It can theoretically distinguish the plaque components, including lipid, fibrous element, calcified region and thrombus, as well as the plaque disruption. Some promising results have been obtained in animal models or human subjects [Skinner et al., 1995; Toussaint et al., 1996]. However, MR still lacks sufficient resolution (currently 0.4 mm) for accurately measuring

cap thickness and imaging lesions within coronary arteries due to their small size as well as cardiac and respiratory motion [Fayad et al., 2000].

1.5 Nuclear scintigraphy imaging techniques

Nuclear scintigraphy images arise from injected radioactive tracers which subsequently emit radiation from within body organs. It is based on the specific binding of radioactively labeled molecules to the target tissue, in this case the atherosclerotic lesion. Because the detection method evaluated in the work of this thesis is related to nuclear tracer imaging, this approach will be discussed in some detail in this section.

An ideal radiotracer for visualizing the vulnerable plaque should meet the following criteria [Vallabhajosula and Fuster, 1997]:

(1) it must be specific for lipid core, macrophage density or thrombus;

(2) it must be able to detect lesions in all atherosclerotic artery types that are related to clinical symptoms;

(3) it must be able to assess progression-regression of atherosclerosis;

(4) it must be able to predict clinically significant events;

(5) it must be able to provide prognostic indicators in population studies;

(6) it must have a kit formulation for instant preparation, high specificity and sensitivity, fast blood clearance and high lesion to blood ratios.

There are no single radiotracers that meet all these conditions. Attempts to image areas of active atherosclerosis started with the labeling of one of the major but nonspecific components of plaques, LDL or Oxidized LDL (OxLDL), and have progressed to the use of smaller antibody fragments and peptides against specific components of the atherosclerotic plaque or thrombus, such as macrophages, smooth muscle cells, endothelial adhesion molecules and platelets [Narula et al., 1999]. These tracers were radiolabeled with radioiodine, ^{99m}Tc, ^{111}In, or ^{125}In, and showed significant uptake in experimental atherosclerotic lesions. Table 1.3 lists the potential targets for vulnerable plaque imaging [Cerqueira, 1999]. However, the limited clinical trials could not demonstrate their utility because of the slow clearance of radiotracers from the circulation and poor target/background ratios [Vallabhajosula and Fuster, 1997; McConnell, 2000]. In addition, relatively low spatial resolution and high blood-pool signal have limited the clinical application of nuclear techniques to date.

A common drawback of all radiolabeled native products, including LDLs, peptides, and immunoglobulins, is that once these radiotracers are taken up by the target tissues, they will be quickly degraded within the lysosomal compartment inside the cell and then be excreted, which compromises the selectivity of these targeting tracers for long-term monitoring. Attempts to overcome this problem have led researchers to study agents that

would remain in the cell once internalized. To this end, cholesteryl 1,3-diiopanoate glyceryl ether (C2I), a novel cholesterol analogue, was first synthesized by our lab.

Table 1.3. Potential targets for imaging vulnerable atherosclerotic plaques

LDL cholesterol
Proliferating smooth muscle cells
Up-regulated receptors
Tyrosine kinase activity: Endothelin-1derivative, ^{99m}TC-ZK167054*
G-protein signaling related: Purine analog, ^{99m}TC-Ap4A**
Surface antigenic moieties: ^{111}In-Z2D3†
Macrophage infiltration in atherosclerotic plaques
Large lipid cores in atherosclerotic lesions: ^{123}I-SP4‡

[* Dinkelborg et al., 1998; ** Elmaleh et al., 1998; † Narula et al., 1995; ‡ Hardoff et al., 1993]

As shown in Figure 1.2, the C2I molecule contains an ether bond, which is resistant to endocellular hydrolysis. Moreover, each C2I molecule bears six iodines, providing it a great potential for a high specific radioactivity after these iodines are exchanged by their radioactive counterparts, such as ^{125}I and ^{123}I. This lipophilic compound has been incorporated into acetylated LDL (AcLDL) and preliminarily examined in a rabbit model for the detection of atheroeclerotic lesions *ex vivo* [Xiao[2] et al., 1999].

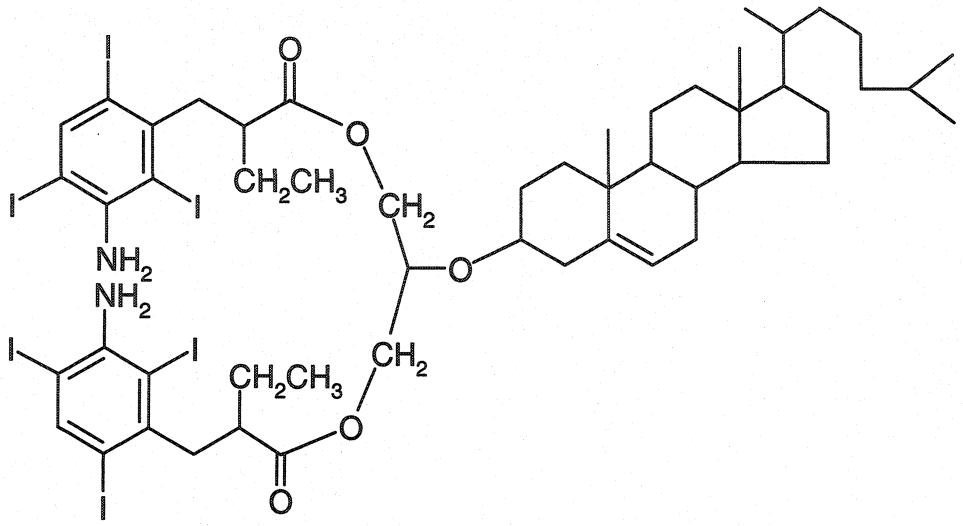

Figure 1.2. The structure of cholesteryl 1,3-diiopanoate glyceryl ether (C2I)

In the current project, apoE and LDLR double knockout mice, which are homozygous for targeted disruptions of the genes for both apoE and the LDLR [apoE(-/-); LDLR(-/-)], were chosen as the animal model to evaluate the potential of the above radiotracer, ^{125}I labeled C2I (^{125}I-C2I), since they can develop atherosclerotic lesions closely-resembling those of humans [Smith and Breslow, 1997]. AcLDL was used as a selective carrier for ^{125}I-C2I because (1) the hydrophobic core of AcLDL particle provides a large space for retaining such lipophilic compounds; (2) it is known that macrophages in atherosclerotic plaques express a scavenger receptor for modified LDL such as OxLDL and AcLDL. Therefore it is rational to use the differential uptake of AcLDL as an approach to deliver radioimaging probes for the detection of early atherosclerotic lesions.

In addition, AcLDL had been proven to have a faster blood clearance than native LDL [Van Berkel et al., 1991], which would facilitate its utility in nuclear imaging by enhancing the tissue-background ratio of radioactivity. On the other hand, ^{125}I-C2I was also formulated into a lipid emulsion which can be considered as an artificial lipoprotein particle imitating chylomicron remnant, a known atherogenic factor. Although the chylomicron remnant is physiologically metabolized mainly in the liver, it can also be internalized by extrahepatic tissues including macrophages in the artery wall [Terpstra, 2000]. We therefore expected the chylomicron-like emulsion formulation to deliver ^{125}I-C2I to early atherosclerotic lesions.

1.6 Treatment strategies for atherosclerosis and gene therapy for FH

As atherosclerosis is a chronic disease requiring prevention over the course of a lifetime, modification of life-style is the first basic step. Preventive measures including regular exercising, quitting smoking, and replacing dietary saturated fatty acids with unsaturated fats, have proven merits. In addition to the control of diseases that may contribute to atherosclerosis, such as hypertension and diabetes, medical interventions that markedly alter the balance of atherogenic *vs* antiatherogenic lipoproteins are associated with inhibition of lesion progression. It has been shown that aggressively lowering LDL cholesterol reduces cardiovascular morbidity and mortality, and prevents the development

of atherosclerosis [Chait and Heinecke, 1999]. Statins, the first-line cholesterol-lowering drugs, are capable of stabilizing atherosclerotic plaques independent of their hypolipidemic effect [Brown et al., 1993; Shah, 1997]. A novel cholesterol transport inhibitor, ezetimibe, can selectively inhibit the uptake of cholesterol from the intestinal lumen, and offers a new therapeutic option for decreasing LDL cholesterol [Gagne et al., 2002]. Some other medications including angiotensin-converting enzyme (ACE) inhibitors may also, at least in part, decrease the plaque vulnerability [Pitt, 2000]. Antioxidants have been recommended as well in order to reduce the risk, although the therapeutic benefits of inhibition of oxidative processes are still in clinical trial stages. For acute coronary syndromes, besides mechanical interventions, there are several pharmacological strategies that have been developed to dissolve preformed thrombi and inhibit thrombogenesis. These agents can be subdivided by their mechanisms of action into three categeries: fibrinolytics, inhibitors of the intrinsic coagulation cascade (e.g. heparins, antithrombins), and antiplatelet agents [Corti et al., 2002].

Gene engineering technology using overexpression or knockout genes of interest has provided genetically manipulated mice models for the study of underlying molecular mechanisms of atherosclerosis and thus accelerated the pace of discovering novel therapeutic agents. Small molecule-based approaches targeting enzymes or transcription factors involved in atherogenic process have been found to have great potential [Glass and

Witztum, 2001]. Moreover, gene therapy represents an ultimate means to correct some genetic disorders leading to atherosclerosis, in particular, FH.

Current therapy for FH is a combination of a stringent diet to decrease cholesterol intake and pharmacological agents to increase the removal of cholesterol, as well as plasma exchange or LDL apheresis in some severe cases [Goldstein et al., 2001]. However, some patients cannot achieve optimal LDL cholesterol levels with the above approaches. The majority of these patients are homozygous FH. Although LDLRs are expressed ubiquitously, the hepatic LDLR has the greatest quantitative effect in controlling plasma LDL levels. Importantly, a limited number of patients with homozygous FH have undergone liver transplantation and have experienced substantial reduction in LDL cholesterol levels [Goldstein et al., 2001]. Success of the liver transplantation suggests that gene therapy targeted toward the liver would likely be an effective strategy for the treatment of FH.

Gene therapy can be defined as the transfer of genetic material to specific target cells/tissues of a patient where its expression produces a therapeutic effect, ultimately preventing or altering a particular disease state. Carriers or delivery vehicles for therapeutic genetic material are called vectors, and there are viral and non-viral vectors being studied now [Jain, 1998]. Introduction of functional LDLR genes in the liver through an *ex vivo* gene therapy approach has been conducted in five FH homozygous

patients with coronary artery disease [Grossman et al., 1995]. In this clinical trial, liver cells were transfected *ex vivo* with a retrovirus expressing the LDLR and then reintroduced into the liver via the portal vein 3 days after the initial surgery. All patients were found to have tolerated the procedure without significant complications. Transgene expression was detected in a limited number of hepatocytes and liver tissue harvested 4 months after gene transfer from all five patients. Significant and prolonged reduction in LDL cholesterol was demonstrated in three of the five patients. However, the marginal effectiveness and the complexity of the process preclude more widespread use of this method of the treatment. The development of *in vivo* gene therapies based on recombinant adenoviruses encoding LDLR or VLDL receptor may facilitate a broader application of these approaches. Although encouraging results have been observed in several animal experiments [Kozarsky et al., 1994; Ishibashi et al., 1993; Kozarsky et al., 1996], immunogenicity and higher toxicity of viral vectors so far make them less attractive than non-viral vectors.

Cationic liposomes are a promising group of non-viral vectors for gene transfer, which exhibited adequate features for *in vivo* use. In the last decade, extensive effort has been devoted to the development and optimization of this strategy [Lee and Huang, 1997]. Numerous novel preparations of cationic liposomes have been formulated and several clinical trials using cationic liposome-DNA complexes (lipoplexes) have been performed

for the treatment of cystic fibrosis and cancer [Nabel et al., 1993; Caplen et al., 1995]. It has been shown that a LPD (cationic liposome/polycationic peptide such as protamine/DNA) complex has great potential for intravenous gene delivery [Li et al., 1998]. However, transgene expression is widely distributed throughout the body of the living host following systemic administration. In our project, a liver targeting LPD complex was developed using a malaria peptide as the hepatocyte-specific ligand. The final objective of this project is to correct LDLR deficiency in LDLR knockout mice, an animal model of human FH, using the liver-specific LPD vector carrying mouse LDLR gene. However, the work conducted in the thesis, as summarized in chapter 3, was focused on *in vitro* studies of the malaria peptide-LPD formulations.

The other work, using LDL as a potential targeting carrier for lipophilic antitumor drugs, was also summarized as an appendix in this thesis. Because its content is somewhat far from the major project, it will be briefly introduced and discussed in chapter 4.

Chapter 2. *Ex vivo* evaluation of a novel polyiodinated compound for early detection of atherosclerosis*

2.1 Introduction

CVD remains the leading cause of morbidity and mortality in Western countries [Lusis, 2000; Glass and Witztum, 2001]. Perhaps the major obstacles to significantly reducing the problems associated with the disease are the multifactorial nature of the disease and its slow and insidious development. While the management of CVD includes both prevention and treatment, strategies aimed at prevention are known to be more cost effective and beneficial than those focused on treatment of the disease at more advanced stages [Farquhar, 1995]. Successful prevention, however, depends on early assessment of individuals at great risk. Angiography, although the "gold standard" for diagnosis of atherosclerosis, is invasive, and it detects only advanced lesions since stenosis of the blood vessel is required for the technology. There are several noninvasive methods available clinically such as X rays, ultrasound, CT, MR, and nuclear scintigraphy, but they all have unique advantages and limitations [McConnell, 2000]. There remains a need for an effective and noninvasive diagnostic method for the early detection of atherosclerosis.

---

* Published in part in *Radiation Research* (Vol.160, No.4, pp460-466, 2003), Kang, Z., Scott, T. M., Wesolowski, C., Feng, L., Wang, J., Wang, L. and Liu, H.

Atherosclerosis is a long-term process developed in a complex inflammatory and hyperlipidemic environment [Lusis, 2000; Glass and Witztum, 2001]. It involves monocyte-macrophages in the arterial intima and the accumulation of lipids from LDL to form cholesteryl esters (CEs) enriched foam cells. It is known that macrophages express a scavenger receptor for modified LDL such as OxLDL and AcLDL [Voyta et al., 1984; Brown et al., 1980]. It has been found that accumulation of LDL in the arterial wall is increased in areas involved in lesions [Roberts et al., 1983; Poledne et al., 1986]. Use of this differential uptake of LDL as an approach to deliver radioimaging probes for the early detection of atherosclerotic lesions seems to be a valid rationale considering the critical role played by LDL in the early stage of atherogenesis. Furthermore, an imaging modality would theoretically permit the visualization of the lesion itself.

Although strategies of employing radiolabeled cholesterol for the detection of atherosclerosis have been investigated previously, the results suggested that the radiolabeled probes suffered from instability due to rapid enzymatic digestion in macrophages [DeGalan et al., 1988]. To overcome this limitation, in this study, we used a radioiodinated cholesterol analogue, ^{125}I-C2I, which was first synthesized in our lab [Xiao et al., 2003], as a radioimaging agent. ^{125}I-C2I was incorporated into AcLDL, a lesion-specific carrier, or prepared as a phospholipid emulsion formulation. The resultant ^{125}I-C2I/AcLDL and ^{125}I-C2I emulsion were examined for their potential to be used for the

detection of early atherosclerotic lesions in homozygous apoE/LDL receptor (LDLR) knockout mice. The double targeted mutant mice are associated with spontaneous elevations in plasma cholesterol level; when fed with normal chow diet, they develop atherosclerotic lesions closely-resembling those of humans [Ishibashi et al., 1994]. They have become the most frequently used animal models in recent atherosclerosis studies [Smith and Breslow, 1997; Dansky et al., 1999]. The rationale for studying ^{125}I-C2I emulsion, in addition to ^{125}I-C2I/AcLDL, was because lipid emulsion has been suggested to simulate chylomicron metabolism and thus can be internalized by macrophages including those involved in atherosclerotic lesions [Redgrave, 2001].

2.2 Materials and methods

2.2.1 Materials

Thin layer chromatography (TCL) was carried out on silica gel-60, F-254 polyethylene-backed plates (Fisher Scientific, Ottawa, ON, Canada). Sodium dodecyl sulfate polyacrylamide gel electrophoresis (SDS-PAGE) was performed on a Mini-PROTEAN® II Electrophoresis Cell (Bio-Rad Laboratories Ltd., Mississauga, ON, Canada). Sonication was executed with Virsonic Cell Disrupter Model 16-850 (VirTis Company Inc., Gardiner, NY, USA). Sephadex® G-25 (medium, from Amersham Biosciences, Quebec, Canada) gel filtration was carried out using a Poly-Pre®

chromatography column (Bio-Rad). Radioactivity was measured using an LKB-Wallac 1277 GAMMAMASTER automatic gamma counter (Wallac Oy, Turku, Finland).

Carrier free $Na^{125}I$ was purchased from NEN Life Science Products, Inc. (Guelph, ON, Canada). SDS-PAGE molecular weight standards and bovine serum albumin (BSA) were obtained from Bio-Rad. All other chemicals were from Sigma-Aldrich Canada Ltd. (Oakville, ON, Canada) unless otherwise indicated.

2.2.2 Preparation of ^{125}I-C2I

C2I was synthesized according to a method developed previously in this lab [Xiao et al., 2003] and radiolabeled with ^{125}I via an iodine exchange reaction in a pivalic acid melt [Weichert et al., 1986]. The ^{125}I-labeled C2I was purified by chromatography. The radiochemical purity of ^{125}I-C2I was determined by TLC using chloroform as the mobile phase in conjunction with AR-2000 Imaging Scanner (BIOSCAN, Inc., Washington, DC, USA).

2.2.3 Preparation of AcLDL

LDL was isolated from fresh human plasma obtained from healthy volunteers by sequential ultracentrifugation [Schumaker and Puppione, 1986] using a Beckman L8-M ultracentrifuge and 60/75 Ti rotors. All LDL preparations were dialysed at 4°C overnight against a buffer containing 0.3 mM EDTA, 150 mM NaCl and 50 mM Tris (pH 7.4). AcLDL was prepared by adding excess acetate anhydride and sodium acetate to the LDL

preparation obtained above [Basu et al., 1976], then subjected to 1% agarose gel electrophoresis. The protein integrity of AcLDL was examined using 6-20% gradient SDS-PAGE [Laemmli, 1970]. Protein concentrations were determined by the method of Bradford [Bradford, 1976] using a Bio-Rad protein assay kit with BSA as the standard.

2.2.4 Preparation of ^{125}I-C2I emulsion

^{125}I-C2I emulsion was prepared according to a previously published method [Xiao[1] et al., 1999]. In brief, a mixture of 12 mg L-α-phosphatidylcholine (PC), 8 mg DL-α-phosphatidylethanolamine dipalmitoyl (DPPE), 20 mg seal oil (Terra Nova Fishery, Newfoundland, Canada) and 10 mg ^{125}I-C2I in chloroform were dried under a nitrogen stream and re-suspended in 10 ml of saline. The suspension was then sonicated for 2 h at 0°C and centrifuged at 40,000 rpm for 7 h at 4°C. The emulsion that floated to the top of the centrifuge tube was collected and the radioactivity was determined. Emulsions were used for experiments within 5 days of preparation.

2.2.5 Preparation of ^{125}I-C2I/AcLDL

^{125}I-C2I/AcLDL was prepared by incubating ^{125}I-C2I emulsion with AcLDL obtained as described above at 37°C for 8 h after which ^{125}I-C2I/AcLDL was separated by ultracentrifugation. ^{125}I-C2I/AcLDL was then characterized by gel filtration [Xiao[1] et al., 1999; Xiao[2] et al., 1999]. Briefly, 500 µl ^{125}I-C2I/AcLDL preparation was loaded onto a Sephadex® G-25 chromatography column and eluted with phosphate buffered saline (pH

7.4). Fractions of 500 μl were collected, and radioactivity and protein content of each fraction were determined by gamma counter and the Bradford method, respectively. Results were then plotted.

2.2.6 Animal model and protocol

ApoE/LDLR knockout mice (B6;129-Apoe^{tm1Unc}Ldlr^{tm1Her} mice, female, age 7-8 weeks, average weight 22 g) were purchased from the Jackson Laboratory (Bar Harbor, MA, USA) and maintained on a normal chow diet during the whole study. They were randomly divided into two test groups: ^{125}I-C2I/AcLDL group (n = 10) and ^{125}I-C2I emulsion group (n = 6), and 3 extra mice were used for the examination of atherosclerotic lesions. C57 mice (n = 8, female, age 6~7 weeks, average weight 20 g) were kindly provided by Dr. C. Kovacs (Faculty of Medicine, Memorial University of Newfoundland) and used as a control. The animal study was reviewed and approved by the University's animal care committee. Blood samples were obtained from the retroorbital plexus every 4 weeks when the mice were anesthetized with inhalation of diethyl ether (BDH Inc., Toronto, ON, Canada), and plasma cholesterol levels were determined enzymatically with an assay kit from Sigma. After 8 weeks of feeding, early stage atherosclerotic lesions were found in the aortas of three apoE/LDLR knockout mice that were examined (age 15-16 weeks). Two weeks later, each animal (age 18~20 weeks) was anesthetized with inhalation of diethyl ether and then injected with ^{125}I-C2I/AcLDL (1.85 MBq/kg) or ^{125}I-

C2I emulsion (3.33 MBq/kg) via the tail vein. The mice were sacrificed humanely 24 h postinjection by over exposure to diethyl ether, and Zamboni's fixative (2% paraformaldehyde in 0.1M phosphate buffer with 15% v/v saturated picric acid, pH 7.2) was perfused through the heart. Various organs including liver, kidney, adrenal gland, spleen, lung, aorta, blood and thyroid were collected, and radioactivity associated with each sample was determined using a gamma counter. It should be noted that the radioactivity for the aorta was based on the weight of the entire aorta and that the specific radioactivity for just the plaque was not assessed.

2.2.7 *Ex vivo* aorta imaging

The aorta samples collected were further cleaned by removing the connective tissues and were fixed in Zamboni's fixative overnight. Then the aortas were stained with Sudan IV dye, and subsequently exposed to a Cyclone™ Phosphor Storage Screen (Packard Instrument Company, Inc., Meriden, CT, USA) at room temperature for 6-8 h following which the results were read by a Cyclone™ scanner.

2.2.8 Data analysis

Statistical analysis of the data was performed using a nonpaired Student's *t* test. A *p* value of 0.05 or less was considered to indicate a significant difference between the sets of data.

2.3 Results

A novel compound, C2I, was synthesized and labeled with ^{125}I. TLC scanning of the resultant product showed a radioactive peak at $R_f = 0.47$ which was identical to that of C2I (Figure 2.1). The radiochemical purity was found to be about 95%. ^{125}I-C2I emulsion was then prepared and its specific activity was 2.55 MBq/ml. Incubation of the ^{125}I-C2I emulsion with AcLDL resulted in ^{125}I-C2I/AcLDL (200 ^{125}I-C2I molecules per AcLDL particle). As shown in Figure 2.2, Sephadex® G-25 gel filtration of ^{125}I-C2I/AcLDL revealed that the profiles of radioactivity and protein absorbance were overlapped, indicating that ^{125}I-C2I was associated with AcLDL. The specific radioactivity of ^{125}I-C2I/AcLDL was 0.925 MBq/ml. Agarose gel electrophoresis results demonstrated that ^{125}I-C2I/AcLDL had a greater mobility than LDL (Figure 2.3), which is due to the increased negative charge on the surface of AcLDL [Hu et al., 2000]. When examined by 6-20% gradient SDS-PAGE analysis, the ^{125}I-C2I/AcLDL preparation exhibited a single apoB-100 band identical to that of LDL or AcLDL control. No other protein bands were found, suggesting that there was no protein degradation (Figure 2.4).

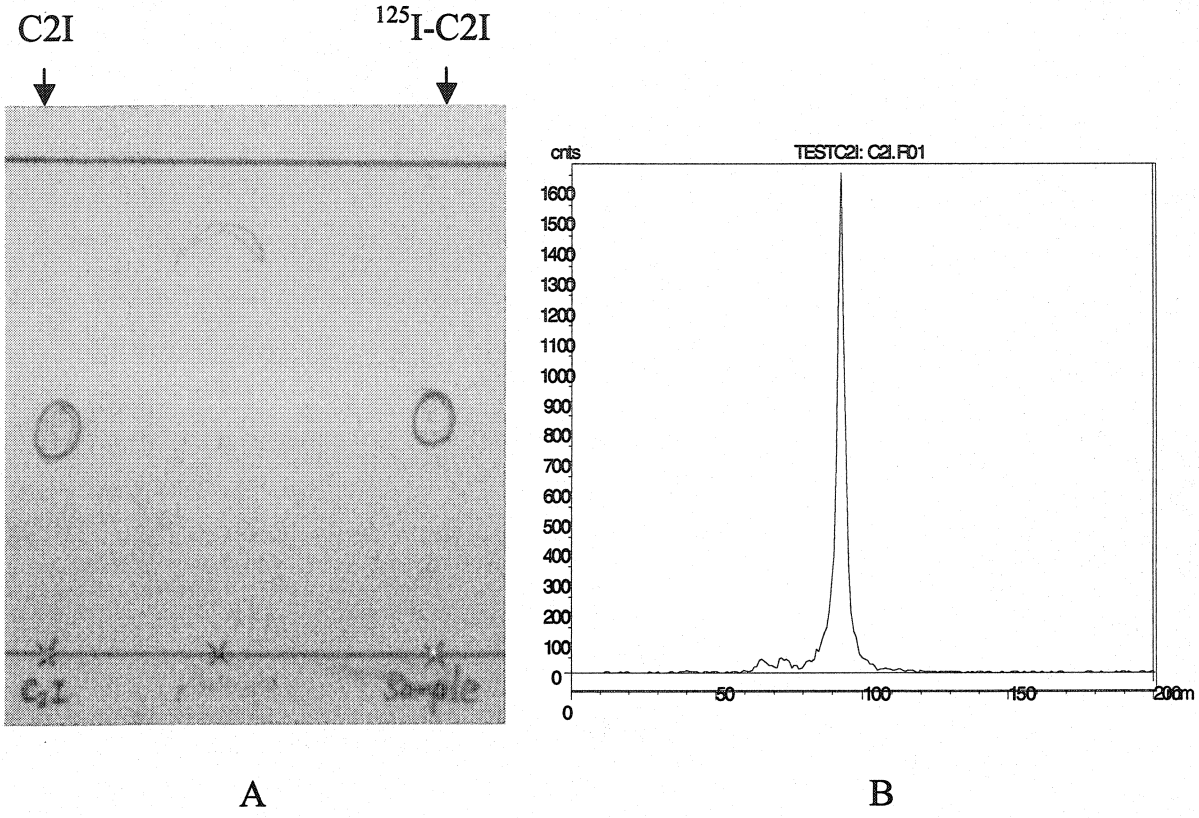

Figure 2.1. Chemical purity and radiochemical purity of ^{125}I-C2I. (A) TLC result of ^{125}I labeled C2I under a mobile phase of 100% chloroform (Rf = 0.47). (B) Radioactivity scanning of TLC plate A along the ^{125}I-C2I running direction showed the Rf value of the radioactivity peak was also 0.47, indicating that it was from the ^{125}I-C2I spot. The horizontal axis represents the height of the plate A and the vertical axis indicates the radioactivity counts per minute.

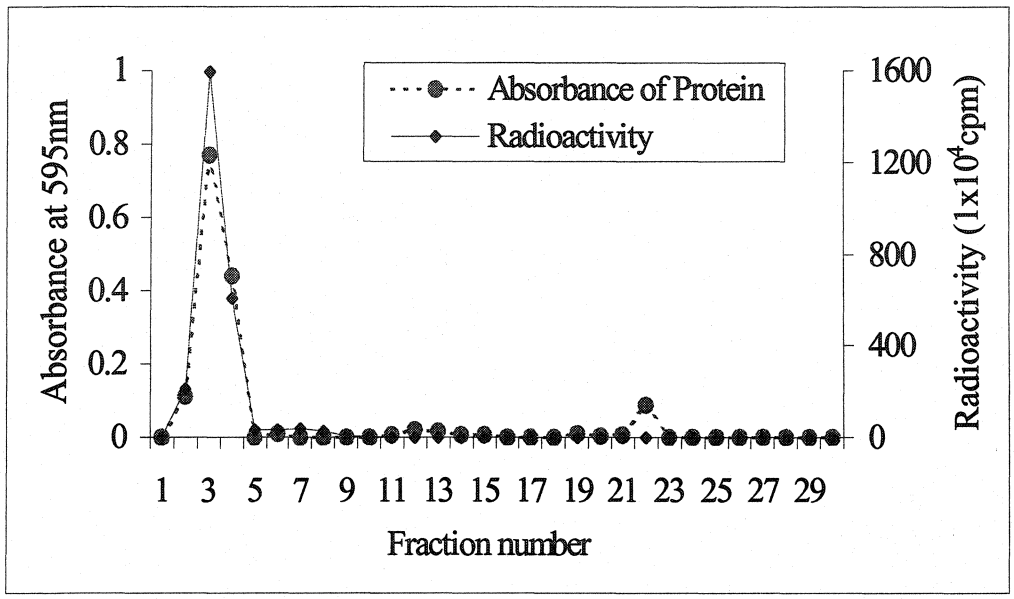

Figure 2.2. Chromatograms of gel filtration (Sephadex® G-25) of ^{125}I-C2I/AcLDL preparation with respect to its radioactivity and protein absorbance at 595 nm (the Bradford method).

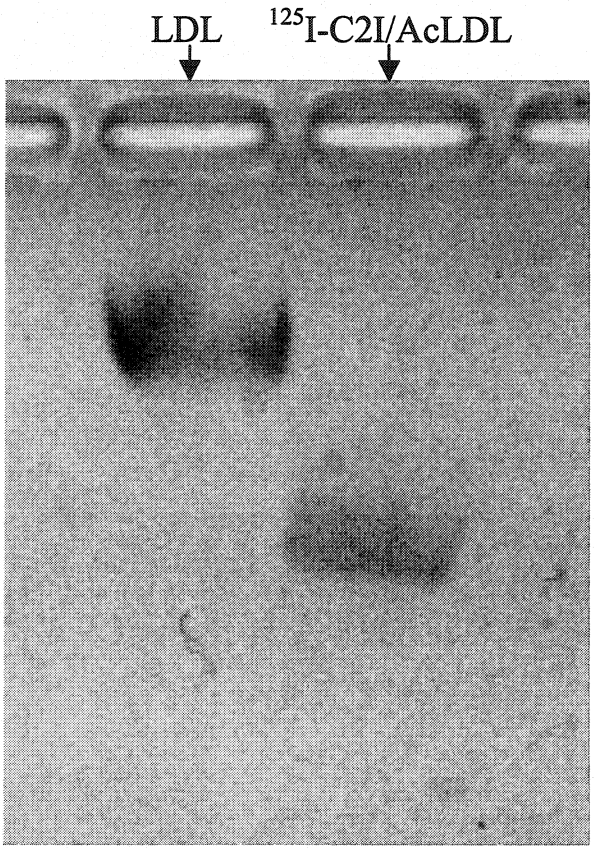

Figure 2.3. Agarose gel (1%) eletrophorosis of LDL and ^{125}I-C2I/AcLDL. The Coomassie blue-prestained samples were run in TBE buffer (89 mM Tris borate, 2 mM EDTA, pH 8.6) at 100 V for 30 min. ^{125}I-C2I/AcLDL showed a faster mobility than LDL due to the increased negative charge on the surface AcLDL.

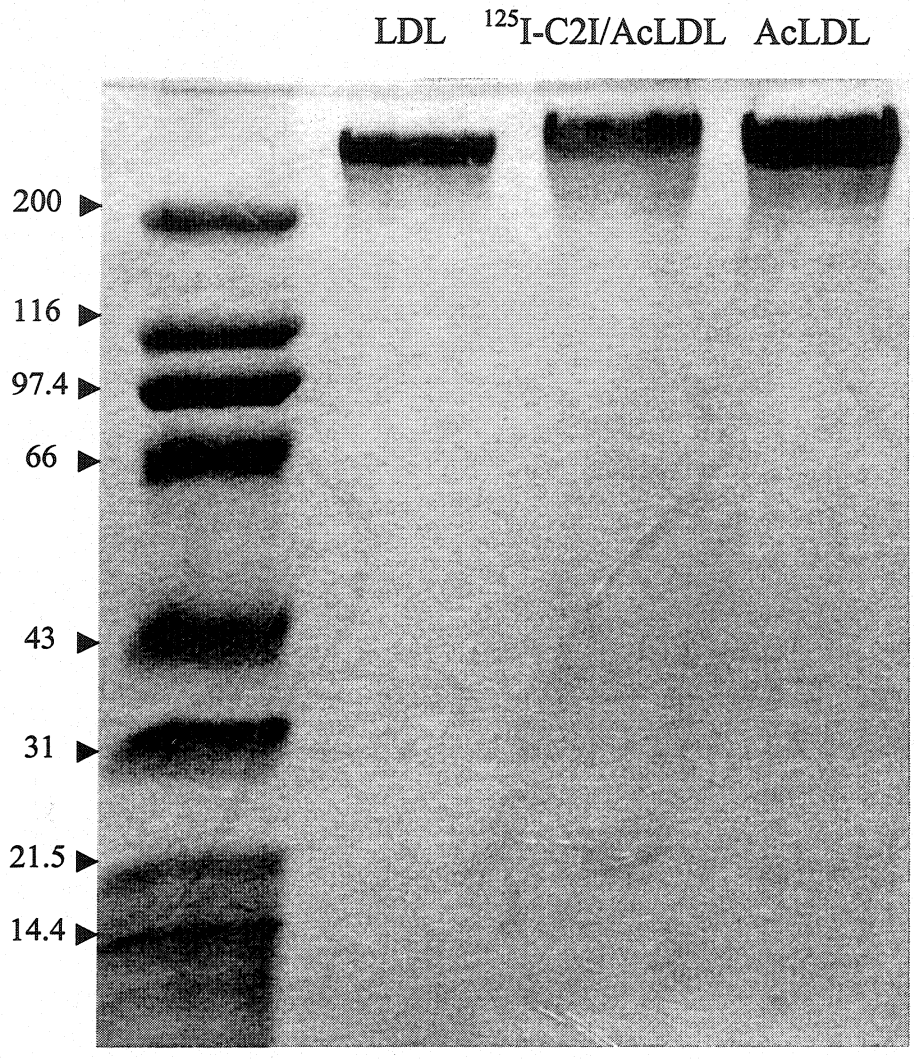

Figure 2.4. Gradient SDS-PAGE (6-20%) analysis of ^{125}I-C2I/AcLDL, AcLDL and LDL. Approximately 1-3 μg protein was loaded for each sample and electrophoresed at 200 V for 45 min. The separating gel was stained with Coomassie blue R250. The positions of a broad range of molecular weight standard (× kDa) are shown with arrow marks.

Both apoE/LDLR knockout and control C57 mice were maintained on a normal chow diet. Plasma cholesterol levels were determined and the results after 8 weeks of feeding are presented in Table 2.1. In comparison to the control group (2.95 mmol/L), the apoE/LDLR knockout mice demonstrated a 5 times higher cholesterol level (15.14 mmol/L), suggesting that atherosclerotic lesions were likely to have developed. Three mice were subsequently dissected and the aortas were examined under a microscope. It was confirmed that early stage atherosclerotic lesions had developed. Two weeks later, ^{125}I-C2I/AcLDL or ^{125}I-C2I emulsion was administered intravenously to both apoE/LDLR knockout mice (at age of 18~20 weeks) and control mice at 1.85 MBq/kg for ^{125}I-C2I/AcLDL and 3.33 MBq/kg for ^{125}I-C2I emulsion. Figures 2.5 and 2.6 illustrated the radioactivity found in various tissues 24 h postinjection of ^{125}I-C2I/AcLDL and ^{125}I-C2I emulsion, respectively. For both apoE/LDLR knockout mice and control mice, it was found that ^{125}I-C2I/AcLDL resulted in the highest accumulation in the adrenal gland followed by the liver, while ^{125}I-C2I emulsion produced the highest level of radioactivity in the liver followed by the spleen. It was also found that, after the administration of ^{125}I-C2I/AcLDL or ^{125}I-C2I emulsion, there was no statistical difference in the radioactivitiy of the liver, spleen, kidney, lung, adrenal gland and fat tissue between the apoE/LDLR knockout mice and control. However, the accumulation of radioactivity in the aorta and blood of the apoE/LDLR knockout mice was significantly higher than that in the control

group. The radioactivity in the aortas of the apoE/LDLR knockout mice was about 11 times higher than that of the control mice after administration of ^{125}I-C2I/AcLDL (1.3×10^4 *vs*.1.1×10^3 cpm/g tissue), and 4.5 times higher after administration of ^{125}I-C2I emulsion (2.4×10^5 *vs*. 5.3×10^4 cpm/g tissue). Table 2.2 summarized the radioactivity distribution expressed as percent of injected dose per gram of organ. It can be seen that ^{125}I-C2I/AcLDL resulted in a faster clearance from the body than ^{125}I-C2I emulsion 24 h after i.v. injection. Another tissue containing high concentration of radioactivity in both groups was found to be thyroid as expected, 3.6×10^6 or 4.1×10^5 cpm/g tissue following administration of ^{125}I-C2I emulsion or ^{125}I-C2I/AcLDL, respectively. As is common for radioiodine-containing reagent, thyroid levels were presumed to reflect the sequestration of radioiodide produced by low rate of metabolic deiodination of compound.

Table 2.1. Cholesterol levels in the blood of apoE/LDLR knockout mice (n = 19) and control C57 mice (n = 8) maintained on normal chow diet for 8 weeks (Average ± SE)

	Cholesterol level	
	apoE/LDLR knockout mice (n = 19)	control mice (n= 8)
mmol/L	15.14 ± 0.89	2.95 ± 0.16
mg/dL	584.7 ± 34.4	113.8 ± 6.1

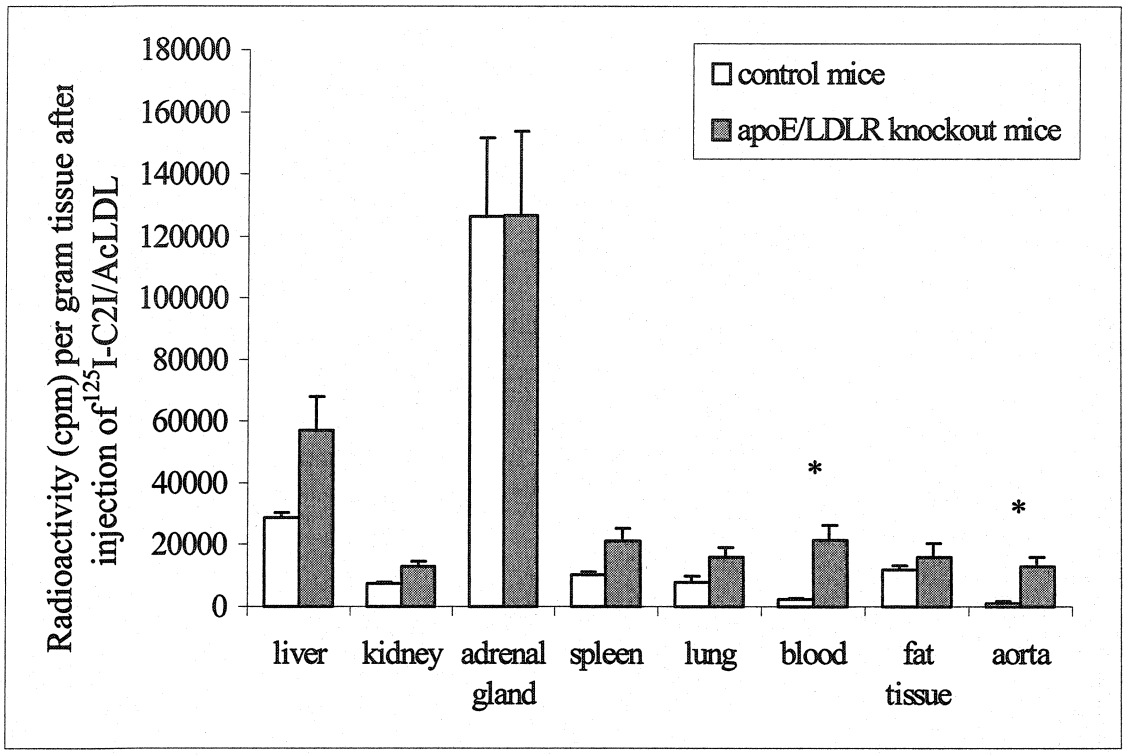

Figure 2.5. Radioactivity found in various organs 24 h after i.v. injection of ^{125}I-C2I/AcLDL at 1.85 MBq/kg in apoE/LDLR knockout mice (n = 10) and control mice (n = 4). Results shown are mean ± SEM (* $p < 0.05$).

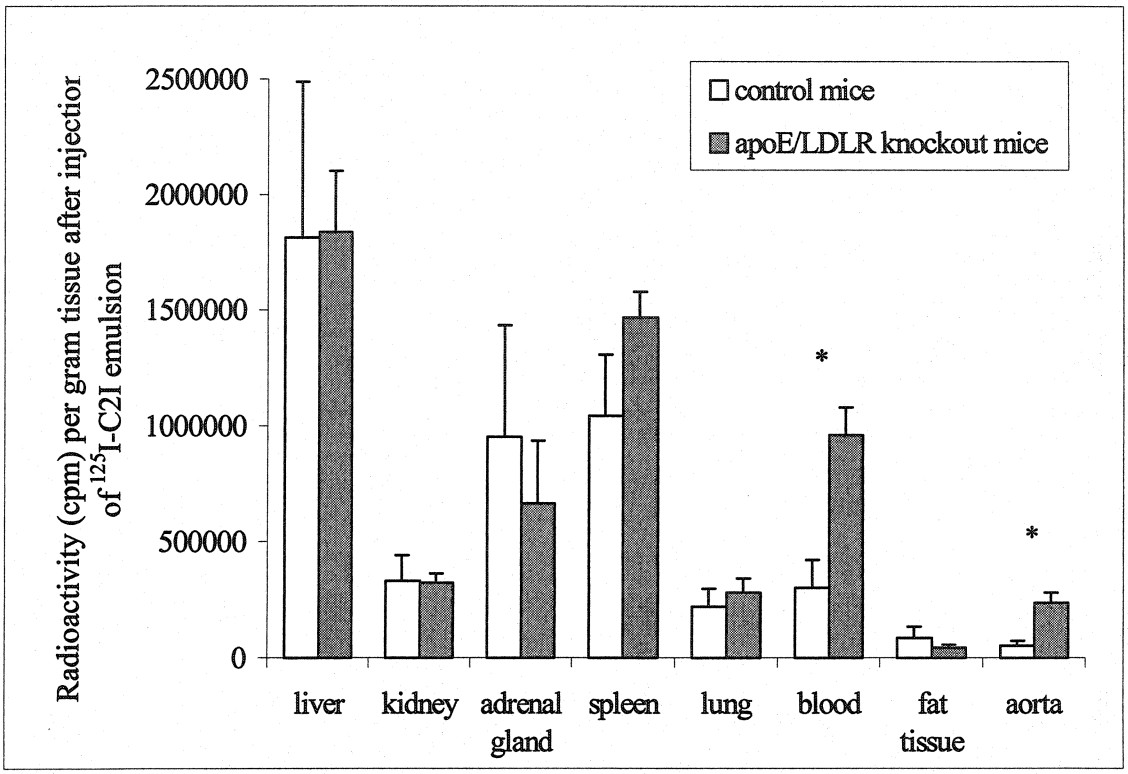

Figure 2.6. Radioactivity found in various organs 24 h after i.v. injection of ^{125}I-C2I emulsion at 3.33 MBq/kg in apoE/LDLR knockout mice (n = 6) and control mice (n = 4). Results shown are mean ± SEM (* $p < 0.05$).

Table 2.2. Biodistribution of radioactivity in various tissues expressed as % injected dose/g tissue 24 h after i.v. injection of 1.85 MBq/kg ^{125}I-C2I/AcLDL or 3.33 MBq/kg ^{125}I-C2I emulsion (Average ± SEM)

Tissue	^{125}I-C2I/AcLDL group (% injected dose per gram tissue)		^{125}I-C2I emulsion group (% injected dose per gram tissue)	
	apoE/LDLR knockout mice (n=10)	Control mice (n=4)	apoE/LDLR knockout mice (n=6)	Control mice (n=4)
liver	2.074±0.397	1.040±0.067	18.468±2.644	18.205±6.789
kidney	0.467±0.066	0.271±0.013	3.276±0.388	3.358±1.099
adrenal gland	4.603±0.984	4.594±0.923	6.700±2.731	9.589±4.832
spleen	0.770±0.151	0.374±0.034	14.755±1.095	10.481±2.639
lung	0.581±0.109	0.287±0.072	2.861±0.594	2.235±0.766
blood	**0.778±0.181***	**0.093±0.008**	**9.671±1.195***	**3.074±1.167**
fat tissue	0.584±0.160	0.434±0.045	0.464±0.109	0.851±0.524
aorta	**0.472±0.113***	**0.042±0.016**	**2.392±0.464***	**0.530±0.198**

* $p < 0.05$

Sudan IV staining of the aorta was performed in order to visualize the atherosclerotic lesions. The red lipid stain is an indication of lipid-laden foam cells, a hallmark of early atherosclerosis. The phosphorimages, which reflect the level of radioactivity, and the Sudan IV results for aortas are illustrated in Figure 2.7. It is clear that the accumulation of radioactivity in the aortas of apoE/LDLR knockout mice as revealed by phosphorimages was superimposed on the lesion identified by the Sudan IV staining. Both phosphorimaging and Sudan IV staining exhibited negative results for the aortas of the control mice: neither accumulation of radioactivity nor atherosclerotic lesions were present.

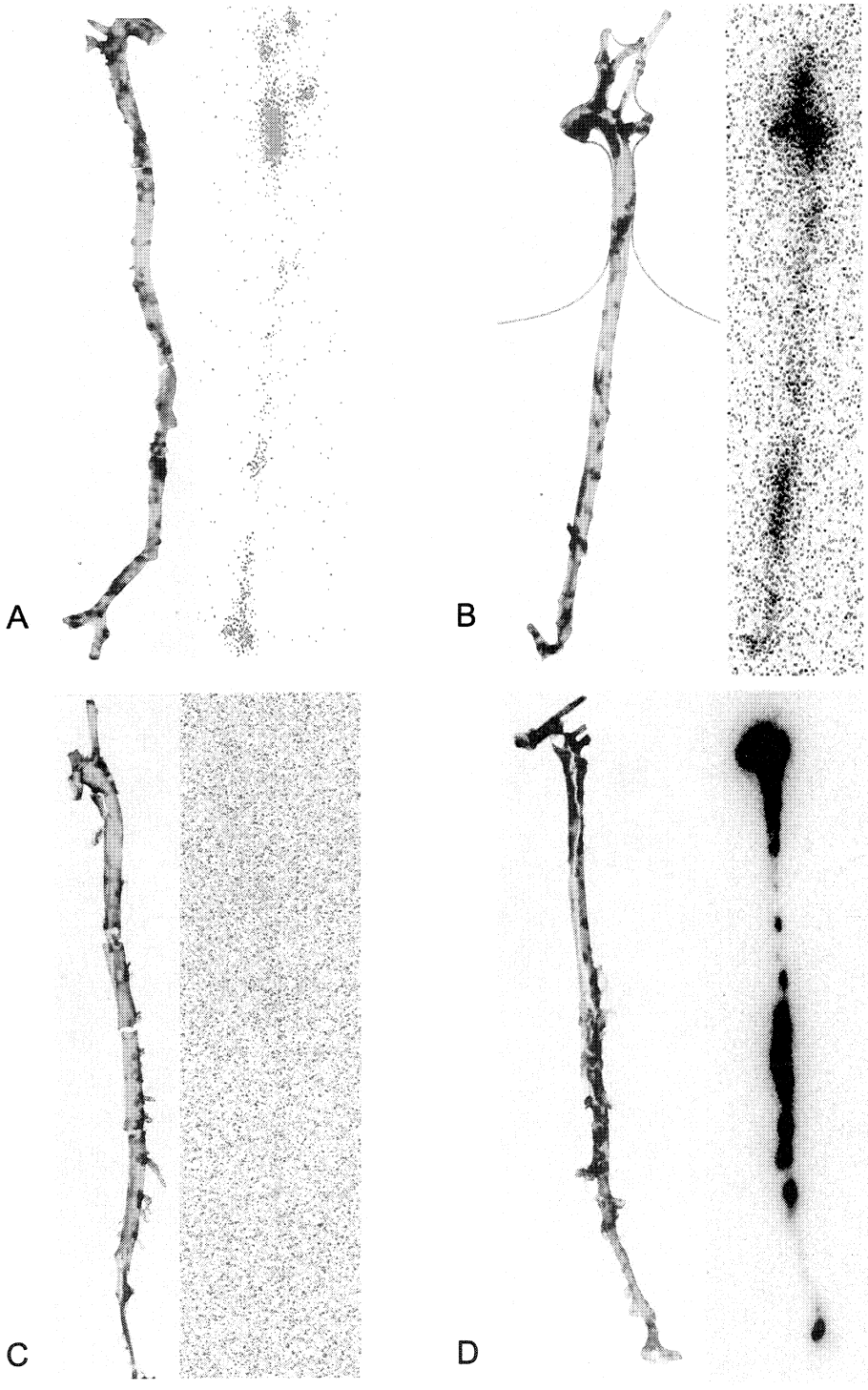
A
B
C
D

2.4 Discussion

It is now becoming clear that vulnerable atherosclerotic plaques are more closely associated with clinical acute coronary syndromes than vessel stenosis severity [McConnell, 2000; Cerqueira, 1999]. Hence, an earlier evaluation and intervention of atherosclerosis would be more effective in reducing the morbidity and mortality due to CVD. The atherosclerotic plaque prone to rupture is usually a modestly advanced lesion, not visible by traditional angiography [McConnell, 2000]. Therefore, reliable diagnostic technologies that can directly image atherosclerotic lesions or detect abnormalities of the vessel wall itself are urgently required. Radionuclide tracer imaging which takes advantage of targeted biological markers or specialized ligands appears to be one of the promising approaches for this purpose [Cerqueira, 1999]. It is known that macrophages play an important role in the formation of atheroslerotic lesions, thus modified LDLs, substrates of receptors present in macrophages, are considered to be promising. Previous studies have demonstrated the feasibility of using radiolabeled LDL or OxLDL as a tracer for experimental arterial lesions in animal models and human atheroslerotic plaques [Atsma et al., 1993; Lees et al., 1983; Lees et al., 1988; Iuliano et al., 1996]. However, when LDL or modified LDL is internalized into the targeted cells, it is rapidly degraded by lysosomal enzymes and then the radiolabeled protein residue is excreted, resulting in rapid clearance of the radiolabeled LDL or OxLDL from the lesion [Goldstein et al., 1979; Brown and Goldstein, 1983]. Attempts to overcome this problem have led researchers to study protein ligands that would remain in the cell once internalized [Pittman and Taylor, 1986]. Since CEs are a major component of the lipophilic core of LDL, ^{125}I-cholestryl

iopanoate (^{125}I-CI), a CE analog, studied earlier by Counsell *et al* [DeGalan et al., 1988; Deforge et al., 1992], has been incorporated into AcLDL and evaluated as an imaging agent for the detection of atherosclerotic lesions in a rabbit model [Xiao[2] et al., 1999]. In this work, C2I, a novel analogue of CI, was studied. Like CI, C2I also possesses an enhanced hydrophobicity and is resistant to hydrolysis by lysosomal enzymes in cells due to the presence of the ether bond in the molecule [Xiao et al., 2003]. Furthermore, C2I contains six iodines for radiolabeling, which is twice the number available with CI, and therefore allows labeling with a higher specific radioactivity. After promising results were obtained in rabbits [Xiao et al., 2003], we used apoE and LDLR double knockout mice in this study to evaluate its *in vivo* behavior when incorporated into AcLDL. In addition, we prepared a chylomicron-like emulsion of C2I using phospholipids and highly unsaturated triglyceride-rich seal oil as the core lipid components, and compared its lesion-seeking ability with C2I/AcLDL. Chylomicron is a type of triglyceride-rich lipoprotein responsible for transporting most dietary lipids from intestine to the blood. With a size range of 80-1000nm in diameter, it is rapidly cleared from plasma by lipolysis and remnants uptake [Spady, 1992]. Although the liver is the main organ for the uptake of chylomicron remnants, extrahepatic tissues including the arterial wall are also involved in its clearance possibly through a receptor-mediated process (endocytosis or phagocytosis), such as apoE-binding receptors and scavenger receptors [Redgrave, 2001; Terpstra et al., 2000]. It has been reported that there is a clear relationship between chylomicron metabolism and progression of atherosclerosis [Redgrave, 2001]. Emulsions with similar lipid composition and particle size as chylomicron will mimic its

metabolizing pathway after intravenous administration, therefore we expect this formulation to deliver the radioiodinated C2I to atherosclerotic lesions.

^{125}I-C2I emulsion used in the experiment was freshly prepared, which was essential due to its thermodynamic instability. During the incubation of emulsion with AcLDL, there was an exchange of lipid components between them, resulting in the incorporation of ^{125}I-C2I into AcLDL. The results from 1% agarose gel electrophoresis showed that the incorporation did not alter the integrity of AcLDL. As revealed by 6-20% SDS-PAGE, apoB-100 also remained intact, which is crucial for recognition of the particles by the scavenger receptor on the macrophages. When ^{125}I-C2I/AcLDL was examined by Sephadex® G-25 gel filtration, the radioactivity chromatogram was superimposed with that of protein, indicating that ^{125}I-C2I was either incorporated into or tightly associated with AcLDL. The lipophilicity of C2I was thought to have facilitated its incorporation into the LDL lipid core. However, the incorporation efficiency of C2I (200 molecules per AcLDL particle) was lower than that of CI (500 molecules per AcLDL particle) [Xiao^2 et al, 1999]. This could be attributed to the larger molecular size of C2I.

Gene targeting and transgenic technology have provided a series of mouse strains with a wide range of lipoprotein profiles and susceptibility to atherosclerosis [Smith and Breslow, 1997; Dansky et al., 1999]. In this study, apoE/LDLR double knockout mice that are prone to the development of atherosclerotic lesions were used as an animal model. After 8 weeks on normal chow diet, the plasma cholesterol level of apoE/LDLR knockout mice (age 15-16 weeks) was 5 times as high as that of the control mice, and a few fatty streaks were already present at the aortic arch and branch points. Two weeks

later, ^{125}I-C2I/AcLDL or ^{125}I-C2I emulsion was injected into mice (at 18-20 weeks of age). A higher radioactivity dose of ^{125}I-C2I emulsion was used, because the targeting specificity of the emulsion formulation was estimated to be lower than that achieved from using ^{125}I-C2I/AcLDL. Tissue biodistribution studies performed 24 h after administration demonstrated that both ^{125}I-C2I/AcLDL and ^{125}I-C2I emulsion were effective in targeting the early atherosclerotic lesions. Although the preparation process was more laborious, ^{125}I-C2I/AcLDL, as we anticipated, showed better specificity than the emulsion. The radioactivity levels accumulated in the aorta of the atherosclerotic apoE/LDLR knockout mice following administration of ^{125}I-C2I/AcLDL and ^{125}I-C2I emulsion were 11 and 4.5 times those found in the aorta of the control mice. A significant amount of radioactivity was also found in the blood of apoE/LDLR knockout mice, which can be explained by their elevated blood cholesterol levels. The strong blood signal would likely provide a large background for *in vivo* detection. However, it should be noted that although the aorta appeared to contain a lower level of radioactivity than blood, the specific radioactivity in the atherosclerotic lesion, which occupied less than 25% of the aorta, would be at least four times as high as that of the aorta. Consequently, the specific radioactivity in the lesion would be higher than that found in the blood following administration of ^{125}I-C2I/AcLDL, while the specific radioactivity in the lesion after administration of ^{125}I-C2I emulsion would be similar to that found in the blood. Even so, it is still important to study the blood clearance profile of ^{125}I-C2I in order to determine the appropriate time interval to perform the *in vivo* detection after administration of the radioimaging agent. An ideal time interval would be the time when the ratio of radioactivity in the suspected lesion to that in the blood is maximum or when there is

enough radioactivity accumulated in the suspected lesion and little radioactivity still in the blood. Further studies are required to address the above concern. Our results also indicated that significant amounts of radioactivity were presented in adrenal and liver following administration of ^{125}I-C2I/AcLDL. While it is known that the liver, being rich in scavenger receptors, can rapidly remove AcLDL [van Berkel et al., 1995], it is unclear what mechanisms are involved in the uptake of ^{125}I-C2I/AcLDL by the adrenal gland, one of the steroid hormone-secreting tissues, especially when LDLR is deficient. Following administration of ^{125}I-C2I emulsion, the highest level of radioactivity was found in the liver as expected, since the liver is the main organ responsible for the metabolism of chylomicrons. As for the elevated level of radioactivity found in thyroid, which is a common drawback of all radioiodine-containing tracers, "cold" iodide such as NaI can be pre-administered prior to the proposed radioimaging agent in order to saturate the iodine-uptaking capacity of thyroid.

Sudan IV staining was employed to reveal the gross distribution of atherosclerotic plaques. As shown in Figure 2.7, foamy cell lesions were formed throughout the arterial tree which is similar to that seen in human atherosclerosis. Histological examinations showed plaques of foam cells, cholesterol clefts and lipid pools, which resembled moderate human lesions (Figure 2.8). The radioactivity images of aorta samples revealed by *ex vivo* scanning using a phosphorimager were superimposed on the results from Sudan IV staining, suggesting that ^{125}I-C2I/AcLDL and ^{125}I-C2I emulsion selectively deposited C2I at the atherosclerotic regions. ^{125}I-C2I was able to remain at the lesions, presumably because of the presence of the ether bond in the molecule of C2I which is resistant to lysosomal hydrolysis. If an appropriate radioisotope such as ^{123}I is used as a

substitute for ^{125}I, the lesions could be visualized externally using appropriate imaging equipment.

In summary, the results obtained in this study are promising. The selective uptake and retention of a radiolabeled polyiodinated probe, ^{125}I-C2I, to early atherosclerotic lesions have been accomplished by using AcLDL or chylomicron-like emulsion as a delivery system. However, more studies are required to address a number of concerns. For example, the blood clearance of the radioactive probe and the optimal time interval for achieving the maximum target-to-background ratio are yet to be determined. Moreover, not all vulnerable plaques may be imaged with the radiolabeled cholesterol analogue because some rupture-prone lesions contain a thin fibrous cap and lack lipid pool. In addition, nuclear imaging has a relatively low spatial resolution (5-10 mm), which will pose a significant challenge to resolve some subclinical atherosclerotic lesions (often < 1 mm diameter) compared to the much large blood-filled vascular lumen (20-30 mm diameter in the aorta, 3-4 mm thick in the coronary arteries).

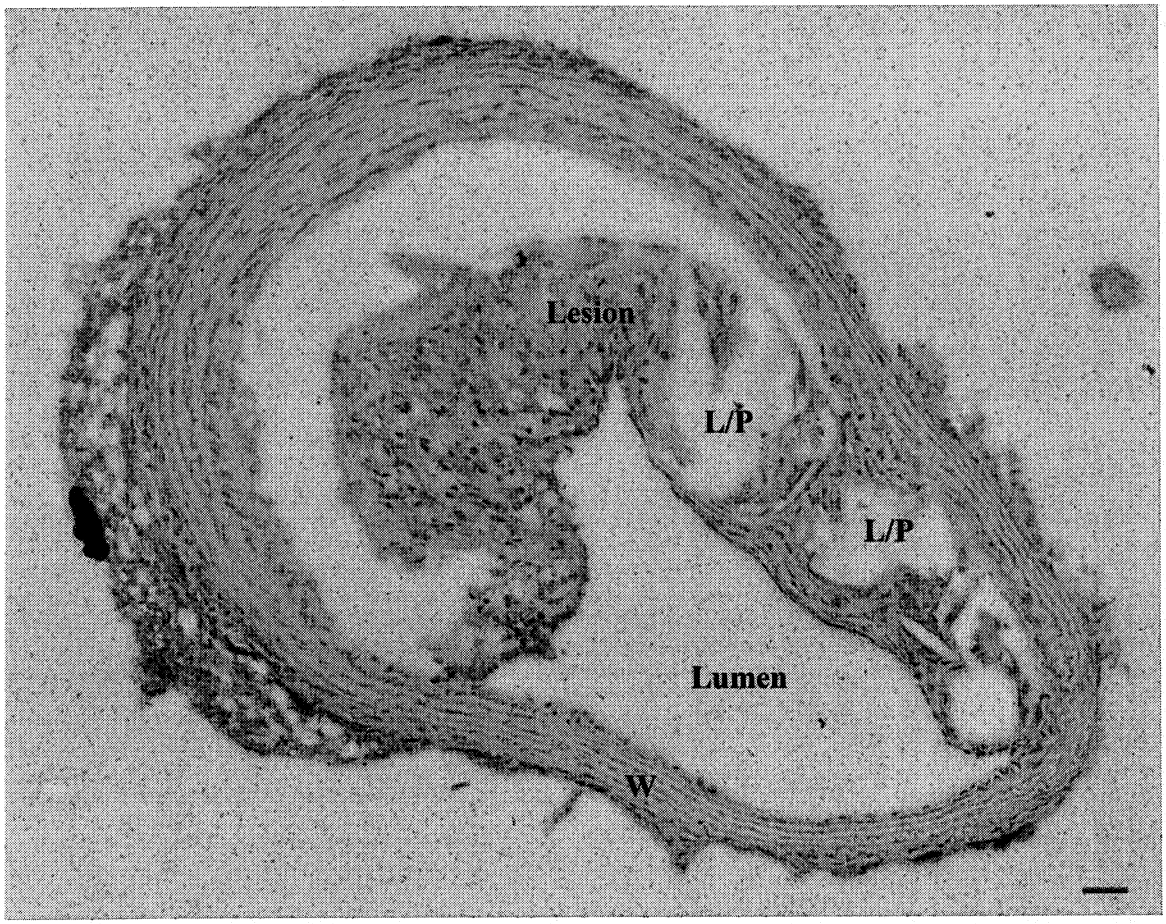

Figure 2.8. Light micrograph (×100) of a cross section of an Hematoxylin and Eosin (H&E) stained atherosclerotic lesion from the aortic arch of an apoE/LDLR knockout mouse. Lesion part, containing foam cells, cholesterol clefts, and lipid pools (L/P), peeled off from the wall (W) of the aorta during the preparation process of the sample. The bar represents 100 μm.

Chapter 3. *In vitro* gene transfection by malaria peptide targeted cationic liposome/protamine/DNA (LPD) complexes

3.1 Introduction

Gene therapy, a new pharmacotherapeutical concept, originally addresses the root causes of many genetic disorders by replacing the defective or missing genes with correct genes and subsequently expressing functional proteins [Crystal, 1995; Jain, 1998; Ledley, 1996]. However, it has long been postponed by the lack of appropriate carriers or vehicles used to deliver therapeutic genes into the right cells/tissues/organs. In order to achieve successful gene therapy, there are at least two delivery systems being examined as carriers: viral and non-viral vectors. Although viral vectors are highly efficient, they usually cause a number of safety problems, such as immune responses, inflammatory reactions, potential recombination or complementation and other toxicities. In addition, it is difficult to make large quantity of viral vectors [Scherman et al., 1998]. Non-viral vectors, on the other hand, are safer and easier to make although they have lower transfection efficiency than viral vectors. The advantages of using non-viral vectors, especially cationic liposomal systems, have recently attracted more research efforts on their development [Scherman et al., 1998; Pedroso de Lima et al., 2001]. LPD complex is one of the widely employed formulations showing great potential in the area of gene therapy [Li et al., 2000]. However, both viral and non-viral vectors lack homing devices to direct DNAs to the specific organ(s) upon direct *in vivo* administration. The

distribution of the delivered genes is generally throughout the whole body of experimental animals [Zhu et al., 1993; Templeton et al., 1997]. Targeted delivery thus needs to be explored to achieve greater gene expression in specific organs and to minimize adverse effects.

Malaria sporozoites enter into human liver just a few minutes after mosquito biting. The speed of infection and target cell selectivity suggest that the invasion is mediated by specific ligand-receptor endocytosis. The major surface protein of malaria parasites (*Plasmodium falciparum*), the circumsporozoite (CS) protein, contains two conserved domains (region I and II) and a domain from CS II was found to be implicated in the selective binding to mammalian hepatocytes [Cerami et al., 1992; Chatterjee et al., 1995]. In this study, we hypothesized that LPD coupled with the peptide derived from CS II would be specifically delivered to the liver after intravenous administration. A palmitoylated 24 amino acid malaria peptide was thus designed according to the published sequence [Cerami et al., 1992; Suarez et al., 2001] (Figure 3.1A). The fatty acid moiety is used to serve as a lipid-chelating anchor. To investigate the transfection ability of this peptide-LPD complex *in vitro*, a plasmid bearing chloramphenicol acetyltransferase (CAT) or enhanced green fluorescent protein (EGFP) encoding reporter gene was used to prepare LPD and then examined in cultured HepG2 (human hepatoma cell line) and Hela cells (human cervical carcinoma cell line, as a control). CAT-LPD preparations with or without the peptide were also injected into wild-type mice as a preliminary evaluation of feasibility of their use for *in vivo* transfection.

Figure 3.1A. Sequence of the palmitoyl derivative of modified peptide (24 amino acids) derived from the domain II of circumsporozoite protein (CS) of malaria parasites (*Plasmodium falciparum*).

The ultimate objective of this project, although beyond the work conducted in this chapter, is to deliver the mouse LDLR (mLDLR) gene to the liver of LDLR-knockout mouse, an animal model closely resembling human FH conditions. FH is one of the most prevalent genetic diseases, and is characterized by a high level of plasma cholesterol and premature atherosclerosis. The culprit is the malfunction of LDLR resulting from a mutation in the gene specifying it [Goldstein et al., 2001]. Normally, LDLR is expressed mainly on the surface of hepatocytes (constituting more than 70% of the body's LDLR) and plays a critical role in the mechanisms underlying the homeostasis of cholesterol. Gene therapy is an ultimate way for the treatment of FH. It has been shown in clinical trials to be useful in lowering plasma cholesterol and reducing atherosclerosis risk, but still needs further study to obtain practical, satisfactory results, especially with respect to the safety concerns of viral delivery systems [Kawashiri and Rader, 2000]. The success of the *in vivo* delivery of the malaria peptide-LPD complex (D = LDLR gene) and subsequent expression of LDLR is expected to correct the elevated plasma cholesterol

level of LDLR knockout mice. Positive results might render the malaria peptide-LPD complex as a promising non-viral delivery alternative for the gene therapy of FH.

3.2 Materials and methods

3.2.1 Materials

1,2-diolelyl-3-trimethylammonium-propane (DOTAP, Figure 3.1B) and mini-extruder including different sizes of polycarbonate membranes were purchased from Avanti Polar Lipids (Alabaster, AL, USA). Protamine sulphate Grade X from salmon, cholesterol, Dulbecco's Modified Eagle's Medium (DMEM) and 1× trypsin-EDTA solution were obtained from Sigma-Aldrich Canada Ltd. (Oakville, ON, Canada). Fetal bovine serum (FBS) was purchased from Hyclone (Logan, UT, USA) and the antibiotics were from Mediatech, Inc. (Herndon, VA, USA). Chloroform and N,N-dimethylformamide (DMF) were obtained from Fisher Scientific (Ottawa, ON, Canada). CAT ELISA (enzyme linked immunosorbent assay) kit was purchased from Roche Diagnostics (Laval, Quebec, Canada). Bio-Rad (Mississauga, ON, Canada) DC (detergent compatible) protein assay reagent was used to determine protein concentration. The palmitoylated malaria peptide derivative was synthesized by Genemed Synthesis, Inc. (San Francisco, CA, USA). The oligonucleotide primers used in the preparation of plasmids were synthesized by Operon, a Qiagen company (Alameda, CA, USA).

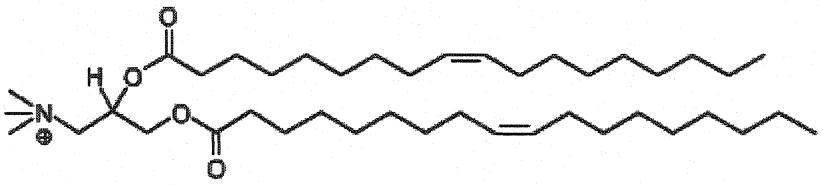

Figure 3.1B. Structure of 1,2-diolelyl-3-trimethylammonium-propane (DOTAP).

3.2.2 Cell culture

HepG2 cells and Hela cells were generously provided by Dr. T. Michalak and Dr. A. Pater (Faculty of Medicine, Memorial university of Newfoundland), respectively. They were maintained in DMEM supplemented with 10% FBS, 100 IU/ml penicillin and 100 mg/ml streptomycin at 37°C with 5% CO_2.

3.2.3 Construction and purification of reporter gene plasmid

CAT cDNA fragment (657 bp) was released from pBlueBac4.5/CAT (Invitrogen Canada Inc., Burlington, ON, Canada) with endonuclease HindIII and subcloned into a mammalian expression vector pcDNA3.1(-)/Myc-HisA (Invitrogen). The positive clone was screened and examined by EcoRI digestion, then amplified in TOP10 strain of *E. Coli*. A QIAGEN Plasmid Mega kit (Valencia, CA, USA) was used to isolate and purify CAT plasmid according to the manufacturer's instruction. EGFP plasmid was a kindly gift from Dr. K. Mearow (Faculty of Medicine, Memorial University of Newfoundland).

All final plasmids were kept in TE buffer (Tris-HCl 10 mM, EDTA 1 mM, pH 8.0) at –20°C.

3.2.4 Preparation of cationic liposome

DOTAP-cholesterol liposome (1:1 molar ratio) was prepared according to the method described by the L. Huang group [Li et al., 2000] with minor modification [Templeton et al., 1997]. Briefly, the lipid mixture was dissolved in HPLC-grade chloroform in a 50 ml round-bottomed flask and dried under vacuum using a rotary evaporator for 30 min. The thus formed thin lipid film was further desiccated under 30 mmHg vacuum for 1 h. The residue was then re-suspended with 5% dextrose water (D5W) and vortexed. The final concentration of DOTAP was 10 mg/ml. The hydrated lipid suspension was rotated at room temperature for 50 min and kept under argon overnight for aging. After 5 min low-frequency sonication (Branson 5200, Branson Ultrasonics Corporation, Danbury, CT, USA) and 10 min heating at 50°C, the lipid suspension was sequentially extruded through polycarbonate membranes with decreasing pore sizes of 0.6, 0.2 and 0.1 μm using a mini-extruder. The obtained liposome was kept under argon gas at 4°C.

3.2.5 Preparation of cationic liposome/protamine/DNA (LPD) complex

Two slightly different methods were used to prepare LPD. First, LPD was prepared as described by a published protocol [Li et al., 2000; Templeton et al., 1997] with minor modification. In brief, the liposome obtained above was mixed with small volume of protamine (5 mg/ml stock in D5W) and the mixture was incubated for 5 min at room temperature. CAT or EGFP plasmid (0.65 mg/ml) was diluted in equal volume of

D5W and then gently added to the liposome-protamine solution. The mixture was incubated at room temperature for 20 min to form LPD complex (1 μg DNA : 0.6 μg protamine : 8.4 μg DOTAP / 3.4 μl volume), which is referred as LPD(a). The LPD(a) samples were subjected to negative stain electron microscopy (EM) examination. LPD was also prepared by the following method. Liposome-protamine mixture and plasmid were respectively diluted in large equal volume of serum/antibiotics-free DMEM first, and then combined together, followed by 20 min incubation at room temperature (under the same ratio as the above in a final volume of 100 μl). The LPD prepared by the second method is referred as LPD(b).

3.2.6 Preparation of complexes of LPD coupled with the palmitoylated malaria peptide

LPD was coupled with the palmitoylated malaria peptide by the following two different methods: (I) Peptide dissolved in DMF (100 μg/μl) was diluted using D5W and added to the LPD(a) preparation at different ratios (0.5, 1, 2, 5, 10 μg peptide/ 1 μg DNA) with final DMF concentration less than 1% (v/v). The mixture was slowly mixed using a pipette tip and incubated at room temperature for 15 min to obtain a peptide-LPD complex referred as LPD-pep; (II) Peptide was introduced to liposome during the hydration step in the preparation of the liposome. As described in section 3.2.4, after thin lipid film was formed and dried, D5W mixed with the peptide in DMF was added and vortexed. The liposome-peptide suspension was then extruded and proceeded with the same procedures as those for LPD(a) or LPD(b); the thus prepared complex is referred as L-pep-PD(a) or L-pep-PD(b) (DNA = CAT). The final ratio of peptide in these L-pep-PD

preparations was 1 μg peptide / 1 μg CAT DNA. DMF-LPD complexes without peptide were also prepared as a control using the above protocols.

3.2.7 Characterization of liposome and LPD complex

The particle size and zeta-potential of cationic liposome or LPD preparations were determined by four-angle dynamic laser light scattering using a Coulter® Delsa 440SX zeta potential analyzer (Beckman Coulter Inc., Miami, FL, USA). The samples were diluted with deionized water (1:200, v/v) and three successive size determinations were made on each sample.

3.2.8 *In vitro* transfection

All the following transfection experiments were done in antibiotic-free DMEM. HepG2 cells (3×10^5 cells/well) and Hela cells (1×10^5 cells/well) were seeded into a 24-well plate with DMEM containing 10% FBS. When they were 85-95% confluent after 36 h, culture medium was changed to 300 μl FBS-free DMEM, and LPD or malaria peptide-LPD preparations were added (1 μg DNA/well) and incubated for 6-8 h. Then cells were washed 3 times with phosphate buffered saline (PBS, pH=7.4) and incubated in DMEM containing 10% FBS. Thirty-six hours later, cells transfected with CAT plasmid were lysed with 300 μl lysis buffer provided in CAT ELISA kit and the protein concentration was determined by Bio-Rad DC protein assay. Expression of CAT protein was measured by a CAT ELISA kit according to the manufacturer's instruction. For EGFP transfection, harvested cells were fixed by 1% paraformaldehyde-PBS solution and examined by flow cytometry. The percentage of transfected cells expressing EGFP-associated fluorescence was analysed by WinMDI software (by Joseph Trotter).

The transfection experiment was also performed in 300 µl DMEM containing 10% FBS for 24 hrs instead of in serum-free medium.

3.2.9 *In vivo* delivery and gene expression

Three 6-week-old C57BL/6 mice (female, ~ 20g) provided by Dr. C. Kovacs (Faculty of Medicine, Memorial University of Newfoundland) were used in this very preliminary *in vivo* experiment. Two mice were injected via the tail vein with 85 µg CAT gene formulated in LPD(a) in a total volume of 200 µl using a 27-gauge syringe needle, and one mouse was injected with the same amount of LPD coupled with 35 µg malaria peptide in LPD-pep formulation. Forty-eight hours following i.v. injection, the mice were sacrificed by over-exposure with diethyl ether, and heart, lung, liver, spleen, kidney, pancreas, small intestine, adrenal gland, bone marrow, and skeleton muscle were collected. The organs were washed with cold saline and quickly frozen with liquid nitrogen. Tissue extracts were prepared by homogenization of respective tissues in lysis buffer (0.05% Triton X-100, 2mM EDTA, 0.1 M Tris, pH 7.8) using a PELLET PESTLE® mixer (Kimble/Kontes, Vineland, New Jersey, USA) followed by 30 min incubation on ice. The homogenates were then centrifuged at 14,000g for 10 min at 4°C. The supernatant was assayed for CAT activity using a CAT ELISA kit and protein content was determined as described above.

3.2.10 mLDLR cDNA cloning and construction into an expression vector

Complete mLDLR cDNA was amplified by RT-PCR from C57BL/6 mouse liver RNA using the following primers: 5'-GATCCAGTGTTTGCAGCGGG-3' and 5'-CGAATTTCAAGCACAGCCAGTAGC-3'. Amplification products were then cloned

into a TA vector pCRII (Invitrogen). Automatic DNA sequencing was performed by Sick Children Hospital (Toronto, ON, Canada). The primers designed for sequencing were:

mLDLRseqM1: 5'-GATCCTCACTGTGCTTCG-3'

mLDLRseqP1: 5'-GATGGCAAGTGCATCTCC-3'

mLDLRseqP2: 5'-TTTGGACAACAATGGTGG-3'

mLDLRseqP3: 5'-AAGGGCGTAAAGAGGAGG-3'

The mLDLR nucleotide sequence and deduced amino acid data were directly submitted to the Genebank (accession number AF425607). The complete cDNA of mLDLR was then released from pCRII vector through XhoI-HindIII restriction endonuclease digestion and subcloned into an eukaryotic expression vector pcDNA3.1(-) /Myc-HisA (Invitrogen).

3.3 Results

3.3.1 Construction of CAT plasmid

Figure 3.2A shows the scheme of the structure of CAT plasmid. Approximately 657 bp CAT cDNA fragment which contains endonuclease EcoRI was inserted into a mammalian expression vector pcDNA3.1(-)/Myc-HisA at the HindIII site. As shown in Figure 3.2B, successful construction of CAT plasmid was demonstrated by the restriction endonuclease EcoRI digestion analysis. Six colonies of CAT plasmid minipreps were examined by 1% agarose gel electrophoresis stained with ethidium bromide (EtBr) after EcoRI digestion. It was found that colonies #2, 4, and 6 were positive with right orientation of CAT insertion. Colonies #1 and 3 were positive but with reverse

orientation of CAT insertion. Colony #5 was negative. Clone #4 was then chosen to be amplified and purified to prepare LPD.

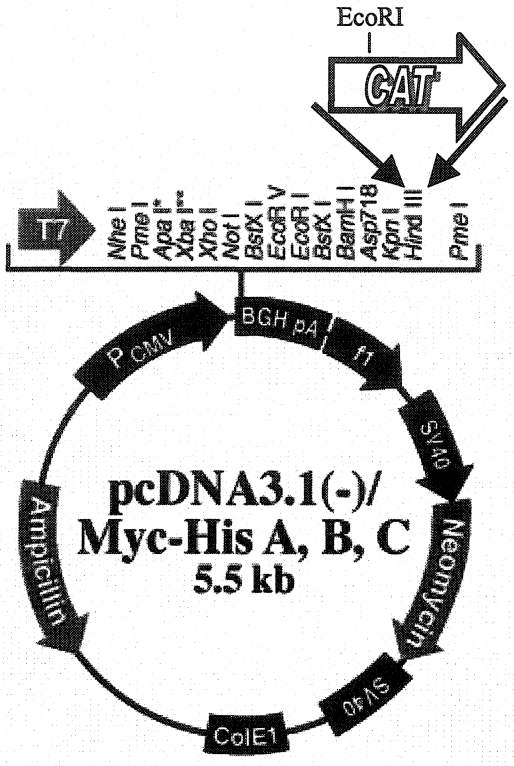

Figure 3.2A. Construction scheme of CAT eukaryotic expression plasmid. CAT gene was released from pBlueBac4.5/CAT with endonuclease HindIII and subcloned into the mammalian expression vector pcDNA3.1(-)/Myc-HisA.

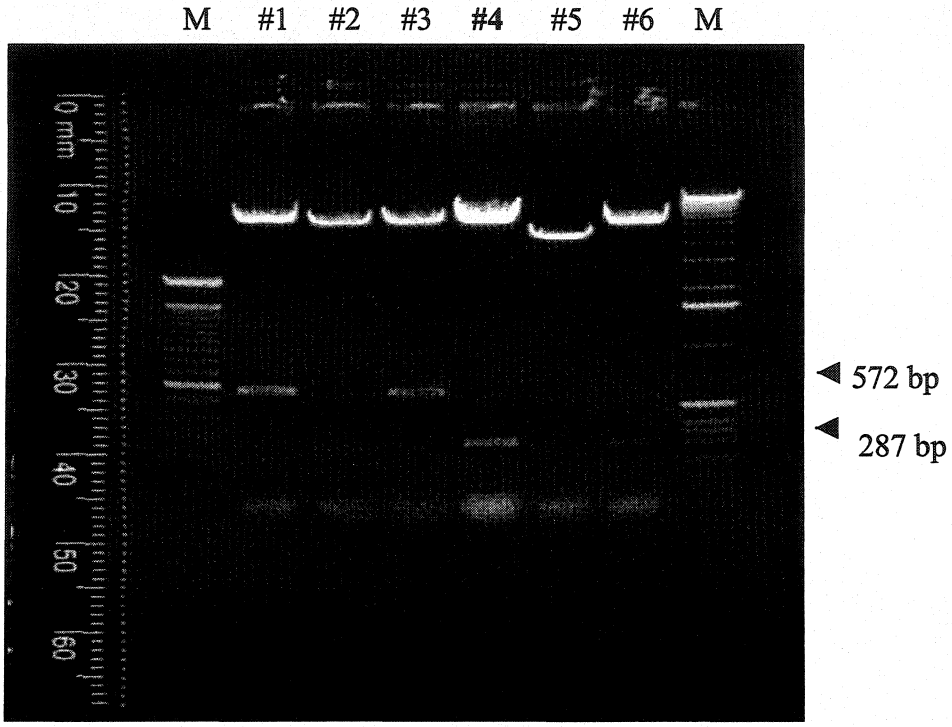

Figure 3.2B. Restriction enzyme (EcoRI) digestion analysis of CAT plasmid minipreps with 6 colonies. The 1% agarose gel was stained with EtBr and visualized under UV.

- Colonies #2, 4, 6 were positive with right orientation of CAT insertion and clone #4 was amplified to prepare LPD.
- Colonies #1, 3 were positive but with reverse orientation of CAT insertion.
- Colony #5 was negative.

3.3.2 Characterization of LPD preparations

DOTAP-cholesterol liposome and LPD were prepared, following which the size and zeta-potential of the resultant particles were measured. As shown in Table 3.1, after final extrusion through 0.1 μm-pore size membrane, the size of cationic liposome was found to be about 130 nm and the zeta-potential was 43 mv. When kept at 4°C for 10 weeks, the particle size of liposome stayed almost unchanged, indicating relatively higher stability of cationic liposomes compared to the traditional liposomes (stable only for 3-4 days). LPD formulation showed an average particle size of 430 nm which was somewhat bigger than that (135 nm) reported by the L. Huang group [Li et al., 1998], indicating that aggregation might have occurred with our LPD preparations despite the use of the suggested ratio of lipid, protamine and DNA. The zeta potential of LPD was found to be 26 mv, which represented a positive charge carried by final particles.

Electron micrographic analysis of the LPD(a) preparation showed similar morphology as reported in the literature [Li et al., 2000]. As seen in Figure 3.3, the LPD preparation is heterogeneous in population, containing both liposome-protamine-DNA complexes and free liposomes. According to the description given in the above literature, the smaller, compact particles are presumed to be LPD.

Table 3.1. Particle size and zeta-potential of cationic liposome and LPD complex (mean ± SD)

	Size (nm)	Zeta-potential (mv)
DOTAP-cholesterol liposome	131 ± 18	43.1 ± 14.5
Liposome/protamine/DNA (LPD)	430 ± 61	26.4 ± 9.0

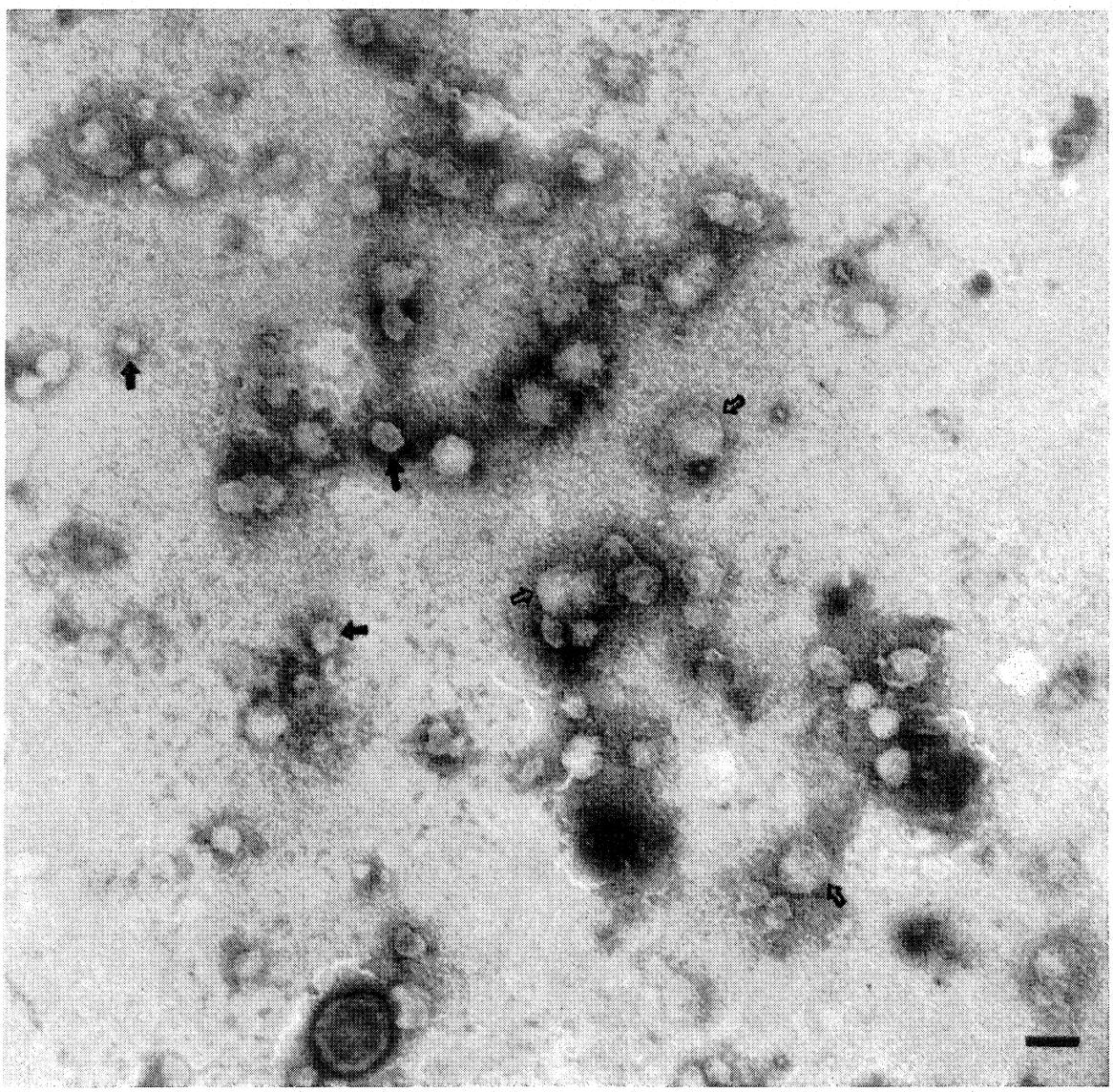

Figure 3.3. Negative stain transmission electron micrograph of LPD(a) complexes, showing both free liposomes (open arrows) and condensed LPD particles (filled arrows). The bar represents 100 nm.

3.3.3 *In vitro* gene transfection

All LPD preparations used in *in vitro* experiments were complexed as 1 μg DNA : 0.6 μg Protamine : 8.4 μg DOTAP and no obvious cytotoxicity was observed during the experiment. As shown in Figure 3.4A and 3.4B, LPD (D = CAT gene) preparations resulted in similar pattern of CAT expression in both Hela and HepG2 cell lines, and Hela cells (Figure 3.4A) exhibited more sensitivity to transfection than did HepG2 cells (Figure 3.4B). When malaria peptide was mixed with LPD complexes for targeting purpose (LPD-pep preparations), there was a dose-dependent effect: lower concentration of peptide showed higher transfection efficiency. An optimal dose of peptide (1 μg peptide/1 μg DNA) was therefore used in the subsequent experiments. In HepG2 cells, peptide-LPD formulations led to 1.5 times (LPD-pep) or 5 times (L-pep-PDa) higher CAT expression than LPD itself (LPDa), respectively. However, no difference was observed in Hela cells for LPD-pep and there were only 1.5 times higher CAT products for L-pep-PDa preparation than LPDa. The DMF-LPD controls did not show either an increase or a decrease in the transfection results (data not shown).

When LPD was prepared with a large volume of serum free medium as diluent to form LPDb or L-pep-PDb, transfection efficiency dramatically increased. Again, L-pep-PDb showed a better result than LPDb in HepG2 cells, while in Hela cells, the transfection difference between LPDb and L-pep-PDb was not obvious.

Another reporter DNA, EGFP, was used to prepare only LPD(a) or LPD-pep during the early experiments. The transfection results of EGFP in cells could be observed under the fluorescence microscope and directly examined by flow cytometry analysis because

EGFP itself is a fluorescence-emitting protein. As revealed in Figure 3.5, the overall transfection efficiency of our formulations was found to be very low. Only 0.6-3% cells were positively transfected when measured by flow cytometry. Apparently, LPD-pep resulted in a higher EGFP expression than LPD in HepG2 cells, whereas no obvious difference was found in Hela cells.

As most research studies suggested, the above transfection experiments were all done in serum and antibiotic free medium for 6-8 h, when the cells were in starvation status. To overcome this problem, we also tried using DME medium containing 10% FBS during transfection, and no obviously different results were obtained (data not shown), indicating that serum had no apparent destabilizing effect on the LPD or peptide-LPD preparations we used.

A.

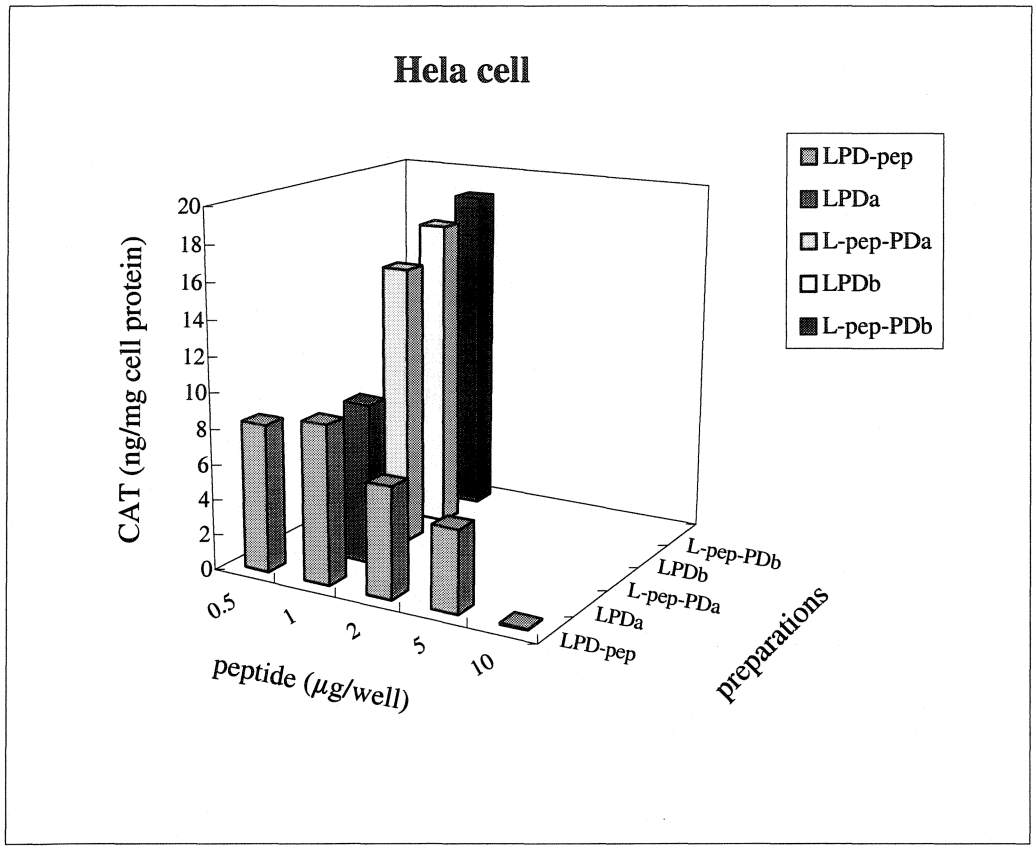

Figure 3.4A. CAT expression after *in vitro* transfection with various LPD or malaria peptide-LPD preparations in Hela cells. The experements were conducted at least 3 times independently and the results are the mean values. Standard errors varied from 2% to 20% of the mean.

B.

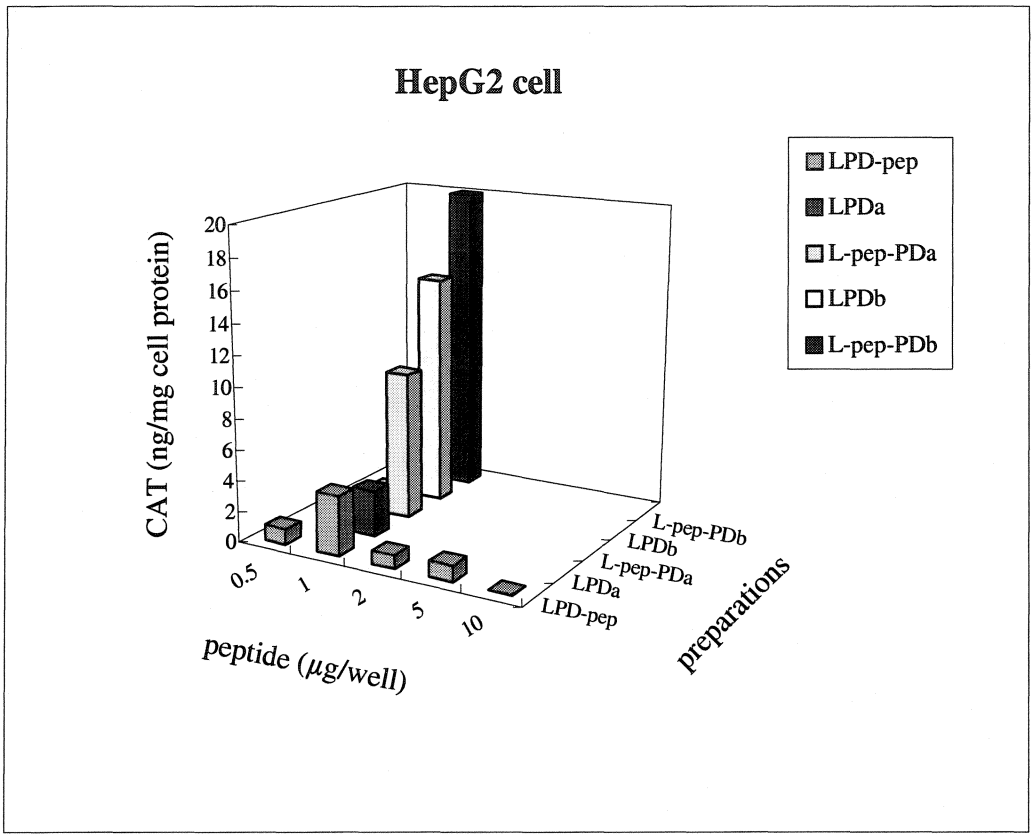

Figure 3.4B. CAT expression after *in vitro* transfection with various LPD or malaria peptide-LPD preparations in HepG2 cells. The experements were conducted at least 3 times independently and the results are the mean values. Standard errors varied from 2% to 25% of the mean.

A.

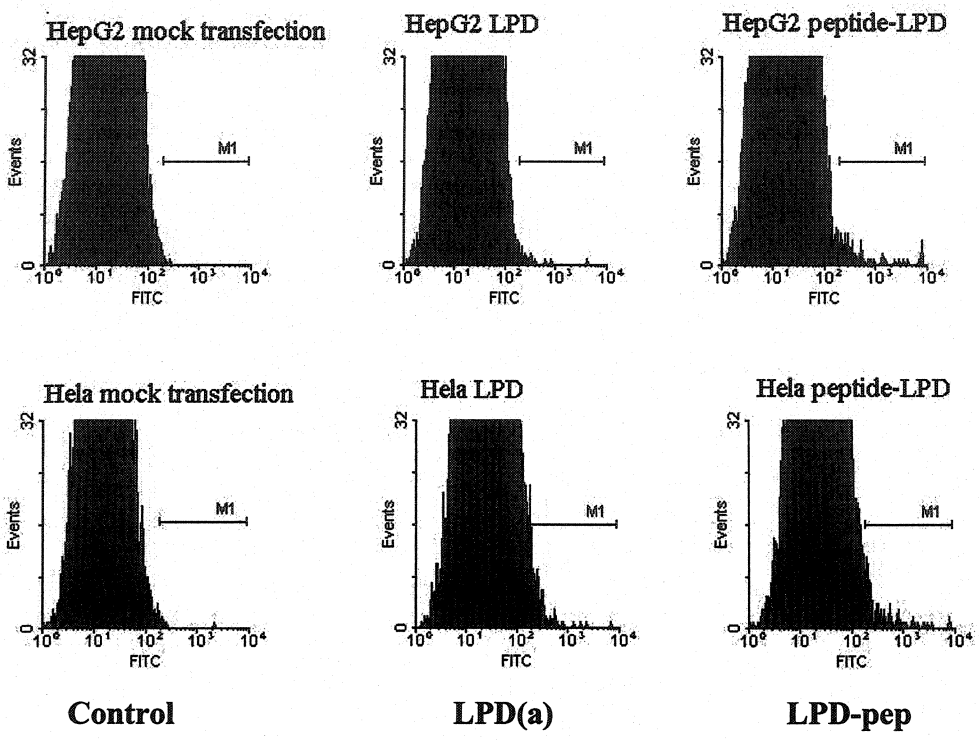
HepG2 mock transfection
HepG2 LPD
HepG2 peptide-LPD
Hela mock transfection
Hela LPD
Hela peptide-LPD
Events
FITC
M1
Control
LPD(a)
LPD-pep

B.

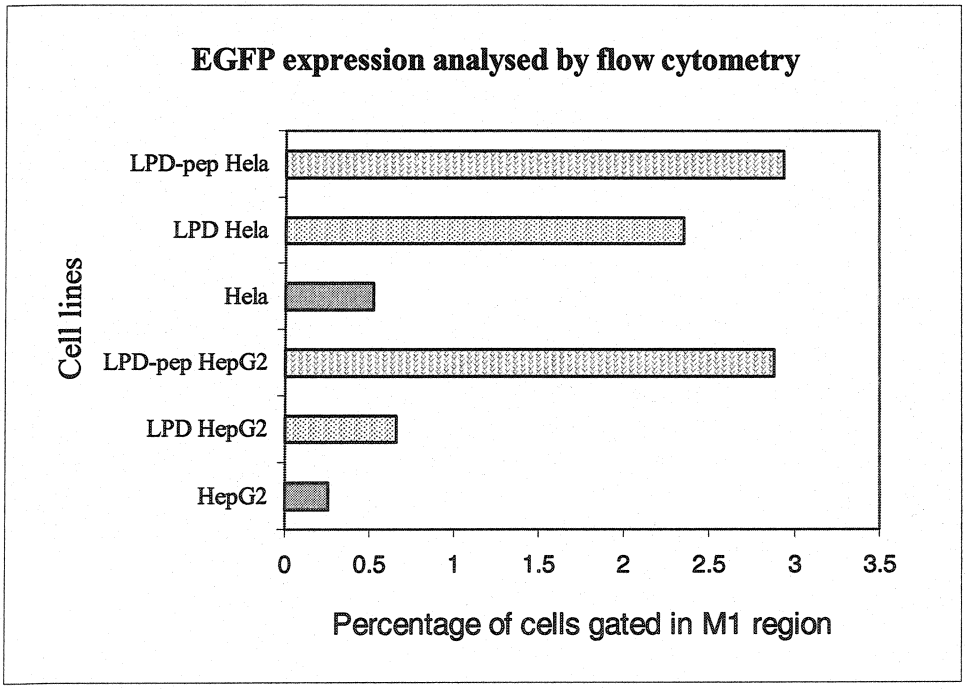
EGFP expression analysed by flow cytometry
LPD-pep Hela
LPD Hela
Hela
LPD-pep HepG2
LPD HepG2
HepG2
Cell lines
0
0.5
1
1.5
2
2.5
3
3.5
Percentage of cells gated in M1 region

3.3.4 *In vivo* gene transfer results

Systemic CAT DNA delivery and gene expression were achieved using LPD(a) formulation at a dose of 85 μg DNA in a 200 μl final volume. Forty-eight hours post-injection, all the organs examined exhibited transgene (CAT) expression. The lung was found to express the highest level of CAT protein, followed by the heart and bone marrow (Figure 3.6). Other organs including the liver showed much less sensitivity to the transfection than the lung. When LPD-pep formulation with 35 μg of peptide and the same amount of CAT DNA was examined for liver targeting effects in one mouse, the pattern of CAT distribution in various organs was identical with that following LPD administration. However, there was no increased CAT production found in the liver compared to that after injection of LPD without the peptide, indicating that the malaria peptide in LPD-pep formulation at a 35 μg dosage failed to deliver more LPD to the liver after systemic administration in this very preliminary experiment.

3.3.5 Cloning of mLDLR cDNA

mLDLR cDNA was successfully cloned. Figure 3.7 shows the screening result of positive pCRII-mLDLR colonies after endonuclease EcoRI digestion. Clone #3 showed bands of 0.8, 2.2, and 3.9 kb which were considered to be a positive construction. Complete sequence of mLDLR cDNA was examined and the accession number of mLDLR sequence by GeneBank is AF425607 (2855bp). The amino acid sequence deducted from mLDLR cDNA has 78% homogeneity as human LDLR according to calculation using OMIGA software (Intelligenetics Inc.). mLDLR plasmid was then constructed using an eukaryotic expression vector pcDNA3.1(-)/Myc-HisA and stored at –20°C prior to use.

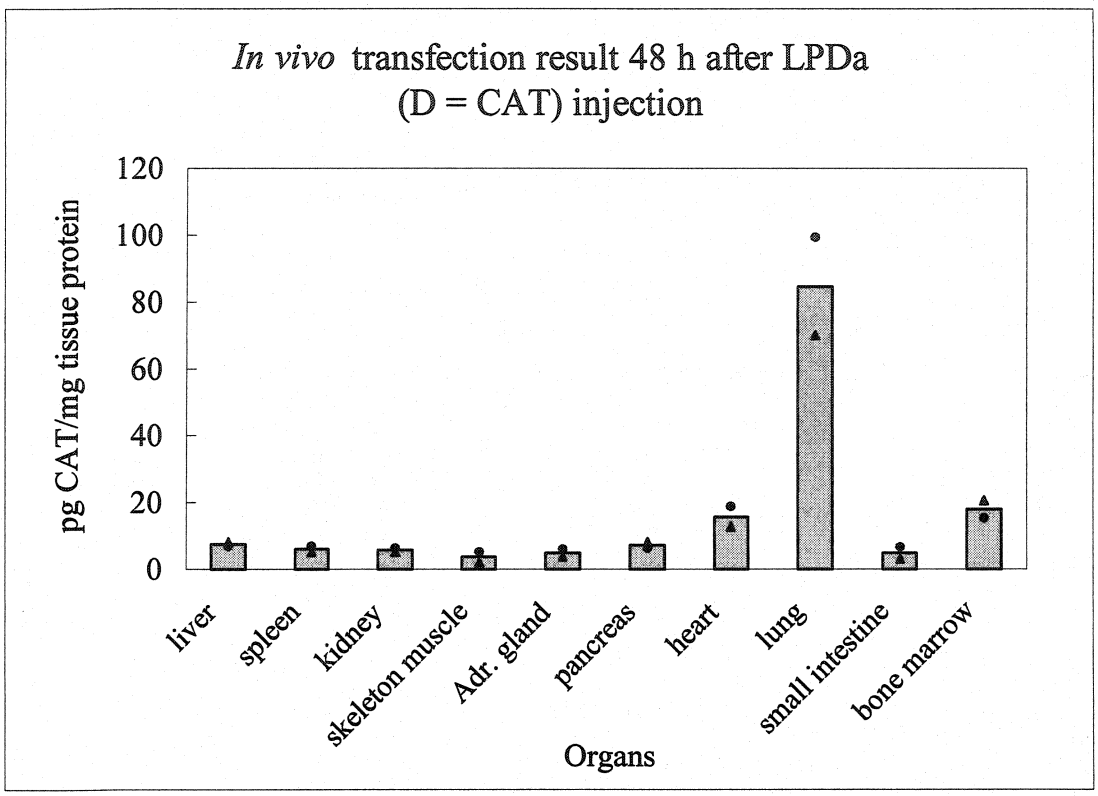

Figure 3.6. CAT expression in various organs 48 h after intravenous injection of LPD(a) complex into C57BL/6 mice (n = 2). CAT production was normalized to protein concentration in the tissue extracts and is presented as the mean value. Individual data from each mouse was also showed: • mouse 1; ▲ mouse 2.

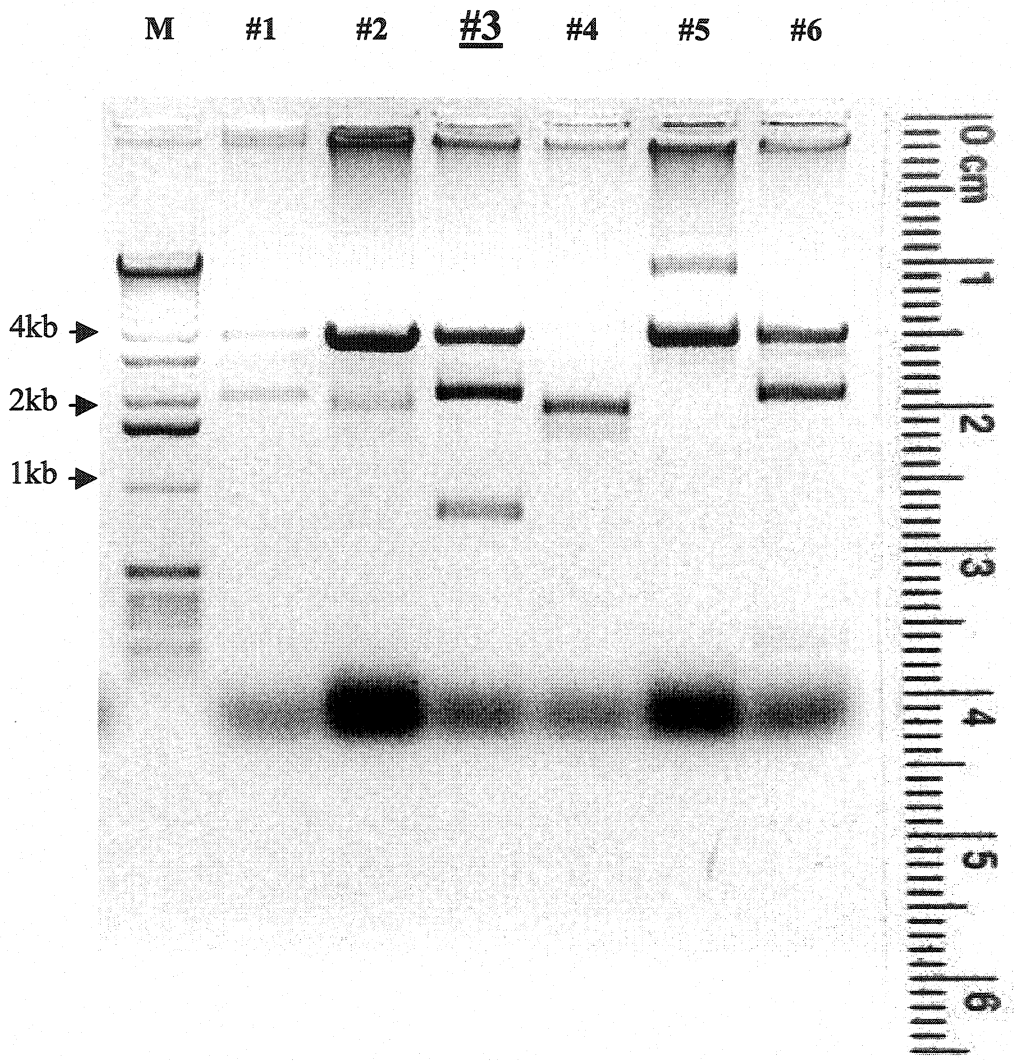

Figure 3.7. Screening of positive pCRII-mLDLR colonies was achieved by EcoRI digestion of plasmid minipreps. Positive construction (#3) showed a pattern of ~0.8kb, 2.2kb and 3.9kb (vector) bands. The ladder (M) is a 1 kb molecular size standard from Invitrogen.

3.4 Discussion

Gene therapy represents an important advance in the treatment of both inherited and acquired diseases. However, success of human gene therapy largely depends upon the development of delivery vehicles or vectors which can selectively deliver therapeutic genes to target cells with efficiency and safety [Walsh, 1998]. In the context of liver disease, such as genetic disorders (e.g. FH), metabolic disorders, viral hepatitis, and liver cancer, somatic gene therapy strategies have been suggested and shown some positive therapeutic effects [Nunes and Raper, 1996]. There are two general approaches to performing liver-targeting gene therapy: *ex vivo* and *in vivo* methods. While the *ex vivo* approach has generally used recombinant retroviruses as a gene delivery vehicle, the *in vivo* method, which is based on both viral and non-viral vectors, is more attractive because of its simplicity and reduced risk and expenses. Cationic liposomes are one of the more promising non-viral vectors for *in vivo* gene therapy [Mahato et al., 1997], and when labeled with a ligand which can be selectively recognized by receptors on hepatocytes, they may be specifically delivered to the liver following systemic administration.

In this study, LPD was chosen as a delivery vector for reporter genes because it had been shown to provide improved gene transfer activity both *in vitro* and *in vivo* [Gao and Huang, 1996; Li and Huang, 1997; Li et al., 1998]. As a type of cationic liposome-based vector, LPD consists of a ternary complex of DOTAP : cholesterol liposome, polycationic protamine with DNA-condensing activity, and plasmid DNA. LPD had been found to be small, compact particles with a core of protamine-condensed DNA coated with a lipidic

shell, very much like enveloped viruses. This unique structure was shown to be less prone to aggregation and offer better protection of plasmid DNA against enzymatic digestion, therefore could dramatically increase the stability and transfection efficiency of liposome-DNA formulation [Sorgi et al., 1997]. Like other lipid-DNA complexes, some characteristics of LPD, including the particular concentrations of cationic lipid, protamine sulfate and DNA, final particle size and charge, and even the addition order of the components during preparation, were all considered to be influential to the transfection efficiency [Ross and Hui, 1999]. The LPD used in our studies consisted of 1 μg DNA : 0.6 μg protamine : 8.4 μg DOTAP, which was shown to be an optimized form for *in vivo* gene transfer via intravenous administration [Li et al., 2000; Birchall et al., 2000].

Most liposomal formulations are essentially colloidal systems, and thermodynamic instability is their inherent characteristic [Lasic and Templeton, 2000]. However, DOTAP-cholesterol liposome prepared in this study was able to retain its particle size of 130 nm for at least 10 weeks. The high positive charge (zeta-potential 43 mv) is believed to contribute to its greater stability via the electrostatic repulsion between particles. In the case of LPD, it was reported to have a particle size of around 135 nm because of the condensation capability of protamine, which had been considered crucial for its increased transfection efficiency [Li and Huang, 1997; Li et al., 1998]. Although the same method was followed in our LPD preparations, the average particle size (430 nm) was not as small as expected, suggesting that aggregation of the resultant complexes might exist [Radler et al., 1997]. The large DNA-liposome aggregates could diminish the transfection activity of LPD formulations. However, production of transfected CAT gene

in our experiments cannot be directly compared with luciferase used in the L. Huang's group [Templeton et al., 1997]. It has also been shown that LPD is a heterogeneous population containing excess amounts of free (empty) liposomes and also small amounts of lipid/DNA complexes. The free liposomes are essential for maximal gene expression in intravenous gene delivery because they can neutralize the action between the plasma components and LPD complexes [Li et al., 1998]. EM examination of the LPD preparation confirmed its heterogeneity and showed some condensed LPD particles and free liposomes.

The 24-amino acid malaria peptide derived from malaria CS II region was modified by attaching a palmitic acid to its N-terminal in order to increase the lipophilicity of the peptide. Theoretically, the fatty acid tail of the peptide is capable of incorporating into the lipid bilayers of the liposome, projecting its amino acid part on the surface of the liposome particle. At the time when the project was designed, we were expecting to conjugate the peptide with liposome by mixing the peptide with lipids (DOTAP and cholesterol) in chloroform during the first step of preparation of liposome. However, the synthesized palmitoylated peptide was found to be poorly dissolved in many organic solvents such as chloroform, methanol, isopropanol, and acetone, except in DMF. We therefore had to use DMF as a solvent of the peptide and control the final concentration of DMF in LPD formulation (in D5W) less than 1%. As described in the method section, two different protocols, other than what we expected, were tried to prepare peptide-LPD complexes. They were referred as LPD-pep or L-pep-PD, respectively, according to the turn of adding the peptide during the preparation process. Although the small amount of DMF neither showed toxicity to the cultured cells nor affected the transfection results of

LPD, it is unclear what interaction is underlying between the peptide and cationic liposome under such conditions.

The *in vitro* transfection experiments were performed using different LPD preparations. It was found that the LPD preparations were able to transfect cultured cells and result in certain level of reporter gene expression without visible toxicity. Compared to LPD(a), LPD(b) resulted in a considerably higher amount of transgene production, 5 times higher in HepG2 cells and 2 times higher in Hela cells, respectively. It is difficult to explain this observation because the only difference between these two preparations is the final mixing method of plasmid DNA with liposome-protamine mixture (see the Materials and methods section). However, the complexing volume of liposome and DNA has been reported to be one of the important parameters for transfection efficiency [Staggs et al., 1997]. In addition, the LPD preparations showed equivalent transfection efficiency in cultured cells under both serum free and serum containing conditions. This can be considered as an advantage of the LPD formulation because it is not needed to eliminate serum during transfection, therefore protecting cells from starvation. Furthermore, the transfection time can be extended when necessary.

The malaria peptide-LPD complex was prepared by two protocols. First, different amounts of peptide were added into the LPD(a) preparation to get what referred as LPD-pep, and a dose-dependent transfection result was observed in both cells. It was found that higher dosage of peptide led to a lower level of transfection, which is possible due to the following reasons: (1) a competitive inhibition between LPD-pep complex and free peptide in the LPD-pep preparation. It is reasonable that higher dosage of peptide could provide more free peptide that were not conjugated with LPD particles; (2) probable

hemolytic activity of the short peptide [Hwang and Vogel, 1998]. An optimal dose of peptide (1 μg peptide/μg DNA/well) showed the highest level of reporter gene expression and therefore was used in the subsequent experiments. In addition, the LPD-pep formulation was found to produce only 1.5 times reporter gene activity as high as that from LPD(a) itself in HepG2 cells, although there was no difference found in control Hela cells. On the other hand, when prepared as L-pep-PD(a) formulation in which the peptide was added into the lipid during the hydration step of the liposome preparation, the transfection efficiency in HepG2 cells was found to be obviously higher, 5 times as high as that of LPD(a) without the peptide. In Hela cells, L-pep-PD(a) also resulted in almost 2 times elevated level of transfection compared to LPD(a), suggesting that Hela cell appeared to possess certain level of receptors for malaria peptide [Ding et al., 1995]. The above results showed the potential targeting effect of the malaria peptide to the liver cells. However, as mentioned before, the association between the peptide and the liposome remains unknown. It is hard to explain the different effects resulted from LPD-pep and L-pep-PD(a). From their preparation method point of view, L-pep-PD(a) is obviously more possible than LPD-pep to provide the chance for the peptide to be associated with liposome, although it is also likely that the peptide may be incorporated into the inner layer of the liposome instead of the surface. Another intricate observation is the fact that when the transfection efficiency was considerably increased using the LPD(b) preparation (compared to LPD(a)), L-pep-PD(b) did not show more improved result than LPD(b) in not only Hela cells but also HepG2 cells.

The preliminary *in vivo* experiment was carried out using only LPD(a) and LPD-pep preparations. It is not surprising that LPD-pep did not lead to increased transfection activity in the liver after intravenous delivery based on the above *in vitro* results. The main significance of this preliminary test is to investigate the *in vivo* behaviour of our LPD preparation. It was found that, as the results published in the literature [Zhu et al., 1993; Liu et al., 1997], the LPD preparation in our studies resulted in a similar biodistribution trend of the reporter gene in the body, in which the lung appeared to have the highest level of transfection activity.

In summary, the cationic DOTAP-cholesterol liposome/protamine/DNA (LPD) preparations could transfect cultured cells *in vitro*, as well as different organs after systemic delivery into mice. A certain level of gene expression had been achieved without visible toxicity. However, the transfection efficiency of cationic liposome vectors is still much lower than that of viral vectors although LPD had been shown to be an improved non-viral formulation. Malaria peptide, when prepared as peptide-LPD complex, showed some targeting effect in human hepatoma cells; however, these results, although promising, were somewhat inconsistent. There is definitely a requirement in future work to figure out more detail information about the peptide-LPD formulations in order to further understand their association and accordingly optimize the preparation protocol. The insolubility of the palmitoylated peptide was a major concern because the introduction of DMF might affect the interaction between the peptide and the liposome. In future, it is probably required to re-design the modification of the peptide, for example, to conjugate the peptide with some other lipophilic chain such as cholesterol.

After a peptide-LPD formulation is proved significantly efficient in liver targeting both *in vitro* and *in vivo* via the reporter gene, the transfection experiments will be conducted in LDLR knockout mice using the mLDLR plasmid in same preparation to explore the possibility of liver-specific gene therapy strategy for FH, the final objective of this project.

Chapter 4. Antiproliferative effect of 3',5'-dipalmitoyl-5-fluorodeoxyuridine incorporated into low density lipoprotein on human cervical cancer cells

4.1 Introduction

In chemotherapy of cancer, toxicity and drug resistance remain as the major challenges. The narrow therapeutic window of antineoplastic drugs hampers the administration of fully effective doses. A therapeutic strategy in which antineoplastic drugs are associated with carriers that are selectively taken up by tumor cells may diminish side effects and allow the administration of more effective doses [Tomlinson, 1987].

The receptor for LDL is an attractive target for the selective delivery of antineoplastic drugs to tumors because it has been found that many tumors of different origins express elevated levels of LDLR [Vitols, 1991; Markel and Brook, 1994]. Especially tumors of gynecological origin and myeloid leukemic cells, but also colon, kidney, lung, and prostate tumors, were found to express exceptionally high amounts of LDLRs [Firestone, 1994]. The elevated expression of LDLRs on cancer cells is probably a result of their accelerated proliferation and to meet their increased demand for cholesterol. LDL, the predominant cholesterol-transporting lipoprotein in human, is a spherical particle of about 23 nm in diameter that consists of a hydrophilic shell of phospholipids and cholesterol, and a lipophilic core of mainly cholesterol esters. A large

part of the particle surface is covered with the apoB-100, which can be specifically recognized by the LDLR. After internalization of LDL via its receptor, the particle is degraded in the lysosomes and the cholesterol is released into the cytoplasm [Brown and Goldstein, 1986].

The fluoropyrimidine antimetabolite 5-fluoro-2'-deoxyuridine (FUdR) has been used extensively for the clinical treatment of carcinomas of the ovary, breast, and gastrointestinal tract [Henn et al., 1993; Xia et al., 1999]. The antineoplastic activity of FUdR is believed to be primarily due to inhibition of DNA biosynthesis by blocking thymidylate synthase (TS), the enzyme which catalyzes the methylation of 2'-deoxyuridine-5'monophosphate to thymidine-5'-monophosphate. FUdR must be phosphorylated intracellularly to afford 5-fluoro-2'-deoxyuridine-5'-monophosphate (FdUMP), a specific competitive inhibitor for TS, to exert its cytotoxic effect [Langenbach et al., 1972; Santi et al., 1974]. In addition, FUdR can also exert cytotoxic effects by incorporating into DNA or RNA following phosphorylation [Kufe et al., 1981]. However, this drug suffers from a number of disadvantages which include high toxicity to normal tissues, rapid blood clearance, low *in vivo* efficacy, and drug resistance. Resistance of human tumor cells to FUdR is thought to be mainly via amplification of TS mRNA and/or increase in TS activity [Murakami et al., 2000], and it can also result from the depletion of activating kinases and uridine phosporylase [Xia et al., 1999].

Different strategies have been studied with an attempt to circumvent the above problems, such as chemical modification [Guo et al., 1995; Xia et al., 1999], preparation of suspension in an oil-water mixture [Ishikawa et al., 1992], and encapsulation in liposomes [Van Borssum Waalkes et al., 1998]. In this study, an alternative strategy,

using LDL as a tumor-targeting carrier for FUdR, was investigated. FUdR was first chemically modified to its lipophilic prodrug, 3',5'-dipalmitoyl-FUdR (dpFUdR) in order to achieve the desired incorporation into LDL. dpFUdR was then incorporated into LDL, resulting in LDL-dpFUdR. The antiproliferative effect of LDL-dpFUdR complex was studied in human cervical cancer cells with acquired FUdR resistance. The underlying interaction between FUdR and cell TS protein was also examined.

4.2 Materials and methods

4.2.1 Materials

FUdR (Floxuridine) was purchased from Sigma-Aldrich Canada Ltd. (Oakville, ON, Canada). Seal oil was provided by Terra Nova Fishery (NL, Canada). The antibodies used in flow cytometry analysis were LDL-R (Ab-1), a monoclonal anti-hLDLR antiboby (primary antibody, from Oncogene, Cambridge, MA, USA), and fluorescein isothiocyanate (FITC) or R-phycoerythrin (PE) labeled goat $F(ab')_2$ anti-mouse IgG (H+L) (secondary antibody, from Cedarlane Laboratories Limited, Hornby, ON, Canada). An enhanced chemiluminescence (ECL) detection kit for Western blotting was obtained from Amersham Biosciences, Inc. (Quebec, Canada). Anti-human thymidylate synthase (sheep) antibody and peroxidase conjugated affinity purified anti-sheep IgG [H&L] (rabbit) were purchased from Rockland Inc. (Gibertsville, PA, USA). All other chemicals and solvents were obtained from Sigma-Aldrich unless otherwise indicated.

Silica gel TLC plates with aluminum backing were obtained from Fisher Scientific (Ottawa, ON, Canada). High performance liquid chromatography (HPLC) analyses were carried out using an HP Series 1050 system (Agilent Technologies, Wilmington, DE, USA) with a Phenomenex Bondclone 10 C18, 150 × 3.9 mm column (Torrance, CA, USA). A Mini-PROTEAN® II Electrophoresis Cell and a Mini Trans-Blot® Electrophoretic Transfer Cell (Bio-Rad Laboratories Ltd., Mississauga, ON, Canada) were used to perform SDS-PAGE and protein transfer, respectively. EM examination was executed by a JOEL 1200EX electron microscope, during which the samples were stained with 1% phosphotungstic acid.

4.2.2 Isolation of LDL

LDL (d = 1.019-1.063 g/ml) was isolated from normolipidemic human plasma (Canadian Red Cross, St. John's, NL, Canada) by sequential ultracentifugation [Schumaker and Puppione, 1986] using a Beckman L8-M ultracentrifuge and 60/75 Ti rotors. The LDL fraction was dialysed at 4°C overnight against a buffer containing 0.3 mM EDTA, 150 mM NaCl and 50 mM Tris (pH 7.4) and then filtered through a Millex-GP filter (pore size 0.22 μm, Millipore Co., Billerica, MA, USA). Protein concentration of the LDL was determined by the method of Bradford using Bio-Rad protein assay kit with BSA as the standard. The LDL (1.6-2.2 mg/ml) was stored at 4°C under argon and used for experiments within 2 weeks.

4.2.3 Preparation of LDL-dpFUdR complex

As illustrated in Figure 4.1, 3',5'-dipalmitoyl-FUdR was synthesized by the reaction of FUdR in dry dichloromethane with palmitic acid according to the published

method [Schwendener et al., 1985; Van Borssum Waalkes et al., 1993]. The purity of dpFUdR was checked by TLC and reverse-phase HPLC. To prepare LDL-dpFUdR, dpFUdR emulsion was first prepared using the method reported previously [Xiao[1] et al., 1999]. Twelve milligram of PC, 8mg of DPPE, 20 mg of seal oil and 10 mg of dpFUdR were dissolved in chloroform, dried under a nitrogen flow and re-suspended in 10 ml of saline. The suspension was sonicated for 2 h at 0°C and centrifuged at 40,000 rpm (Beckman L8-M ultracentrifuge) for 7 h at 4°C. The floating emulsion fraction was collected and then incubated with LDL at 37°C for 8 h at a dpFUdR to LDL molar ratio of 1000:1, following which dpFUdR-LDL complex was purified by ultracentrifugation. To determine its concentration, dpFUdR incorporated into LDL was extracted by chloroform and immediately subjected to HPLC.

To assess and compare the integrity of apoB-100 in native LDL with that loaded with dpFUdR, 8% SDS-PAGE was performed and the separating gel was stained with Coomassie blue R250 (Bio-Rad) to visualize the resultant protein band. The effect of loading dpFUdR on the morphology of LDL particles was analyzed by EM.

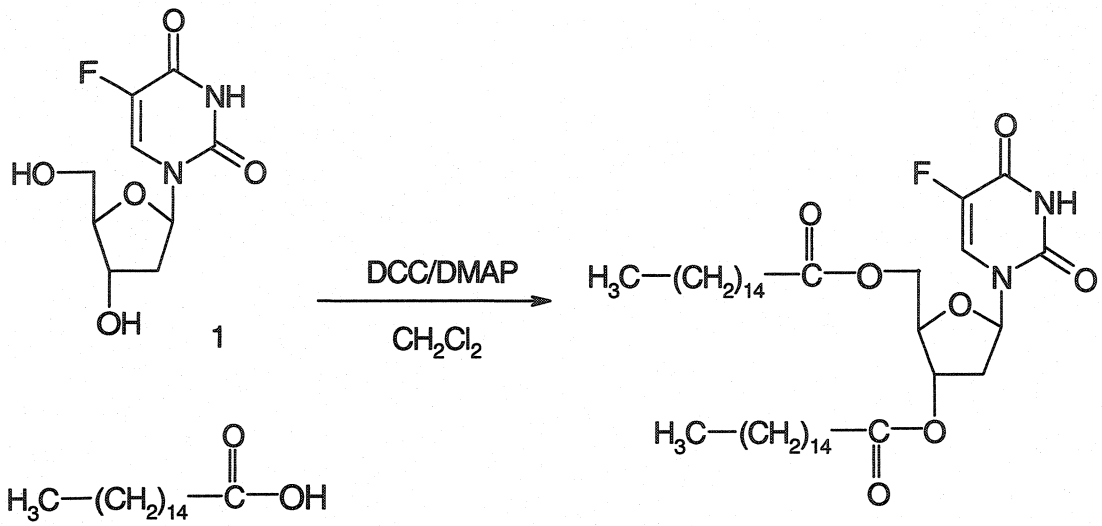

1

2

3

1. 5-Fluoro-2'-deoxyuridine (FUdR)
2. Palmitic acid
3. 3',5'-Dipalmitoyl-5-fluoro-2'-deoxyuridine (dpFUdR)

DCC: Dicyclohexylcarbodiimide

DMAP: Dimethylaminopyridine

CH_2Cl_2: Dichloromethane

Figure 4.1. Scheme of the synthesis of 3',5'-dipalmitoyl-5-fluoro-2'-deoxyuridine (dpFUdR).

4.2.4 Cell culture

Several human cancer cell lines including cervical cancer cells (Hela and Siha) and breast cancer cells (MCF7, BT20, and ZR751) were generously provided by Dr. A. Pater (Faculty of Medicine, Memorial University of Newfoundland) and maintained in DMEM that was supplemented with 10% FBS, 100 IU/ml penicillin and 100 mg/ml streptomycin at 37°C, 5% CO_2. The logarithmically growing cells were harvested by trypsinization and used for the experiments described below. Cell number was counted with a hemocytometer.

4.2.5 Determination of LDLR level on cell surface

Flow cytometry analysis was used to evaluate the LDLR level on the cell surface of the above cultured cell lines. Briefly, each type of cells was harvested and washed with ice-cold PBS, following which approximately 1.5×10^5 cells were incubated with 0.1 μg of monoclonal anti-hLDLR antiboby (primary antibody) in 25 μl of PBS at 4°C for 30 min. After washing 2 times by large volume of PBS (1.3 ml), the cells were stained by FITC or PE-conjugated goat anti-mouse IgG (secondary antibody, 0.7 μg/50 μl PBS) at 4°C for 30 min. The washed cells were then fixed in 200 μl of 1% paraformaldehyde-PBS and subsequently examined by FACS Star®-Plus flow cytometer (Becton Dickinson, Palo Alto, CA, USA). As controls, cells were either unstained during the whole procedure or probed with PBS instead of the primary antibody and then incubated with FITC/PE-conjugated secondary antibody.

4.2.6 Establishment of FUdR-resistant Hela cells

A FUdR resistant subline of Hela, Hela/FUdRr, was developed according to a published method with minor modifications [Murakami et al., 2000]. In brief, Hela cells were cultured until 80-90% confluence, at which time point the medium was changed to DMEM containing 1 μM FUdR. After a 3-day exposure, the cells were cultured in drug-free medium again until the surviving cells re-grew. These cells were then repeatedly exposed for 3 days to step-wise increasing concentrations of FUdR up to 60 μM. FUdR-resistant Hela cells were established by this process over about 6 months and named as Hela/FUdRr cells.

4.2.7 Cytotoxicity assessment by MTT assay

The MTT assay for evaluation of drug cytotoxicity is based on the mitochondrial reduction of a yellow tetrazolium compound, 3-[4,5-Dimethylthiazol-2-yl]-2,5-diphenyltetrazolium bromide (MTT), to a colored formazan product (Mosmann, 1983; Cole, 1986; Sladowski et al., 1993). In brief, Hela or Hela/FUdRr cells in fresh DMEM were seeded into 96-well flat-bottomed plates (Corning Incorporated., Corning, NY, USA) in a volume of 100 μl at 1×10^4 cells/well using a multichannel pipette (BrandTech Scientific, Inc., Essex, CT, USA). The plates were incubated at 37°C for 12 h to allow cells to re-attach and re-equilibrate. The cells were then exposed to various concentrations of LDL-dpFUdR or FUdR (in PBS) prepared by 2 time series dilution for 48 h with equal amounts of dpFUdR emulsion and native LDL as control. Subsequently, most medium was removed from each well and 50 μl of MTT solution (2 mg/ml in PBS) were added. After 4 h of incubation at 37°C, the supernatant was carefully sucked off, and 100 μl/well of dimethylsulfoxide (DMSO) was added to solubilize the formazan

metabolite. Following a brief shaking, the plates were read at wavelength 595 nm in a microplate reader (Bio-Rad, Model 550). Usually four to five replicate wells were used for each group to be tested, and each experiment was repeated at least twice. Controls included wells with cells but no drugs and wells with medium and the highest drug concentration but no cells.

4.2.8 Western blotting analysis

Hela or Hela/FUdRr cells, before and after 24 h exposure to 10 μM FUdR or LDL-dpFUdR, were lysed in a lysis buffer (0.5% Triton X-100, 1mM CDTA, 1 mM PMSF, 1 mg/ml aprotinin, 20 mM MOPS, pH 7.2) for 30 min on ice, followed by centrifugation at 14,000 g for 15 min. Extracts (40 μg protein) were mixed with 4 × SDS sample buffer containing 1% 2-mercaptoethanol and heated at 95°C for 5 min before loading onto a 12% discontinuous SDS polyacrylamide gel. The transfer of proteins to nitrocellulose membranes (Hybond® ECL, from Amersham) was carried out at 100 V for 2 h in a transfer buffer prepared according to the protocol of Bio-Rad. The membranes were washed twice in TBST (10 mM Tris-HCl, 150 mM NaCl, 0.1% Tween-20, pH 8) and then blocked with 1% BSA-TBST for 45-60 min. Primary antibody, sheep anti-human TS, was diluted in TBST and incubated with the membranes overnight at 4°C. After washing, the membranes were incubated for 1 h with secondary antibody (horseradish peroxidase (HRP)-conjugated rabbit anti-sheep IgG) diluted 1:1000 in TBST and then washed again. The detection of protein bands were accomplished using ECL kit as described in Amersham's instruction. The results were analyzed by densitometric scanning using a ChemiImager™ (Alpha Innotech Corporation, San Leandro, CA, USA).

4.3 Results and discussion

The feasibility of chemotherapy in which native LDL loaded with cytotoxic drug is used to inhibit tumors expressing the LDLR had been explored extensively [Firestone, 1994; Filipowska et al., 1992; De Smidt and Van Berkel, 1990]. LDL is a kind of quasispherical endogenous nanoparticle with a long serum half-life of 2-4 days in humans, which provide a further possibility of an increased therapeutic effect of the cytotoxic drug loaded into LDL due to its prolonged circulation time compared to that of the free drug.

FUdR is a water-soluble nucleoside analogue which is effective in the treatment of certain human epithelial tumors. Its activity is up to 100 times higher than that of the parent compound 5-fluorouracil (5-FU) on a molar basis in *in vitro* test. In *in vivo* studies, however, FUdR has been reported to be less potent than 5-FU [Heidelberger et al., 1958; Laskin et al., 1976]. Considering the fast degradation rate of FUdR and the fact that the cytotoxicity of FUdR largely depends on the duration of its exposure to tumor cells [Kanzawa et al., 1980; Yin et al., 1991], it may be postulated that the incorporation of FUdR into LDL should improve its cytotoxic effect by altering its pharmacokinetic properties accompanied by the more specific tumor delivery. The lipid fractions of LDL allow a substantial quantity of lipophilic drug(s) to be stored inside. Therefore, a diester prodrug of FUdR, dpFUdR, was synthesized in the present work. dpFUdR is highly lipophilic and should be a better candidate for the incorporation into LDL than hydrophilic FUdR. The design of an esterified prodrug is a common strategy to improve the lipophilicity and pharmacokinetic/pharmacodynamic properties of the drugs

containing a carboxyl or hydroxyl group, since the human body is rich in esterases which are capable of hydrolyzing ester prodrugs and releasing the active prodrug moieties [Bundgaard, 1991].

4.3.1 Characterization of LDL-dpFUdR complex

The incorporation of dpFUdR into LDL was achieved using a method established in our lab through the incubation of dpFUdR-seal oil emulsion and LDL. The concentration of dpFUdR loaded in LDL was measured by HPLC after dpFUdR was recovered by chloroform extraction from LDL-dpFUdR complex. As shown in Figure 4.2, HPLC was performed using a mobile phase of methanol (MeOH) : H_2O (98:2, v/v) at a flow rate of 1 ml/min in conjunction with a UV detector (268 nm) and the retention time of dpFUdR was 9 min. According to the calculation of both drug and LDL protein concentration, it was found that there were approximately 220 dpFUdR molecules conjugated with one LDL particle. To characterize the integrity of apoB-100 and probably the whole LDL particle, LDL-dpFUdR was compared with native LDL using SDS-PAGE and EM examination, respectively. As can be seen in the result of 8% SDS-PAGE (Figure 4.3), there was only one stained band equivalent to the size of apoB-100 in both lanes, and neither had degradation products. EM photographs (Figure 4.4) also showed particles similar in morphology, as well the size for both samples. The above results indicate that the incorporation of dpFUdR did not alter the integrity of LDL, and the apoB-100 remained intact. The latter is thought to be crucial for the recognition of the particles by LDLR on the cell surface.

A.

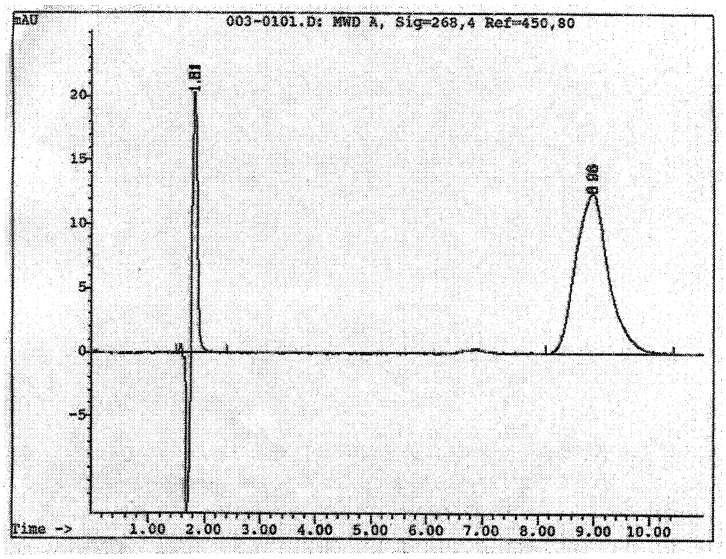

B.

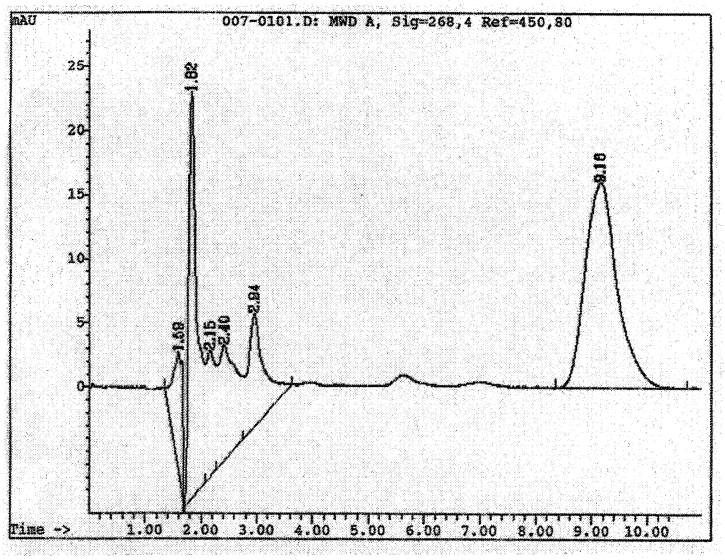

Mobile phase: MeOH: H_2O 98:2 (v/v)

Flow rate: 1 ml/min

Detector: UV, 268 nm (reference 450 nm)

Injection: 10 µl, ~0.15 mg/ml

Figure 4.2. Chromatograms of dpFUdR in mobile phase using HPLC. (A) dpFUdR standard in mobile phase; (B) dpFUdR extracted from LDL-dpFUdR complex.

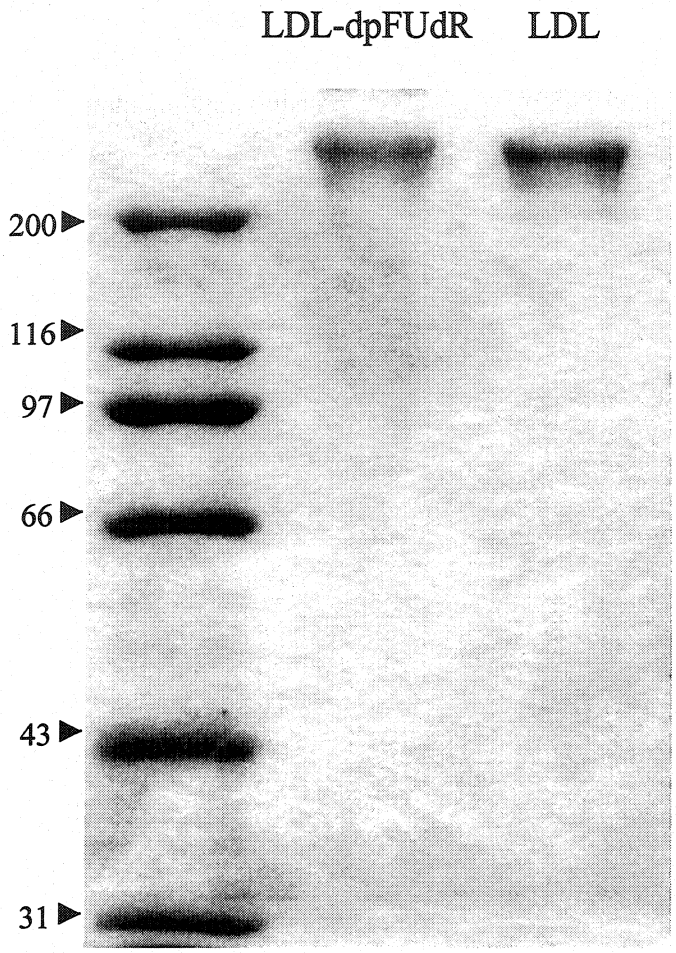

Figure 4.3. 8% SDS-PAGE of LDL-dpFUdR complex and native LDL. Approximately 0.5-1 μg protein was loaded for each sample and electrophoresed at 200 V for 40 min. The separating gel was stained with Coomassie blue R250. The positions of a broad range of molecular weight standard (× kDa) are shown with arrow marks.

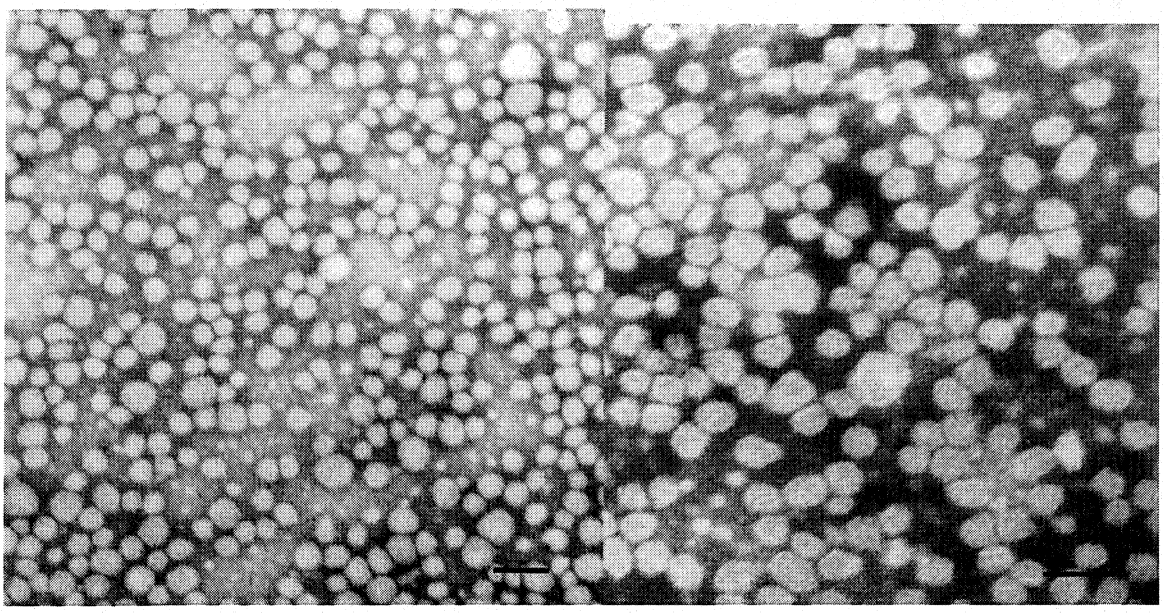

A. LDL (75,000×3 ×) **B.** LDL-dpFUdR (79,800×3 ×)

Figure 4.4. Electron micrographs (3×) of LDL and LDL-dpFUdR preparations. The samples (10-20 μg protein/ml) were applied to formvar and carbon-coated copper grids and negatively stained with 1% phosphotungstate solution, followed by examination using a JOEL 1200EX electron microscope at a magnification of 75,000 × or 79,800 ×. (A) native LDL; (B) LDL-dpFUdR. The bar represents 50 nm.

4.3.2 Evaluation of cell surface LDLR level

Several human cancer cell lines were stained with monoclonal anti-hLDLR antibody and analyzed by flow cytometry. Figure 4.5 demonstrates the result from Hela cells. As can been seen, cell numbers (counts) were plotted against the log of fluorescence intensity (PE-Height) and the histogram of Hela cells stained with anti-hLDLR antibody (red color) was overlaid on those of control cells (non-stained cells and cells incubated with only secondary antibody but no anti-hLDLR antibody, green and black color respectively). The right shift indicates the expression of LDLR on the cell surface. The histograms of other cell lines showed similar pattern as that of Hela cells, whereas the shift was less. The Hela cell was then considered to possess the highest level of LDLR among these cell lines when tested by this method, and therefore a good candidate for the LDL-mediated cell-specific targeting of antiproliferative drugs. In the subsequent experiments, the Hela cell line was chosen to develop the acquired FUdR-resistant subline.

It has to be pointed out that, unlike the classical binding assay using radioiodine-labeled LDL [Goldstein and Brown, 1974; Xiao[3] et al., 1999], the flow cytometry analysis used in this experiment could not quantify the absolute receptor amount on cell surface. However, it is a simple and fast means to screen or compare the LDLR level of different cell lines without a need to manipulate radioisotope.

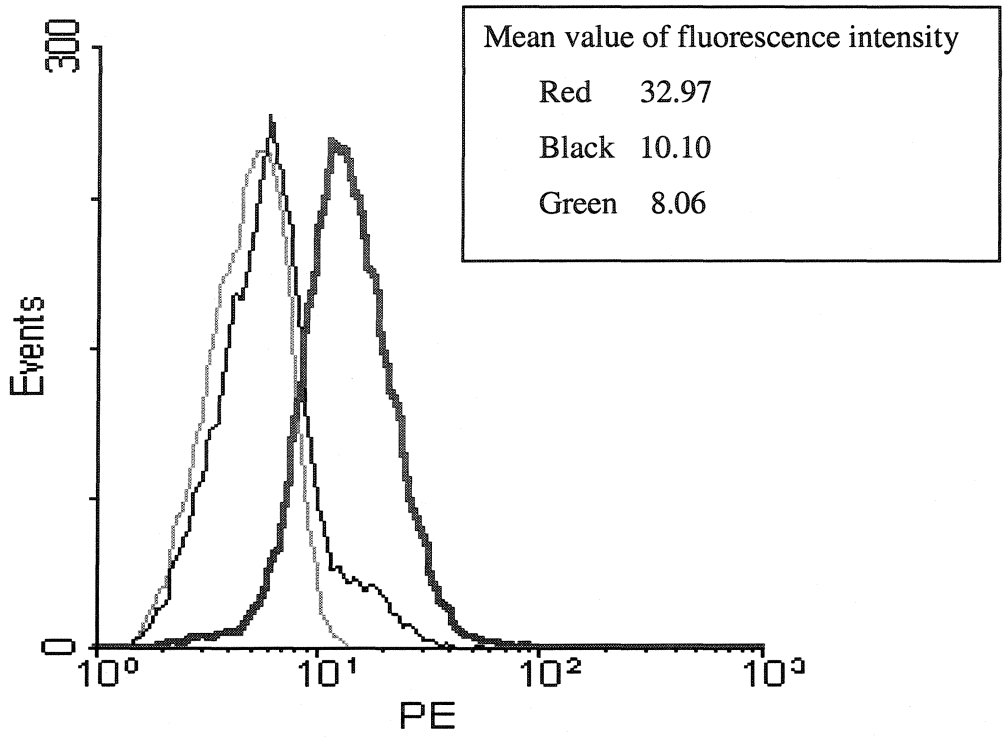

Figure 4.5. Flow cytometry analysis of LDLR level on the surface of Hela cells. The histogram of Hela cells stained with monoclonal anti-hLDLR antibody (red line) was overlaid on the histograms of controls: non-stained cells (green line) and cells stained with only secondary antibody (black line). Cell numbers (counts) are plotted against the log of fluorescence intensity (PE-Height). The number inside the panel indicates the mean values.

4.3.3 Cytotoxicity assay

Human cervical cancer cells with acquired resistance to FUdR, referred here as Hela/FUdRr cells, were established by step-wise exposure of Hela cells to FUdR. As shown in Figure 4.6A, 4.6B, and Table 4.1, Hela/FUdRr cells were proved to be relatively FUdR-resistant. After 48 h exposure, the IC_{50} value of FUdR was 8.9 μM against Hela cells, and approximately 10% cells were found to be able to survive from a high concentration of FUdR (150 μM); whereas in Hela/FUdRr cells, the IC_{50} of FUdR was more than 2 times higher (20.2 μM) and up to 30% cells still remained resistant to 150 μM of FUdR.

dpFUdR, a prodrug of FUdR, was prepared as a emulsion formulation and subsequently incorporated into LDL, resulting in LDL-dpFUdR complex. Cytotoxic effects of LDL-dpFUdR versus free FUdR or dpFUdR emulsion on Hela and Hela/FUdRr cells after 48 h treatment were evaluated by MTT assay and illustrated in Figure 4.6 and Table 4.1. In Hela cells, LDL-dpFUdR showed an IC_{50} value of 7.5 μM after 48 h exposure, indicating an equivalent toxicity as the parent drug, FUdR (IC_{50} 8.9 μM). Nevertheless, at the concentration of 21 μM, LDL-dpFUdR was capable of inducing 100% cell death. In Hela/FUdRr cells, LDL-dpFUdR resulted in similar results as in Hela cells with an IC_{50} value of 4.7 μM and also a completed toxicity at the concentration of 21 μM. However, when compared to FUdR, LDL-dpFUdR demonstrated a 5-fold lower IC_{50} value (4.7 μM versus 20.2 μM), indicating an increased cytotoxic effect of LDL-dpFUdR in FUdR resistant cells. On the other hand, dpFUdR emulsion presented 5-7 fold lower toxicity, as revealed by the IC_{50} values, than LDL-dpFUdR in both cells, and

LDL itself did not show any contribution to the toxicity of LDL-dpFUdR in all experiments.

Since the loading of the prodrug into LDL did not influence the integrity of apoB-100, it was believed that the internalization of LDL-dpFUdR complex by Hela or Hela/FUdRr cells was mainly via LDL receptor-mediated process instead of a simple diffusion [Xiao[3] et al., 1999; Westesen et al., 1995; Masquelier et al., 1986]. Compared with dpFUdR emulsion, LDL carried dpFUdR resulted in an increased cytotoxicity in both cell types, implying a targetted delivery and enhanced uptake through the LDLR pathway. Although LDL-dpFUdR did not lead to higher toxicity than free FUdR in Hela cells according to the IC_{50} value, it could overcome the FUdR resistance of Hela cells, which was encountered when using FUdR. This advantage of LDL-dpFUdR complex was further demonstrated in drug-resistant Hela/FUdRr cells by its decreased IC_{50} value compared to FUdR and 100% toxicity at a relatively lower concentration.

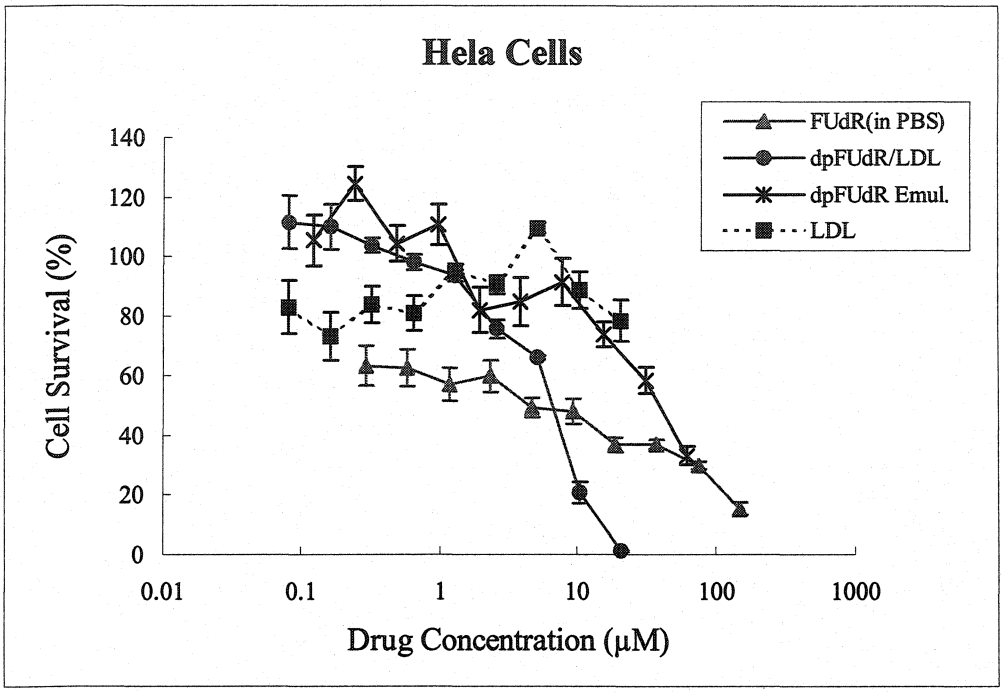

Figure 4.6A. Cytotoxic effect on human cervical Hela cells after 48 h exposure to various concentrations of FUdR, LDL-dpFUdR complex, dpFUdR emulsion and LDL (control). Cells were subjected to the MTT assay. The results are represented as the average ± SE from three independent experiments.

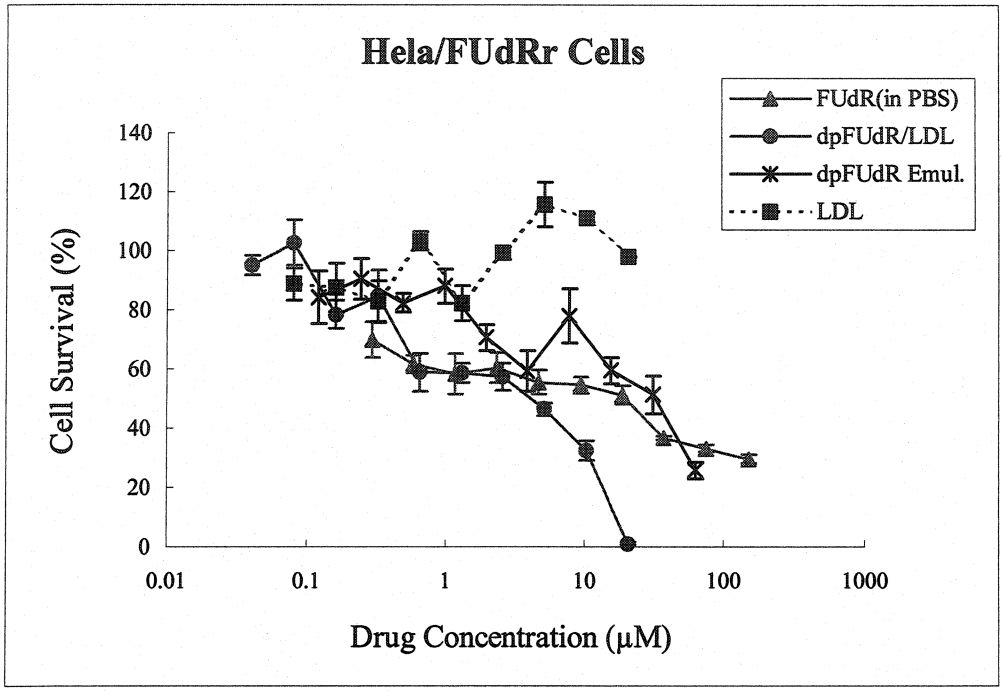

Figure 4.6B. Cytotoxic effect on FUdR-resistant Hela/FUdRr cells after 48 h exposure to various concentrations of FUdR, LDL-dpFUdR complex, dpFUdR emulsion and LDL (control). Cells were subjected to the MTT assay. The results are represented as the average ± SE from three independent experiments.

Table 4.1. Concentrations of FUdR, LDL-dpFUdR complex and dpFUdR emulsion to cause a 50% inhibition of the growth of Hela or Hela/FUdRr cells after 48 h exposure

Cells	IC_{50} (μM)		
	FUdR (in PBS)	LDL-dpFUdR	dpFUdR emulsion
Hela	8.9	7.5	39.3
Hela/FUdRr	20.2	4.7	33.3

It should also be noted that, there was a "concentration threshold" [Kawaguchi[1] et al., 1985] for the cytocoxicity of the prodrug, dpFUdR, in both Hela and Hela/FUdRr cells based on the MTT results regardless of its formulation, either incorporated into LDL or prepared as an emulsion. When the concentration is lower than "threshold", the cell growth inhibition potency of LDL-dpFUdR or dpFUdR emulsion appears similar to that of FUdR. However, after the concentration exceeds the "threshold", both dpFUdR formulations significantly enhance the cytotoxicity as indicated by a decrease of cell growth curve slope. In all cases, FUdR retained the gentle slope without considerable change over a wide range of concentrations, implying that FUdR could not kill all of the cells due to drug resistance. Possible explanations for this observation might be the fact that the hydrolytic rate of the prodrug, dpFUdR, by the cytoplasmic enzyme was slow at the low concentration of prodrug and high at its high concentration [Kawaguchi[2] et al., 1985].

4.3.4 TS level in cells analyzed by Western blotting

TS is a key regulatory enzyme that catalyzes the methylation of deoxyuridine monophosphate in the de novo pathway of pyrimidine synthesis. It is known that TS is also an important cellular target for fluoropyrimidine cytotoxic drugs such as FUdR. Intracellularly, FUdR is converted to FdUMP, which inhibits TS by forming a stable ternary complex with methylene tetrahydrofolate (CH_2THF), leading to cytotoxicity [Drake et al., 1993]. One of the main reasons of FUdR resistance is reported to be increased TS activity and/or TS overproduction. Quantitation of TS protein level has been carried out by clinics to prognose cancer activity and the resistance of malignant

tumor to anticancer drugs such as 5-FU and FUdR [Kuniyasu et al., 1998]. Measurement of TS includes [^{3}H]-FdUMP binding assay, enzyme activity assessment, as well as the polymerase chain reaction based procedure which determines the level of TS mRNA [Suzuki et al., 1998]. In this study, Western blotting was used to analyze TS levels in Hela and Hela/FUdRr cells before or after FUdR treatment, and a newly developed polyclonal antiserum that is highly specific for TS, and at the same time could recognize a broad range of epitopes, was chosen to probe TS signal [Haqqani et al., 1999].

As shown in Figure 4.7, the 36 kDa band was recognized as TS, while the shifting band (38.5 kDa) represented the ternary complex (TS + FUdR metabolite + CH_2THF), which migrates more slowly. In the absence of drug treatment, only TS bands were observed in both Hela and Hela/FUdRr cell extracts (see lane 1 and 2), and the latter showed a relatively denser band (96 vs. 76 as quantitated by densitometric scanning), suggesting a slightly higher TS level in Hela/FUdRr cells. Although the increase of TS expression in Hela/FUdRr cell is not obvious in comparison to Hela cell, as revealed in this analysis, the result indicated the trend of TS overexpression in FUdR-resistant cells. After 24 h of FUdR or LDL-FUdR exposure, two bands were observed for each sample: the TS band and the ternary complex band. It was found that there was no distinct difference in the density of the corresponding bands. However, a trend could also be detected that LDL-dpFUdR led to a denser complex band than FUdR in Hela/FUdRr cells (lane 3 and 4), indicating that more dpFUdR molecules were transported into FUdR-resistant cells by LDL and subsequently hydrolyzed to free FUdR. This is presumed to be the mechanism for LDL-dpFUdR to overcome the acquired FUdR-resistance of cancer cells. In Hela cells (lane 5 and 6), on the other hand, LDL-dpFUdR resulted in an

equivalently dense complex band as FUdR, which is also matching the MTT result, that is, the cytotoxicity of LDL-dpFUdR and free FUdR were similar.

In summary, FUdR is a highly potent antiproliferative compound in *in vitro* test, and its lipophilic ester prodrug, dpFUdR, can be converted to FUdR by intracellular hydrolysis to execute the cytotoxic effect. When incorporated into LDL, dpFUdR could be more actively taken up by human cervical cancer cells (Hela) via the LDL receptor-mediated pathway. In comparison with the parent drug, FUdR, LDL-dpFUdR was also found to be able to overcome the acquired FUdR-resistance. Although LDL has not been paid the same attention as a tumor targeting vehicle in chemotherapy compared to years ago, it remains as a potential carrier for some anti-cancer drugs.

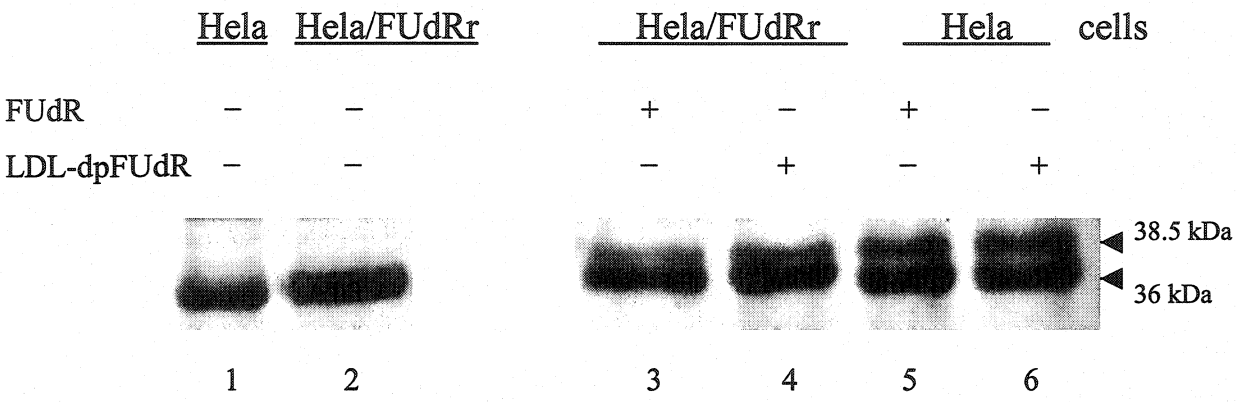

Figure 4.7. Western blotting analysis of TS level in Hela or Hela/FUdRr cells before and after 24 h treatment with 10 μM FUdR and LDL-dpFUdR. The result shown here is a representive of three independent experiments. The 36 kDa band was recognized as TS, while the shifting band (38.5 kDa) represented the ternary complex (TS + FUdR metabolite + CH_2THF), which migrates more slowly. Without drug treatment, only TS bands were observed, and Hela/FUdRr cells showed a relatively denser band than Hela cells, indicating a slightly higher TS level (lane 1 and 2). After drug exposure, two bands were observed for each sample, and there was no distinct difference in the density of the corresponding bands (lane 3, 4 and 5, 6).

Chapter 5. Summary

Targeting delivery of pharmaceuticals has been a long-term research interest in the field of pharmacy. Many different types of delivery system have been explored, ranging from numerous synthetic carriers (e.g. emulsions, liposomes, microspheres) through to naturally occurring materials such as lipoproteins and viruses. These approaches have been extensively investigated in attempts to reduce the risk of cardiovascular diseases. In the work of this thesis, modified LDL was evaluated as a selective carrier of a radioimaging agent for the diagnosis of atherosclerosis. A liver-targeting liposome formulation was also developed with an ultimate objective of delivering therapeutical gene in the treatment of FH, a prevalent genetic disorder leading to atherosclerosis.

LDL is the main lipoprotein particle responsible for the transportation of cholesterol in the plasma. It had been demonstrated to have a close relationship with the development of atherosclerosis due to the fact that continuous deposition of LDL cholesterol in the artery wall contributes to the formation as well as the growth of atherosclerotic lesions. In the development of malignant tumors, LDL also plays an important role because numerous cancer cells presumably need much cholesterol from LDL to meet the requirement for their proliferations. LDL is taken up by cells mainly via a specific receptor-mediated process, which provides a rational to use naturally originated LDL as a targeting carrier for compounds to the cells expressing high level of LDL-receptors.

In chapter 2, one of the main parts of the thesis, a radioimaging agent for detection of early atherosclerosis was evaluated by incorporation of a non-hydrolyzable radiotracer, C2I, into AcLDL, a modified form of LDL. Our results demonstrated the great potential of the C2I/AcLDL agent for imaging atherosclerotic lesions. Besides its diagnostic usage, LDL was also examined as a delivery system for an antiproliferative drug in cancer chemotherapy. As described in chapter 4, the prodrug, dpFUdR, was successfully conjugated with LDL, and LDL-dpFUdR, compared to free FUdR, resulted in overcoming the acquired FUdR resistance of human cervical cancer cells.

As a type of synthetic carrier, cationic liposome is one of the most promising vehicles used in the area of gene therapy. The second objective of the thesis was to develop a liver-targeting liposome-DNA complex for the purpose of correcting LDLR deficiency of FH model. Chapter 3 summarized the experiments conducted so far which were concentrated on *in vitro* studies. A malaria peptide derivative conjugated LPD formulation was developed and showed encouraging, however, somewhat inconsistent, transfection results in human hepatoma cells.

On the basis of results in this thesis, further studies will be performed: (1) using other radionuclides, such as ^{131}I, and other atherosclerotic animal models, such as mini-pig to study the blood clearance profile of C2I/AcLDL and image atherosclerosis *in vivo*; (2) to modify the malaria peptide derivative, optimize the preparation condition of the peptide-LPD complex and examine the *in vivo* behaviour of the formulation.

References

Atsma D. E., Feitsma R. I., Camps J., van't Hooft F. M., van der Wall E. E., Nieuwenhuizen W., Pauwels E. K. Potential of ^{99m}Tc-LDLs labeled by two different methods for scintigraphic detection of experimental atherosclerosis in rabbits. *Arterioscler Thromb.* 1993, 13(1): 78-83.

Basu S. K., Goldstein J. L., Anderson G. W., Brown M. S. Degradation of cationized low density lipoprotein and regulation of cholesterol metabolism in homozygous familial hypercholesterolemia fibroblasts. *Proc Natl Acad Sci U S A.* 1976, 73(9): 3178-3182.

Birchall J. C., Kellaway I. W., Gumbleton M. Physical stability and in-vitro gene expression efficiency of nebulised lipid-peptide-DNA complexes. *Int J Pharm.* 2000, 197(1-2): 221-231.

Bradford M. M. A rapid and sensitive method for the quantitation of microgram quantities of protein utilizing the principle of protein-dye binding. *Anal Biochem.* 1976, 72: 248-254.

Brown B. G., Zhao X. Q., Sacco D. E., Albers J. J. Lipid lowering and plaque regression. New insights into prevention of plaque disruption and clinical events in coronary disease. *Circulation.* 1993. 87(6): 1781-1791.

Brown M. S., Basu S. K., Falck J. R., Ho Y. K., Goldstein J. L. The scavenger cell pathway for lipoprotein degradation: specificity of the binding site that mediates the uptake of negatively-charged LDL by macrophages. *J Supramol Struct.* 1980, 13: 67-81.

Brown M. S., Goldstein J. L. A receptor-mediated pathway for cholesterol homeostasis. *Science.* 1986, 232(4746): 34-47.

Brown M. S., Goldstein J. L. Lipoprotein metabolism in the macrophage: implications for cholesterol deposition in atherosclerosis. *Annu Rev Biochem.* 1983, 52: 223-261.

Bundgaard H. Novel chemical approaches in prodrug design. *Drugs of the Future.* 1991, 16: 443-458.

Callister T. Q., Cooil B., Raya S. P., Lippolis N. J., Russo D. J., Raggi P. Coronary artery disease: improved reproducibility of calcium scoring with an electron-beam CT volumetric method. *Radiology.* 1999, 208(3): 807-814.

Caplen N. J., Alton E. W., Middleton P. G., Dorin J. R., Stevenson B. J., Gao X., Durham S. R., Jeffery P. K., Hodson M. E., Coutelle C., Huang L., Porteous D. J., Williamson R., Geddes D. M. Liposome-mediated CFTR gene transfer to the nasal epithelium of patients with cystic fibrosis. *Nat Med.* 1995, 1(1): 39-46.

Cerami C., Frevert U., Sinnis P., Takacs B., Clavijo P., Santos M. J., Nussenzweig V. The basolateral domain of the hepatocyte plasma membrane bears receptors for the circumsporozoite protein of Plasmodium falciparum sporozoites. *Cell.* 1992, 70(6): 1021-1033.

Cerqueira M. D. Current status of radionuclide tracer imaging of thrombi and atheroma. *Semin Nucl Med.* 1999, XXIX(4): 339-351.

Chait A., Heinecke J. W. Lipoproteins, modified lipoproteins and atherosclerotic vascular disease. In *The metabolic & molecular bases of inherited disease (Vol. II)* (Scriver C. R., Beaudet A. L., Sly W. S. and Valle D., Eds.), 8th ed. McGraw-Hill, New York. 2001, pp597-605.

Chatterjee S., Wery M., Sharma P., Chauhan V. S. A conserved peptide sequence of the Plasmodium falciparum circumsporozoite protein and antipeptide antibodies inhibit Plasmodium berghei sporozoite invasion of Hep-G2 cells and protect immunized mice against P. berghei sporozoite challenge. *Infect Immun.* 1995, 63(11): 4375-4381.

Cole S. P. C. Rapid chemosensitivity testing of human lung tumor cells using the MTT assay. *Cancer Chemother Pharmacol.* 1986, 17(3): 259-263.

Corti R., Farkouh M. E., Badimon J. J. The vulnerable plaque and acute coronary syndromes. *Am J Med.* 2002, 113(8): 668-680.

Crystal R. G. The gene as the drug. *Nat Med.* 1995, 1(1): 15-17.

Dansky H. M., Charlton S. A., Sikes J. L., Heath S. C., Simantov R., Levin L. F., Shu P., Moore K. J., Breslow J. L., Smith J. D. Genetic background determines the extent of atherosclerosis in ApoE-deficient mice. *Arterioscler Thromb Vasc Biol.* 1999, 19(8): 1960-1968.

De Smidt P. C., van Berkel T. J. Prolonged serum half-life of antineoplastic drugs by incorporation into the low density lipoprotein. *Cancer Res.* 1990, 50(23): 7476-7482.

Deforge L. E., Degalan M. R., Ruyan M. K., Newton R. S., Counsell R. E. Comparison of methods for incorporating a radioiodinated residualizing cholesteryl ester analog into low density lipoprotein. *Int J Rad Appl Instrum B.* 1992, 19(7): 775-782.

DeGalan M. R., Schwendner S. W., Skinner R. W., Longino M. A., Gross M., Counsell R. E. Iodine-125 cholesteryl iopanoate for measuring extent of atherosclerosis in rabbits. *J Nucl Med.* 1988, 29: 503-508.

Ding Z. M., Cristiano R. J., Roth J. A., Takacs B., Kuo M. T. Malarial circumsporozoite protein is a novel gene delivery vehicle to primary hepatocyte cultures and cultured cells. *J Biol Chem.* 1995, 270(8): 3667-3676.

Dinkelborg L. M., Duda S. H., Hanke H., Tepe G., Hilger C. S., Semmler W. Molecular imaging of atherosclerosis using a technetium-99m-labeled endothelin derivative. *J Nucl Med.* 1998, 39(10): 1819-1822.

Drake J. C., Allegra C. J., Johnston P. G. Immunological quantitation of thymidylate synthase-FdUMP-5,10-methylenetetrahydrofolate ternary complex with the monoclonal antibody TS 106. *Anticancer Drugs*. 1993, 4(4): 431-435.

Elmaleh D. R., Narula J., Babich J. W., Petrov A., Fischman A. J., Khaw B. A., Rapaport E., Zamecnik P.C. Rapid noninvasive detection of experimental atherosclerotic lesions with novel 99mTc-labeled diadenosine tetraphosphates. *Proc Natl Acad Sci U S A*. 1998, 95(2): 691-695.

Falk E., Shah P. K., Fuster V. Coronary plaque disruption. *Circulation*. 1995; 92: 657-671.

Farquhar J. W. The Victoria Declaration on heart health: its international implications. In *Atherosclerosis X* (Woodford F. P., Davignon J., and Sniderman A., Eds.). Elsevier Scientific, Amsterdam-Lausanne-New York-Oxford-Shannon-Tokyo. 1995, pp144-146.

Fayad Z. A., Fuster V. Clinical imaging of the high-risk or vulnerable atherosclerotic plaque. *Circ Res*. 2001, 89(4): 305-316.

Fayad Z. A., Fuster V., Fallon J. T., Jayasundera T., Worthley S. G., Helft G., Aguinaldo J. G., Badimon J. J., Sharma S. K. Noninvasive in vivo human coronary artery lumen and wall imaging using black-blood magnetic resonance imaging. *Circulation*. 2000, 102(5): 506-510.

Fazio G. P., Redberg R. F., Winslow T, Schiller N. B. Transesophageal echocardiographically detected atherosclerotic aortic plaque is a marker for coronary artery disease. *J Am Coll Cardiol*. 1993, 21(1): 144-150.

Filipowska D., Filipowski T., Morelowska B., Kazanowska W., Laudanski T., Lapinjoki S., Akerlund M., Breeze A. Treatment of cancer patients with a low-density-lipoprotein delivery vehicle containing a cytotoxic drug. *Cancer Chemother Pharmacol*. 1992, 29(5): 396-400.

Firestone R. A. Low-density lipoprotein as a vehicle for targeting antitumor compounds to cancer cells. *Bioconjug Chem.* 1994, 5(2): 105-113.

Fuster V. Mechanisms Leading to Myocardial Infarction: Insights From Studies of Vascular Biology. *Circulation.* 1994, 90(4): 2126-2146.

Fuster V., Badimon L., Badimon J. J., Chesebro J. H. The pathogenesis of coronary artery disease and the acute coronary syndromes. *N Engl J Med.* 1992; 326: 242-250.

Gagne C., Bays H. E., Weiss S. R., Mata P., Quinto K., Melino M., Cho M., Musliner T. A., Gumbiner B.; Ezetimibe Study Group. Efficacy and safety of ezetimibe added to ongoing statin therapy for treatment of patients with primary hypercholesterolemia. *Am J Cardiol.* 2002, 90(10): 1084-1091.

Gao X., Huang L. Potentiation of cationic liposome-mediated gene delivery by polycations. *Biochemistry.* 1996, 35(3): 1027-1036.

Gimbrone M. A. Jr. Vascular endothelium, hemodynamic forces, and atherogenesis. *Am J Pathol.* 1999, 155(1): 1-5.

Glass C. K., Witztum J. L. Atherosclerosis: the road ahead. *Cell.* 2001, 104: 503-516.

Goldstein J. L., Brown M. S. Binding and degradation of low density lipoproteins by cultured human fibroblasts. Comparison of cells from a normal subject and from a patient with homozygous familial hypercholesterolemia. *J Biol Chem.* 1974, 249(16): 5153-5162.

Goldstein J. L., Ho Y. K., Basu S. K., Brown M. S. Binding site on macrophages that mediates uptake and degradation of acetylated low density lipoprotein, producing massive cholesterol deposition. *Proc Natl Acad Sci U S A.* 1979, 76(1): 333-337.

Goldstein J. L., Hobbs H. H., Brown M. S. Familial hypercholesterolemia. In *The metabolic & molecular bases of inherited disease (Vol. II)* (C. R. Scriver, A. L.

Beaudet, W. S. Sly and D. Valle, Eds.), 8th ed. McGraw-Hill, New York. 2001, pp2863-2913.

Gronholdt M. L. Ultrasound and lipoproteins as predictors of lipid-rich, rupture-prone plaques in the carotid artery. *Arterioscler Thromb Vasc Biol.* 1999, 19(1): 2-13.

Grossman M., Rader D. J., Muller D. W., Kolansky D. M., Kozarsky K., Clark B. J. 3rd, Stein E. A., Lupien P. J., Brewer H. B. Jr, Raper S. E., Wilson J. M. A pilot study of ex vivo gene therapy for homozygous familial hypercholesterolaemia. *Nat Med.* 1995, 1(11): 1148-1154.

Guo X., Lerner-Tung M., Chen H. X., Chang C. N., Zhu J. L., Chang C. P., Pizzorno G., Lin T. S., Cheng Y. C. 5-Fluoro-2-pyrimidinone, a liver aldehyde oxidase-activated prodrug of 5-fluorouracil. *Biochem Pharmacol.* 1995, 49(8): 1111-1116.

Haqqani A. S., Cowling R. T., Maroun J. A., Birnboim H. C. Characterization of a polyclonal antibody to human thymidylate synthase suitable for the study of colorectal cancer specimens. *J Histochem Cytochem.* 1999, 47(12): 1563-1574.

Hardoff R., Braegelmann F., Zanzonico P., Herrold E. M., Lees R. S., Lees A. M., Dean R. T., Lister-James J., Borer J. S. External imaging of atherosclerosis in rabbits using an ^{123}I-labeled synthetic peptide fragment. *J Clin Pharmacol.* 1993, 33(11): 1039-1047.

Heidelberger C., Griesbach L., Cruz O., Schnitzer R. J., and Grunberg E. Fluorinated pyrimidines VI. Effects of 5-fluorouridine and 5-fluoro-2'-deoxyuridine on transplanted tumors. *Proc. Soc. Exp. Biol. Med.* 1958, 97: 470-475.

Henn T. F., Garnett M. C., Chhabra S. R., Bycroft B. W., Baldwin R. W. Synthesis of 2'-deoxyuridine and 5-fluoro-2'-deoxyuridine derivatives and evaluation in antibody targeting studies. *J Med Chem.* 1993, 36(11): 1570-1579.

Hu J, Liu H, Wang L. Enhanced delivery of AZT to macrophages via acetylated LDL. *J Control Release*. 2000, 69(3): 327-335.

Hwang P. M., Vogel H. J. Structure-function relationships of antimicrobial peptides. *Biochem Cell Biol*. 1998, 76(2-3): 235-246.

Ishibashi S., Brown M. S., Goldstein J. L., Gerard R. D., Hammer R. E., Herz J. Hypercholesterolemia in low density lipoprotein receptor knockout mice and its reversal by adenovirus-mediated gene delivery. *J Clin Invest*. 1993, 92(2): 883-893.

Ishibashi S., Herz J., Maeda N., Goldstein J. L., Brown M. S. The two-receptor model of lipoprotein clearance: Tests of the hypothesis in knockout mice lacking the low density lipoprotein receptor, apolipoprotein E, or both proteins. *Proc Natl Acad Sci U S A*. 1994, 91: 4431-4435.

Ishikawa M., Kikuta H., Imaizumi A., Suzuki E., Takayanagi Y., Sasaki K. Sustained release of 5-fluorouracil from oil/water emulsions. *Res Commun Chem Pathol Pharmacol*. 1992, 76(2): 245-248.

Iuliano L., Signore A., Vallabajosula S., Colavita A. R., Camastra C., Ronga G., Alessandri C., Sbarigia E., Fiorani P. Violi F. Preparation and biodistribution of ^{99m}technetium labelled oxidized LDL in man. *Atherosclerosis*. 1996, 26: 131-141.

Jain K. K. Introduction and historical aspects. In *textbook of gene therapy*. Hogrefe & Huber publishers, Toronto. 1998, pp1-4.

Kanzawa F., Hoshi A., Kuretani K. Differences between 5-fluoro-2'-deoxyuridine and 5-fluorouridine in their cytotoxic effect on growth of murine lymphoma L5178Y cells in in vivo and in vitro systems. *Eur J Cancer*. 1980,16(8): 1087-1092.

Kawaguchi[1] T., Saito M., Suzuki Y., Nambu N., Nagai T. Specificity of esterases and structure of prodrug esters. II. Hydrolytic regeneration behavior of 5-fluoro-2'-deoxyuridine (FUdR) from 3',5'-diesters of FUdR with rat tissue homogenates and

plasma in relation to their antitumor activity. *Chem Pharm Bull (Tokyo).* 1985, 33(4): 1652-1659.

Kawaguchi[2] T., Suzuki Y., Nakahara Y., Nambu N., Nagai T. Activity of esterase in the hydrolysis of 3',5'-diesters of 5-fluoro-2'-deoxyuridine in relation to the structure of the diester prodrugs. *Chem Pharm Bull (Tokyo).* 1985, 33(1): 301-307.

Kawashiri M. A., Rader D. J. Gene therapy for lipid disorders. *Curr Control Trials Cardiovasc Med.* 2000, 1: 120-127.

Kozarsky K. F., Jooss K., Donahee M., Strauss J. F. 3rd, Wilson J. M. Effective treatment of familial hypercholesterolaemia in the mouse model using adenovirus-mediated transfer of the VLDL receptor gene. *Nat Genet.* 1996, 13(1): 54-62.

Kozarsky K. F., McKinley D. R., Austin L. L., Raper S. E., Stratford-Perricaudet L. D., Wilson J. M. In vivo correction of low density lipoprotein receptor deficiency in the Watanabe heritable hyperlipidemic rabbit with recombinant adenoviruses. *J Biol Chem.* 1994, 269(18): 13695-13702.

Kufe D. W., Major P. P., Egan E. M., Loh E. 5-Fluoro-2'-deoxyuridine incorporation in L1210 DNA. *J Biol Chem.* 1981, 256(17): 8885-8888.

Kuniyasu T., Nakamura T., Tabuchi Y., Kuroda Y. Immunohistochemical evaluation of thymidylate synthase in gastric carcinoma using a new polyclonal antibody: the clinical role of thymidylate synthase as a prognostic indicator and its therapeutic usefulness. *Cancer.* 1998, 83(7): 1300-1306.

Laemmli U. K. Cleavage of structural proteins during the assembly of the head of bacteriophage T4. *Nature.* 1970, 227(259): 680-685.

Langenbach R. J., Danenberg P. V., Heidelberger C. Thymidylate synthetase: mechanism of inhibition by 5-fluoro-2'-deoxyuridylate. *Biochem Biophys Res Commun.* 1972, 48(6): 1565-1571.

Lasic D. D., Templeton N. S. Bioorganic colloids: macromolecules, DNA, self-assembled particles, and their complexes. In *Gene therapy: therapeutic mechanisms and strategies* (Templeton N. S. and Lasic D. D., Eds.). Marcel Dekker, Inc., New York. 2000, pp241-266.

Laskin J. D., Jordan E. F., Kenny L.N., Sugg D., Divekar A. Y., and Hakala M. T. Differences in the sensitivity to culture. *Proc. Am. Assoc. Cancer Res.* 1976, 17: 71-76.

Ledley F. D. Pharmaceutical approach to somatic gene therapy. *Pharm Res.* 1996, 13(11): 1595-1614.

Lee R. J., Huang L. Lipidic vector systems for gene transfer. *Crit Rev Ther Drug Carrier Syst.* 1997, 14(2): 173-206.

Lees A. M., Lees R. S., Schoen F. J., Isaacsohn J. L., Fischman A. J., McKusic K. A., Strauss H. W. Imaging human atherosclerosis with 99m-Tc-labeled low density lipoproteins. *Arteriosclerosis.* 1988, 8: 461-470.

Lees R. S., Lees A. M., Strauss H. W. External imaging of human atherosclerosis. *J Nucl Med.* 1983, 24: 154-156.

Li B., Li S., Tan Y., Stolz D. B., Watkins S. C., Block L. H., Huang L. Lyophilization of cationic lipid-protamine-DNA (LPD) complexes. *J Pharm Sci.* 2000, 89(3): 355-364.

Li S., Huang L. In vivo gene transfer via intravenous administration of cationic lipid-protamine-DNA (LPD) complexes. *Gene Ther.* 1997, 4(9): 891-900.

Li S., Rizzo M. A., Bhattacharya S., Huang L. Characterization of cationic lipid-protamine-DNA (LPD) complexes for intravenous gene delivery. *Gene Ther.* 1998, 5(7): 930-937.

Libby P. Molecular bases of the acute coronary syndromes. *Circulation*. 1995; 91: 2844-2850.

Liu Y., Mounkes L. C., Liggitt H. D., Brown C. S., Solodin I., Heath T. D., Debs R. J. Factors influencing the efficiency of cationic liposome-mediated intravenous gene delivery. *Nat Biotechnol*. 1997, 15(2): 167-173.

Lusis A. J. Atherosclerosis. *Nature*. 2000, 407: 233-241.

Mahato R. I., Takakura Y., Hashida M. Nonviral vectors for in vivo gene delivery: physicochemical and pharmacokinetic considerations. *Crit Rev Ther Drug Carrier Syst*. 1997, 14(2): 133-172.

Markel A., Brook G. J. Cancer and hypocholesterolemia. *Isr J Med Sci*. 1994, 30(10): 787-793.

Masquelier M., Vitols S., Peterson C. Low-density lipoprotein as a carrier of antitumoral drugs: in vivo fate of drug-human low-density lipoprotein complexes in mice. *Cancer Res*. 1986, 46(8): 3842-3847.

McConnell M. V. Imaging techniques to predict cardiovascular risk. *Curr Cardiol Rep*. 2000, 2: 300-307.

Mosmann T. Rapid colorimetric assay for cellular growth and survival: application to proliferation and cytotoxicity assays. *J Immunol Methods*. 1983, 65(1-2): 55-63.

Murakami Y., Kazuno H., Emura T., Tsujimoto H., Suzuki N., Fukushima M. Different mechanisms of acquired resistance to fluorinated pyrimidines in human colorectal cancer cells. *Int J Oncol*. 2000, 17(2): 277-283.

Nabel G. J., Nabel E. G., Yang Z. Y., Fox B. A., Plautz G. E., Gao X., Huang L., Shu S., Gordon D., Chang A. E. Direct gene transfer with DNA-liposome complexes in melanoma: expression, biologic activity, and lack of toxicity in humans. *Proc Natl Acad Sci U S A*. 1993, 90(23): 11307-11311.

Narula J., Petrov A., Bianchi C., Ditlow C. C., Lister B. C., Dilley J., Pieslak I., Chen F. W., Torchilin V. P., Khaw B. A. Noninvasive localization of experimental atherosclerotic lesions with mouse/human chimeric Z2D3 F(ab')2 specific for the proliferating smooth muscle cells of human atheroma. Imaging with conventional and negative charge-modified antibody fragments. *Circulation.* 1995, 92(3): 474-484.

Narula J., Virmani R., Iskandrian A. E. Strategic targeting of atherosclerotic lesions. *J Nucl Cardiol.* 1999, 6(1 Pt 1): 81-90.

Nunes F. A., Raper S. E. Liver-directed gene therapy. *Med Clin North Am.* 1996, 80(5): 1201-1213.

Packard C. J., Shepherd J. Physiology of the lipoprotein transport system: an overview of lipoprotein metabolism. In *The metabolic & molecular bases of inherited disease (Vol. II)* (C. R. Scriver, A. L. Beaudet, W. S. Sly and D. Valle, Eds.), 8th ed. McGraw-Hill, New York. 2001, pp19-27.

Pasterkamp G., Falk E., Woutman H., Borst C. Techniques characterizing the coronary atherosclerotic plaque: influence on clinical decision making? *J Am Coll Cardiol.* 2000, 36(1): 13-21.

Pedroso de Lima M. C., Simoes S., Pires P., Faneca H., Duzgunes N. Cationic lipid-DNA complexes in gene delivery: from biophysics to biological applications. *Adv Drug Deliv Rev.* 2001, 47(2-3): 277-294.

Pitt B. The anti-ischemic potential of angiotensin-converting enzyme inhibition: insights from the heart outcomes prevention evaluation trial. *Clin Cardiol.* 2000, 23(7 Suppl 4): IV9-14.

Pittman R. C., Taylor C. A. Jr. Methods for assessment of tissue sites of lipoprotein degradation. *Methods Enzymol.* 1986, 129 (part B): 612-628.

Poledne R., Reinis Z., Lojda Z., Hanus K., Cihova Z. The inflow rate of low density lipoprotein cholesterol to the arterial wall in experimental atherosclerosis. *Physiol Bohemoslov. (ABBR).* 1986, 35: 313-318.

Radler J. O., Koltover I., Salditt T., Safinya C. R. Structure of DNA-cationic liposome complexes: DNA intercalation in multilamellar membranes in distinct interhelical packing regimes. *Science.* 1997, 275(5301): 810-814.

Redgrave T. G. Chylomicrons. In *The metabolic & molecular bases of inherited disease (Vol. II)* (Scriver C. R., Beaudet A. L., Sly W. S. and Valle D., Eds.). McGraw-Hill, New York. 2001, pp31-44.

Roberts A. B., Lees A. M., Lees R. S., Strauss H. W., Fallon J. T., Taveras J., Kopiwoda S. Selective accumulation of low density lipoproteins in damaged arterial wall. *J Lipid Res.* 1983, 24: 1160-1167.

Ross P. C., Hui S. W. Lipoplex size is a major determinant of in vitro lipofection efficiency. *Gene Ther.* 1999, 6(4): 651-659.

Santi D. V., McHenry C. S., Sommer H. Mechanism of interaction of thymidylate synthetase with 5-fluorodeoxyuridylate. *Biochemistry.* 1974, 13(3): 471-481.

Scherman D., Bessodes M., Cameron B., Herscovici J., Hofland H., Pitard B., Soubrier F., Wils P., Crouzet J. Application of lipids and plasmid design for gene delivery to mammalian cells. *Curr Opin Biotechnol.* 1998, 9(5): 480-485.

Schumaker V. N. and Puppione D. L. Sequential flotation ultracentrifugation. *Methods Enzymol.* 1986, 128: 155-170.

Schwendener R.A., Supersaxo A., Rubas W., Weder H. G., Hartmann H. R., Schott H., Ziegler A., Hengartner H. 5'-O-Palmitoyl- and 3',5'-O-dipalmitoyl-5-fluoro-2'-deoxyuridine--novel lipophilic analogues of 5'-fluoro-2'-deoxyuridine: synthesis,

incorporation into liposomes and preliminary biological results. *Biochem Biophys Res Commun.* 1985, 126(2): 660-666.

Shah P. K. New insights into the pathogenesis and prevention of acute coronary syndromes. *Am. J. Cardiol.* 1997, 79: 17-23.

Smith J. D., Breslow J. L. The emergence of mouse models of atherosclerosis and their relevance to clinical research. *J Intern Med.* 1997, 242: 99-109.

Skinner M. P., Yuan C., Mitsumori L., Hayes C. E., Raines E. W., Nelson J. A., Ross R. Serial magnetic resonance imaging of experimental atherosclerosis detects lesion fine structure, progression and complications in vivo. *Nature Med.* 1995, 1(1): 69-73.

Sladowski D., Steer S. J., Clothier R. H., Balls M. An improved MTT assay. *J Immunol Methods.* 1993, 157(1-2): 203-207.

Sorgi F. L., Bhattacharya S., Huang L. Protamine sulfate enhances lipid-mediated gene transfer. *Gene Ther.* 1997, 4(9): 961-968.

Spady D. K. Lipoproteins in biological fluids and compartments: synthesis, interconversions, and catabolism. In *Lipoproteins as carriers of pharmacological agent* (Shaw J. M., Eds.). Marcel Dekker, Inc. New York-Basel-Hong Kong. 1992, pp.1-12.

Staggs D. R., Burton D. W., Deftos L. J. Importance of liposome complexing volume in transfection optimization. *Biotechniques.* 1996, 21(5): 792-795.

Stary H. C., Chandler A. B., Dinsmore R. E., Fuster V., Glagov, S., Insull J. W., Rosenfeld M. E., Schwartz C. J., Wagner W. D., Wissler R. W. A Definition of Advanced Types of Atherosclerotic Lesions and a Histological Classification of Atherosclerosis: A Report From the Committee on Vascular Lesions of the Council

on Arteriosclerosis, American Heart Association. *Circulation*. 1995, 92(5): 1355-1374.

Stary H. C., Chandler A. B., Glagov S., Guyton J. R., Insull W. J., Rosenfeld M. E., Schaffer S. A., Schwartz C. J., Wagner W. D., Wissler R. W. A Definition of Initial, Fatty Streak, and Intermediate Lesions of Atherosclerosis: A Report From the Committee on Vascular Lesions of the Council on Arteriosclerosis, American Heart Association. *Circulation*. 1994, 89(5): 2462-2478.

Stehbens W. E. Coronary heart disease, hypercholesterolemia, and atherosclerosis I. false premises. *Exp. Mol. Pathol.* 2001, 70: 103-119.

Suarez J. E., Urquiza M., Puentes A., Garcia J. E., Curtidor H., Ocampo M., Lopez R., Rodriguez L. E., Vera R., Cubillos M., Torres M. H., Patarroyo M. E. Plasmodium falciparum circumsporozoite (CS) protein peptides specifically bind to HepG2 cells. *Vaccine*. 2001, 19(31): 4487-4495.

Suzuki M., Okabe H., Tsukagoshi S., Kawai T., Fukushima M., Sato I. Immunohistochemical investigation of thymidylate synthase in cervical cancer. *Oncology*. 1998, 55(6): 564-568.

Templeton N. S., Lasic D. D., Frederik P. M., Strey H. H., Roberts D. D., Pavlakis G. N. Improved DNA: liposome complexes for increased systemic delivery and gene expression. *Nat Biotechnol.* 1997, 15(7): 647-652.

Terpstra V., van Amersfoort E. S., van Velzen A. G., Kuiper J., van Berkel T. J. Hepatic and extrahepatic scavenger receptors: function in relation to disease. *Arterioscler Thromb Vasc Biol.* 2000, 20(8): 1860-1872.

Thieme T., Wernecke K. D., Meyer R., Brandenstein E., Habedank D., Hinz A., Felix S. B., Baumann G., Kleber F. X. Angioscopic evaluation of atherosclerotic plaques: validation by histomorphologic analysis and association with stable and unstable coronary syndromes. *J Am Coll Cardiol.* 1996, 28(1): 1-6.

Tomlinson E. Theory and practice of site-specific drug delivery. *Adv. Drug. Deliv. Rev.* 1987, 1: 87-198.

Toussaint J. F., LaMuraglia G. M., Southern J. F., Fuster V., Kantor H. L. Magnetic resonance images lipid, fibrous, calcified, hemorrhagic, and thrombotic components of human atherosclerosis in vivo. *Circulation.* 1996, 94(5): 932-938.

Vallabhajosula S., Fuster V. Atherosclerosis: imaging techniques and the evolving role of nuclear medicine. *J Nucl Med.* 1997, 38(11): 1788-1796.

Van Berkel T. J., De Rijke Y. B., Kruijt J. K. Different fate in vivo of oxidatively modified low density lipoprotein and acetylated low density lipoprotein in rats. Recognition by various scavenger receptors on Kupffer and endothelial liver cells. *J Biol Chem.* 1991, 266(4):2282-2289.

Van Berkel T. J., Fluiter K., van Velzen A. G., Vogelezang C. J., Ziere G. J. LDL receptor-independent and -dependent uptake of lipoproteins. *Atherosclerosis.* 1995, 118 Suppl: S43-50.

Van Borssum Waalkes M., Goris H., Dontje B. H., Schwendener R. A., Scherphof G., Nijhof W. Toxicity of liposomal 3'-5'-O-dipalmitoyl-5-fluoro-2'-deoxyuridine in mice. *Anticancer Drug Des.* 1998, 13(4): 291-305.

Van Borssum Waalkes M., van Galen M., Morselt H., Sternberg B., Scherphof G. L. In-vitro stability and cytostatic activity of liposomal formulations of 5-fluoro-2'-deoxyuridine and its diacylated derivatives. *Biochim Biophys Acta.* 1993, 1148(1): 161-172.

Vitols S. Uptake of low-density lipoprotein by malignant cells--possible therapeutic applications. *Cancer Cells.* 1991, 3(12): 488-495.

Voyta J. C., Via D. P., Butterfield C. E., Zetter B. R. Identification and isolation of endothelial cells based on their increased uptake of acetylated-low density lipoprotein. *J Cell Biol.* 1984, 99: 2034-2040.

Walsh G. Nucleic acid therapeutics. In *Biopharmaceuticals: biochemistry and biotechnology*. John Wiley & Sons, New Yolk. 1998, pp387-402.

Weichert J. P., Van Dort M. E., Groziak M. P., Counsell R. E. Radioiodination via isotope exchange in pivalic acid. *Int J Rad Appl Instrum Part A.* 1986, 37(8): 907-913.

Westesen K., Gerke A., Koch M. H. Characterization of native and drug-loaded human low density lipoproteins. *J Pharm Sci.* 1995, 84(2): 139-147.

Woolf N. Pathology of atherosclerosis. In *The metabolic & molecular bases of inherited disease (Vol. II)* (C. R. Scriver, A. L. Beaudet, W. S. Sly and D. Valle, Eds.), 8th ed. McGraw-Hill, New York. 2001, pp533-539.

Xia Z., Wiebe L. I., Miller G. G., Knaus E. E. Synthesis and biological evaluation of butanoate, retinoate, and bis(2,2,2-trichloroethyl)phosphate derivatives of 5-fluoro-2'-deoxyuridine and 2',5-difluoro-2'-deoxyuridine as potential dual action anticancer prodrugs. *Arch Pharm (Weinheim).* 1999, 332(8): 286-294.

Xiao W., Scott T. M., Feng L., Yu Z., Wang L., Hughes J. A., Liu H. Acetylated low-dencity lipoprotein (AcLDL) encapsulated cholesteryl 1,3-diiopanoate glycery ether (C2I) for the detection of atherosclerosis in rabbits. *J Nucl Med.* 2003, 44: 770-773.

Xiao[1] W., Wang L., Davis J. P., Liu H. Microemulsion of seal oil markedly enhances the transfer of a hydrophobic radiopharmaceutical into acetylated low density lipoprotein. *Lipids.* 1999, 34(5): 503-509.

Xiao[2] W., Wang L., Scott T. M., Counsell R. E., Liu H. Radiolabeled cholesteryl iopanoate/acetylated low density lipoprotein as a potential probe for visualization of early atherosclerotic lesions in rabbits. *Pharm Res.* 1999, 16(3): 420-426.

Xiao[3] W., Wang L., Ryan J. M., Pater A., Liu H. Incorporation of an (125)I-labeled hexa-iodinated diglyceride analog into low-density lipoprotein and high specific uptake by cells of cervical carcinoma cell lines. *Radiat Res.* 1999, 152(3): 250-256.

Yin M., and Rustum Y. M. Comparative DNA strand breakage induced by FUra and FdUrd in human ileocecal adenocarcinoma (HCT-8) cells: relevance to cell growth inhibition. *Cancer Commun.* 1991, 3(2): 45-51.

York P. G., Fitzgerald P. J. Intravascular ultrasound: state of the art and future directions. *Am. J. Cardiol.* 1998, 81: 27E-32E.

Zhu N., Liggitt D., Liu Y., Debs R. Systemic gene expression after intravenous DNA delivery into adult mice. *Science.* 1993 Jul 9;261(5118):209-11.